1998

Effects of heat on the hydrophobicity of EPDM composite insulators.

Liwen Cao
University of Windsor

INFORMATION TO USERS

This manuscript has been reproduced from the microfilm master. UMI films the text directly from the original or copy submitted. Thus, some thesis and dissertation copies are in typewriter face, while others may be from any type of computer printer.

The quality of this reproduction is dependent upon the quality of the copy submitted. Broken or indistinct print, colored or poor quality illustrations and photographs, print bleedthrough, substandard margins, and improper alignment can adversely affect reproduction.

In the unlikely event that the author did not send UMI a complete manuscript and there are missing pages, these will be noted. Also, if unauthorized copyright material had to be removed, a note will indicate the deletion.

Oversize materials (e.g., maps, drawings, charts) are reproduced by sectioning the original, beginning at the upper left-hand corner and continuing from left to right in equal sections with small overlaps.

Photographs included in the original manuscript have been reproduced xerographically in this copy. Higher quality 6" x 9" black and white photographic prints are available for any photographs or illustrations appearing in this copy for an additional charge. Contact UMI directly to order.

Bell & Howell Information and Learning
300 North Zeeb Road, Ann Arbor, MI 48106-1346 USA
800-521-0600

EFFECTS OF HEAT ON THE HYDROPHOBICITY OF EPDM COMPOSITE INSULATORS

BY

LIWEN CAO

A THESIS
SUBMITTED TO THE
FACULTY OF GRADUATE STUDIES AND RESEARCH
THROUGH THE DEPARTMENT OF ELECTRICAL ENGINEERING
IN PARTIAL FULFILMENT OF THE REQUIREMENT FOR
THE DEGREE OF MASTER OF APPLIED SCIENCE AT
THE UNIVERSITY OF WINDSOR

WINDSOR, ONTARIO, CANADA
1998

APPROVED BY:

Dr. R. Hackam (Supervisor)
Electrical Engineering

Dr. B.B. Budkowska
Civil and Environmental Engineering

Dr.G.R. Govinda Raju
Electrical Engineering

Dr.J.Soltis, Electrical Engineering
Chair of Examining Committee

ABSTRACT

Polymeric materials have been widely used as high voltage outdoor insulators since the early 1970s. This is due to their excellent electrical performance compared to ceramic insulators. Although glass and porcelain were the preferred materials for housing, insulators, bushings, terminations and surge arresters for many years, because of their high surface energy, they wet readily when exposed to fog, dew and rain. When these traditional insulators operate under moisture and contamination conditions, there is a high possibility of suffering from leakage current, leading to flashover which is followed with an outage of the power system.

Polymeric insulators can help solve this problem in certain cases by remaining hydrophobic after being subjected to dry-band-arcing. When polymeric materials like silicon rubbers, ethylene propylene diene monomer (EPDM), teflon (PTFE), and epoxy resin etc, were introduced into high voltage insulator technology about 25 years ago, it turned out that all these materials were characterized as hydrophobic due to their water-repellent properties. Because of good performance in the presence of pollution and other advantages such as light weight, resistance to vandalism easy handling and installation, composite insulators are now applied widely when replacing the traditional insulators and in newly built transmission and distribution power lines.

Long-rod composite insulators, with weather sheds made of ethylene propylene diene monomer (EPDM) have been broadly used as insulation material. The experience gained in electrotechnology from the use of EPDM has influenced the choice of shed material

for composite insulators. Thus the majority of the manufacturers include in their production program composite insulators with EPDM sheds. However, there have been very few published reports on the physical or chemical mechanisms of electrical performance of EPDM due to commercial reasons.

This thesis presents a laboratory study on the hydrophobic performance of EPDM, on the effects of heat treatment and surface analysis. It has been found that the maintenance of the water repellency of the surface of EPDM, after a temporary loss of its hydrophobicity, is due to the diffusion of low molecular weight (LMW) fluid from the bulk to the surface. The LMW fluid could be regenerated by the scissions of long molecular chains. A detailed study of the regenerated LMW fluid during heating in an electrical oven and after laser beam bombardments has been carried out. A study on the decomposition of ATH filler has also been done. A study to determine the surface hydrophobicity before and after the heat treatment is reported. A study on the photo-micrographs of fracture surface of EPDM and quantitative surface elemental analysis by using Scanning Electron Microscopy (SEM) is carried out. A study of the identification of the LMW fluid using Nuclear Magnetic Resonance (NMR) is reported. A study on the chain length of the siloxane and its concentration using Gas Chromatograph (GC-MS) has been done. The study on the molecular bonds and diffusion process of LMW fluid in the EPDM specimens by the use of ATR attached Fourier transform infrared spectroscopy (FT-IR) has also been performed.

Dedicated to my parents

ACKNOWLEDGEMENTS

I am greatly indebted to my program supervisor Dr.R.Hackam for his guidance, support and encouragement throughout the course of this work. It has indeed been a privilege to work with him.

I would like to thank Dr.Budkowska, a member of my Advisory Committee who has provided useful criticisms and suggestions for which I am grateful.

I would like to thank the Windsor Utility Commission of Windsor, Ontario, for providing EPDM insulators for this study.

I would like to thank Dr.R.Aroca and Dr.H.Ma of the Chemistry & Bio-Chemistry Department for their useful suggestions throughout the course of this work.

I would like to thank Mr.D.Liebsch, Central Research Workshop, and members of his staff for their assistance during the work.

I would like to thank Mr.M.Fuerth of the Chemistry Department for his technical assistance and permission to use the FTIR spectrometer and the NMR analyzer, Dr.R.Lazar of the Great Lake Institute in the Biology Department and Mr.W.Henderson in the Environmental Engineering Department for their technical assistance and permission to use the GC-MS analyzer, Mr.A.Johns and Mr.J.M.Novosad of the Electrical Engineering Department for their technical assistance and Mr.J.Robinson of the Department of Mechanical Engineering for his assistance with the SEM analysis.

TABLE OF CONTENTS

LIST OF FIGURES

CHAPTER I
INTRODUCTION

The use of porcelain and glass as high voltage outdoor insulators has been in existence for over 100 years. They comprise at the present time the vast majority of the installed insulators in both transmission and distribution lines. For over a century of insulation service in electrical power systems, these insulators demonstrated a good resistance to environmental aging and an excellent mechanical strength. Even though glass and porcelain insulators had the ability to withstand substantial arcing without serious degradation, the effect of large leakage current and flashover is a major practical limitation to attain reliable supply of electrical power, because of power system outages. This type of disruption could be very costly [1]. For example, a power interruption lasting a short time can shut down a paper mill, resulting in down time, possible equipment damage, and lost production.

The problem of uncontrolled leakage current say in porcelain insulators is due to the inherent hydrophilic surface of inorganic materials [2-5]. There is a continuous formation of a water film on the insulator surface during high humidity conditions such as rain, dew and fog. The environmental contaminations such as dust, bird pollution, clays and salt spray accumulate on the insulator surface and are partially dissolved into the water film, and create a conductive electrolyte. These deposits decrease the surface resistance and encourage the development of leakage current. The water layer is heated and dries out locally. In consequence dry band arcings take place, which might result in a complete

flashover. Therefore, the contamination problem on outdoor insulators becomes a major concern to the electric power utilities [6,7].

With the development of the composite polymers technology, non-ceramic insulators have been increasingly used in industry and utilities to replace porcelain and glass insulators during the last three decades. After approximately 30 years of service history, the advantages of polymer insulators have been well accepted, such as light weight, ease of handling, reduced installation and maintenance costs, vandalism resistance, and superior contamination performance [1,8-11]. The quality and electrical performance of the polymer insulators have undergone significant improvements during service. Currently, in the United States, non-ceramic insulators represent approximately 60-70% of all newly installed high-voltage insulators [8,11,12]. The most commonly used base polymers or elastomers for the weathersheds of non-ceramic insulators are EPM (ethylene propylene monomer), EPDM (ethylene propylene diene monomer), silicone rubber, alloys of EPDM (or EPM) and silicone, and EVA (ethylene-vinyl acetate) [8].

Before the present work, there was no published information about the additives or the compound of the fluid in the EPDM specimens provided by the manufacturers. During this study, the specimens were investigated and identified to be the alloys of EPDM with silicone, and the fluid in the bulk also has been identified to be silicone oil. The EPDM weathershed used in this study was manufactured by K-Line Insulators, of Scarborough, Ontario Ltd., which was in service at the Windsor utility for 6 years.

1.1 Nomenclature of EPDM

The polymer chain formed by the reaction of ethylene and propylene is called EPR. A terpolymer can be manufactured by polymerizing a diene monomer with ethylene and propylene. Therefore ethylene propylene diene terpolymer is labeled EPDM by ASTM nomenclature. In EPDM, the "E" stands for ethylene, the "P" for propylene, the "D" for diene, and the "M" for the repeating CH_2 units of the saturated polymer backbone[13]. At room temperature and atmospheric pressure, both ethylene and propylene are gaseous hydrocarbons obtained by cracking natural gas liquids or naphtha from petroleum. Both are composed of carbon and hydrogen atoms[13]. The structure is shown in Fig 1.1.

Ethylene Propylene

Fig.1.1 Chemical structures of Ethylene and Propylene

1.2 The history and manufacture of EPDM

EPDM usually is made in a continuous flow-stirred tank reactors. Hexane, ethylene, propylene, diene and catalyst solution must all be pure and dry because of the sensitivity of the Ziegler-Natta catalyst system to water [13]. The olefin sites or carbon-carbon double bond unsaturation in both molecules can react under certain condition [13]. Ethylene and propylene monomer each has a finite molecular weight. Polymerization fastens these monomers together to form a much higher molecular weight chains. Since

all the chains are not of the same length, the polymer molecular weight are not the same. The distribution of molecular weight is from 10^3 to 10^7 atomic mass units (amu), where the mass of hydrogen atom is 1.008. The average molecular weight is 10^5 [13]. EPM based polymer insulation have continuously been improved during the last three decades [8]. The initially introduced polymer was EPM based compound (EPM-1). It was employed during 1971-1986. Since 1983, EPM-2 was recognized to have improved resistance to oxidation and corona cutting than EPM-1. In 1986, an alloy of EPM and silicone was first commercially introduced. This material had the addition of a silicone compound. In 1989, the base compound in the alloy rubber was changed to EPDM. The accelerated laboratory test in Hubbell Power System and Ohio Brass Company provided the evidence that insulators made of an alloy of EPDM and silicone rubber was the best performing compound [8]. No degradation of Insulator EPM-1 during the aging test indicated that the material would continue to provide satisfactory service even after 30 years of service. Insulators made of an alloy of EPDM and silicone might be considered to be an even better long-term performer, on the basis of comparable results in the environment chamber tests and markedly better performance of the alloy material in the test [8,14,15].

1.3 Properties of EPDM

The special advantages of EPDM derive from the chemical molecular structure. The organic saturated polymer C-C chain backbone is the key to the excellent electrical, chemical, and mechanical properties. Non-conjugated dienes introduce the unsaturation pendant to the EPDM polymer backbone. Thus, oxidative attack by oxygen or ozone on

the olefinic sites in EPDM does not result in cleavage of the backbone. Weathering ability can be achieved without antioxidants or antiozonates. Typically, EPDM has an outstanding resistance to ozone, oxygen and sunlight. It also has excellent weathering and heat resistance and low temperature flexibility [8,12-13,16-17]. There was a report on the wettability of the EPDM elastomer by the Institute of Electrotechnology of Poland [14]. The test showed that modified EPDM had a resistant ability to atmospheric influences and also to polar substances (e.g. water). One of its advantages is a possibility of easy modification of this polymer. A common feature of the EPDM elastomer is chain-line structure containing molecules with axes of easy rotation along their covalent bonds. Some of the EPDM modifications are known under the name of self-sealing rubbers, in which wax-like solid or liquid substances diffuse out of the interior to the surface of an elastomer. Additional benefits of these materials are that they are slow-burning, resistant to an electric arc and also to the action of mould fungi.

1.4 Properties of silicone rubber

The chemical structure of silicone rubber (siloxane elastomers) is partly inorganic and partly organic [8,18]. Polydimethylsiloxane (PDMS) is the base molecule for silicone oil and silicone rubber. The molecule is mainly composed of methyl group(CH_3), silicone (Si) and oxygen (O). In the simple form, the silicone rubber can be considered as an inert silica type molecule attached to organic groups. The backbone of the rubber is a repeating silicone-oxygen (Si-O) bond. Thus, one obtains some of the chemical and thermal stability of silica with solubility and ease of handling of organic compounds [19]. Silicone rubber has the ability to resist heat, sunlight and it also has an excellent water

repellency (hydrophobicity). These advantages derive from the special molecular structure. The methyl group (CH_3) is considered to be an excellent hydrophobic group. It can almost freely rotate about the Si-O bond. The extremely flexible methylsiloxane molecule chain contributes to the hydrophobic ability.

1.5 Alloys of EPDM and Silicone

The alloys of EPDM and silicone may make it possible to combine the properties of the two materials. These materials can be alloyed via a compatibilizer, which has the capability to crosslink to both the EPDM and the silicone. The EPDM compounded with silicone has excellent electrical and mechanical properties due to the presence of EPDM and has hydrophobic ability because of the silicone content. A recent report shows that the EPDM and silicone rubber can be compounded in a weight ratio of up to (10:3) [2]. The maintaince of hydrophobicity of EPDM specimens is due to the diffusion of LMW fluid from the bulk to the surface [20-21].

1.6 Fillers and additives in polymers

There is not a single base polymer material which alone has all the necessary properties for an outdoor insulating application. The inherent disadvantage of polymer materials is also based on its molecular structure. Polymer materials have weaker bonds than porcelain, which means that they can be aged and changed by the multiple stresses encountered in service [14]. For example, in order to resist the surface aging process, the material has to resist the tracking and erosion, weathering, moisture and heat, corona discharge and fungi. Typically, polymer insulation is not rigid or self-supporting, where

an intrinsic mechanical strength is required. In addition, the cost of the polymer raw material is much higher than that of porcelain or glass raw materials [9-10].

In this case, selected additives and fillers can be combined in various proportions with the polymers to enhance the electrical, mechanical and chemical properties. The appropriate additives and fillers mixed with the base polymer may contribute to the achievement of the desired electrical performance and the maintaince of long-term proper service. In order to reduce the cost, lower cost fillers are blended in with the more expensive base polymer. Depending on the specific formulation, fillers and additives can comprise of the order of 20% to 80% by weight of the formulation [14]. Fillers, e.g., silica and alumina trihydrate(ATH), are used to enhance tensile strength, modulus, tear strength, and abrasion resistance and to impart a high resistance to electrical tracking and flammability[8-9,16,20]. In the present research, ATH filler is blended in the EPDM specimens, which may enhance the resistance ability to tracking and erosion. For example: erosion and tracking of EPDM weathersheds may occur when dry band arcing ensues on the insulator surface and the hydrophobicity is temporarily lost. It works by thermal decomposition and is consumed during the surface electrical activity. If the temperatures approach the activation temperature of the ATH, the concentration is reduced and its effects are minimized. In such cases, the electrical performance is severely reduced.

1.7 Electrical performance of EPDM insulators

Lipinski and Michalski [20] in Poland investigated the applications of the EPDM elastomer modified by chloroparaffins, wax and derivatives of crude oil as a coating material. They found that the modified EPDM can fulfill the conditions required by contemporary small and high power devices after thermal treatment (damp, heat-steady state, dry hot at 40°C, dry hot at 70°C, during 14 weeks). During the time of the thermal treatment, an intensive migration of waxen fillers into the surface of rubbers was found. The presence of the hydrated oxide aluminum causes an increase of resistance to the electric arc. However, it decreases the lifetime as it lowers the mechanical properties. A decrease of the amount of crude oil derivatives and chloroparaffins improves the resistivity of EPDM elastomer at higher temperatures. They reached the conclusion that the modified EPDM elastomers were very strongly hydrophobic, and their use as a coating material improved the electrical properties of insulators when subjected to droplets corresponding to the size of dew or light rains.

Kindersberger and Kuhl [15] in Germany conducted a laboratory test in 1989 on the hydrophobicity transfer with various polymeric materials using a pollution layer of quartz flour and applying a temperature of 180°C. They found out that EPDM showed a small but noticable effect of transfer of hydrophobicity, while epoxy resins, PMMA and PTFE were not able to transfer hydrophobic properties.

Since 1987, Chalmers University of Technology applied a long-term research program on various polymeric insulators at Annerberg outdoor field station on the West Coast of Sweden [22]. The aim of the program was to elucidate how the performance of the

outdoor insulators is affected by the design and choice of material. Insulators have been exposed to coastal contamination at the station and energized with $130kV_{rms}$ phase-to-ground HVAC since 1988. They reported the hydrophobicity and the statistics of the leakage current peaks of one porcelain, two EPDM and four silicone rubber transmission line insulators [22]. The field experiment showed that the EPDM rubber insulators lost most of their initial high surface resistivity shortly after their exposure to the environment and as a result high leakage currents developed during their first year of energization. The progressive aging of the EPDM rubber insulator surfaces increased the leakage current activity during the test period and one of the EPDM rubber insulators finally flashed over during the salt-storms in 1993. During the salt-storms the magnitude of the developed arcing current of the EPDM insulators is typically two to three times as high as that of the porcelain insulator. Furthermore, the results also showed that silicone rubber insulators could preserve a high degree of hydrophobicity even after more than seven years of energization.

Gubanski and Vlastos [23] reported in 1990 on the wettability of naturally aged silicone and EPDM insulators. Specimens were taken either directly from insulators or after exposure to corona discharges and/or artificial pollution. The experimental results showed that for the EPDM insulators, the advancing angle on the upper side of the shed was found to be lower than that on the under side of the shed. However, for silicone rubber, the opposite was found to be valid. The contact angle of EPDM insulators were much lower than those obtained with silicone rubber insulators and especially in the case of the aged surface. For EPDM rubber insulators, the contact angle did not recover with

time or even continued to decrease after being subjected to corona discharge or polluted by the salt deposition.

Vlastos and Sherif reported on the aspect of natural aging of EPDM[24]. The EPDM insulators were subjected to long-term tests under realistic environmental and operational conditions DC(600 kV) and AC(462 kV_{rms} phase-to-ground) in Anneberg outdoor field. They found out that composite insulators with sheds made of ethylene propylene rubber (EPDM) performed better at the beginning of their life-time than the porcelain and glass insulators. The experimental results gave the evidence that EPDM insulators of different makes, due to their material composition, filler and design, showed differences both in their electrical performance and in the way the shed material was degraded by aging. The insulators energized by DC were subjected to more flashovers than AC insulators.

Sorqvist and Vlastos reported in 1997 on the long-term performance of silicone rubber and EPDM exposed to HVDC [25]. They found out that EPDM insulators had in the long run performed worse than silicone rubber, due to weathering and aging of their surfaces. The EPDM rubber insulators enhanced with LMW silicone additives without ATH filler showed a good hydrophobicity and lower leakage currents. But the performance of these insulators at severe pollution conditions and/or higher electric stresses is still unknown.

1.8 Accelerated laboratory aging test

Although the use of polymeric insulators for outdoor transmission line insulators has rapidly increased during the last three decade. There was still a very limited experience on the reliability and long-term performance of composite insulators in realistic service conditions. Especially some of the early generation of polymer products did not provide the expected service performance. Therefore, in general, the industry still has questions about such insulators. The major concern is the ability of the non-ceramic insulating weathershed materials to resist physical and chemical degradation. Obviously, the overall characteristics of the new generation insulators can not be evaluated by the three decades service experience. Furthermore, ultimate test in realistic condition is also not a very practical method. Therefore, the relatively short-term, accelerated laboratory aging tests is commonly applied to predict both the performance and the chemical changes of these new generation of insulators for high voltage application.

CHAPTER II
MEASUREMENTS TECHNIQUES

2.1 Introduction

EPDM specimens were cut from the weathersheds of a 46 kV outdoor insulator, which had been in service for 6 years. In the present study, specimens were prepared having dimensions of about 1 x 1 x 0.5 cm^3. The specimens were formulated with 200 parts of alumna trihydrate (ATH) filler per hundred (pph) in weight of EPDM rubber. The filler was used to enhance the resistance ability of EPDM to erosion and tracking from dry band discharges. During this work, the ambient temperature was 23±3°C, and the humidity was 44±4%.

2.2 Measurements of weight

The weight of the specimens was measured using a high precision balance (BP 110S) with a sensitivity of 0.01 mg. (Sartorius Type BP 110S)

2.3 Measurements of contact angle

2.3.1 Principles of contact angle

When a water droplet is in contact with a solid, there is an angle formed between the horizontal surface and the tangent to the droplet, and is called the contact angle. The contact angle depends on the surface wettibility, which is largely related to the surface energy. Materials with high surface energy such as porcelain and glass, can easily be wetted, a water film forms continuously on the surface and therefore, they are

hydrophilic[26-30]. In this condition, the contact angle is zero. On the other hand, materials with low surface energy such as silicone rubber and EPDM, have inherent water-repellency and are called hydrophobic. Therefore water droplets on the surface tend to bead up, and run down in vertical insulators. In the latter case, the contact angle is usually larger than 90°. Hydrophobic or hydrophilic properties of materials are determined by the ratio of the cohesive tension of water to the adhesive tension between water and the solid material. With a given cohesive tension of water, the hydrophobicity is increased with decreasing adhesive tension between water and the solid material. On the other hand, the water-repellent property of a solid material depends on the surface tension of water which can be affected by additives. The shape of a drop of water on the surface of a solid is determined by equilibrium of cohesive, adhesive and gravity forces. Therefore, the contact angle was used in this work as a measure of the hydrophobicity of EPDM. It has been shown to be an effective way to provide reliable information on the hydrophobicity condition [31-37].

2.3.2 Experimental setup

In the present study, the contact angles were measured using a goniometer with a sessile drop of distilled water (2.5μS/cm) having a volume of about 6.8μl. The conductivity of the water droplet in the range of (2.5-10,000 μS/cm) had no effect on the measurements of the contact angle [32]. The contact angle depends on the volume of the droplet but in the range 2-9μl had no effect on the measurements [32]. The contact angle was measured within 1 min after placing the water droplet on the surface of the specimens in order to

avoid the influence of long durations of the presence water. The contact angle was measured at 6 locations of the surface and an average reading was determined.

2.4 Measurements using gas chromatography (GC-MS)

2.4.1 Principles of GC-MS

Chromatography is a collective name for all separation processes where the separation of the components is effected by their partition between a stationary (fixed) phase with a large surface and a moving (percolating) phase which flows over the first [38-39]. The decisive factor is the relative flow between the phases. In elution chromatography the sample under investigation is swept through the column by elution with a fluid (eluent) or gas (carrier gas). The eluent gas passes through the column in a constant stream into which the sample to be analyzed is fed. The various components in the sample will travel, under the rinsing effect of the eluent, with different velocities through the column where the velocity will depend on the sorptivity of the component. Provided there is a sufficient difference between the partition coefficients, the components will leave the column after a certain distance completely separated. The method applied in gas chromatography, namely temperature and flow programming, offer possibilities of changing the temperature and the rate of flow of the carrier gas during analysis, thereby accelerating the elution of the high boiling, more strongly sorbed components in the sample[38-40].

2.4.2 Experimental setup

In the present work, the carrier gas is helium(He), which was fed into a column at approximately 30 cm/s and determined at 100°C (1ml/min). The column head pressure is

$0.9x10^5$Pa (13psi). Samples started running in the SCAH-Model. The initial temperature was 35°C, and the initial time was 2 min. The rate of increasing temperature was 20°C/per min to 180°C (hold 1 min), and then it was adjusted to 15°C/per min from 180°C to 300°C. Only 1μl samples is injected. Sample extracted is analyzed on a Hewlett Packard's model (5890/5970GC/MSD). The detector was mass selective (quadruple mass analyzer, 70 eV). The column is 30m x 0.25mm I.D. x 0.25 μm. DB-5 film was used. The GC-MSD interface temperature was 280°C, and the injector temperature was 250°C.

2.5 Measurements using nuclear magnetic resonance (NMR)

2.5.1 Principles of NMR

Nuclear magnetic resonance (NMR) spectroscopy is a tool for chemical structural analysis [41]. All atomic nuclei have charge and mass, while many also possess angular momentum and magnetic moments; as a result, the latter behave as spinning bodies. The theory of the NMR is based on the nuclear spin (I). Nuclei with odd mass numbers have spins whose value, I, is an odd-intergral multiple of ½. Nuclei with even mass are spinless if the nuclear charge is even, or have intergral spin if the charge is odd[42]. Nuclei spin is in units of $h/2\pi$, where h is Planck constant. When a magnetic field B is applied, the nuclear moments orient themselves with only certain allowed orientations or spin states (2I+1). The nuclear magnetic moment (μ) is directly proportional to the spin I, as $\mu = \gamma Ih/2\pi$, where the proportionality constant γ is the magnetogyric ratio which is constant for each particular nucleus. These states are degenerate in the absence of a magnetic field, but in the presence of an applied field these correspond to different potential energy levels. The detection and measurement of transitions between these spin

states is NMR spectroscopy. For example, when a nucleus of magnetogyric ratio γ is placed in a magnetic field B, the resonant condition is satisfied when the frequency of the applied radiation ν is given by $\nu = \gamma B/2\pi$. The relationship between field (B) and frequency (ν) extends to the methods of obtaining spectra. The NMR signal obtained is directly proportional to the number of nuclei producing it[41-44]. One of the most important features in NMR spectra is the chemical shift, which has its origin in the magnetic screening produced by electrons. Chemical shift is defined as the nuclear shielding divided by the applied field. The unit of chemical shifts is parts per million (ppm). The chemical shift is only a function of the nucleus and its environment, i.e. it is a molecular quantity[42].

2.5.2 Experimental procedure

Nuclear Magnetic Resonance (NMR) techniques were used to identify the LMW fluid extracted from the EPDM. In order to extract the fluid, the specimens were cut into small pieces (about 1mmx1mmx1mm) and were immersed in hexane for 120h, and the vessel was connected to a reflux condenser. In order to separate the LMW fluid from the solution containing hexane, the solution was heated at 50°C, the temperature is close to the boiling point of hexane. This process was very carefully controlled by using nitrogen protection during the whole reflux procedure to obviate spontaneous combustion. After 120h of immersion, extract and reflux processes, a viscid liquid was obtained. About 20 mg of fluid was extracted from 2.5 g (0.8%) of EPDM. It was found that the fluid was transparent, viscous, and highly concentrated. A high-resolution spectrometer (Bruker AC500, 500Hz) was used with chloroform-d as solvent. Three different solutions were

used to identify the composition of the material in the fluid. 1. analytical hexane, 2. silicone fluid (20 centipoise viscosty) and 3. a mixture of hexane and the LMW fluid which was extracted from EPDM. A drop of each solution was used and placed in a NMR tube with the chloroform-d solvent. The composition of the material extracted from the EPDM samples was identified as a PDMS molecular structure.

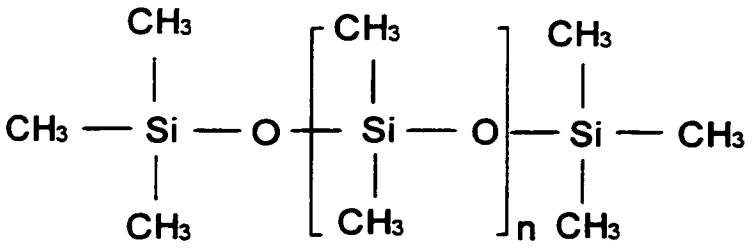

Fig.2.1 Chemical formular of PDMS

2.6 Measurements using scanning electron microscopy (SEM)

2.6.1 Principles of SEM

The principles of SEM is that, the electron beam leaves the electron column, enters the specimen chamber, and strikes the specimen at a single location on the optical axis of the column[45]. The electron beam interacts both elastically and inelastically with the specimen, forming the limiting interaction volume from which the various types of radiation emerge, including backscattered, secondary, and absrobed electrons, etc. By measuring the magnitudes of these signals with suitable detectors, a certain surface properties of the specimens can be made at the single location where the electron beam strikes. In order to construct an image, the beam must be moved from place to place by

means of a scanning system. The SEM uses the secondary electrons produced by the scanning beam to give a life-like, almost three-dimensional image of the surface of the specimen being scanned. The magnification range of the SEM is extraordinarily wide: from 10 to 10^5 or more[31,19,46].

2.6.2 Experimental setup

To study the surface of the specimens, A SEM instrument type Semko Nano Lab7 with a 15 keV electron beam in the pressure range of 10^{-4} to10^{-3} Pa used. The penetration of the electron beam into the surface of EPDM specimens at 15 keV was about 10μm. The specimens were studied before and after heating in an electrical oven and laser beam bombardment. The compositions of the elements of aluminum (Al), silicone (Si) and oxygen (O) on the surface of the specimens was determined by an energy dispersive X-ray counter. Scanning was done on 4 locations of each specimen. Two specimens were used for each case. The dimension of the specimens was about 1.0x1.0x0.5cm^3.

2.7 Measurements using Fourier transform infrared spectroscopy (ATR-FTIR)

2.7.1 Principles of ATR-FTIR

The technique of infrared spectroscopy is used to measure the transmission of a light beam passing through the entire thickness of the sample material, as a function of the wavelength [40,45,47]. Coupled with attenuated total reflection (ATR) can be used to get the spectra of thin films on a polymer surface which might have major interfering infrared bands. The atoms in the specimens are excited by the absorbed infrared light. The absorbed energy is translated into vibrational and rotational energies. The energy

absorbed by the molecules that result in the vibrational motions are several hundred times larger than those associated with the rotational motion. The transmission, neglecting reflection losses, follows the law:

$$I_T / I_A = e^{-\alpha d}$$

where I_A and I_T are applied and transmitted light intensities, respectively. α is the absorption coefficient and d, the sample thickness. ATR is due to absorbing coupling mechanism whereby the reflectivity for total internal reflection can be continuously adjusted at some value between 0 and 100% by placing an absorbing medium in contact with the reflecting surface. The resulting reflection is to be attenuated; the energy of infrared light is absorbed and is not transmitted but may be converted to another energy, such as exciting molecular energy states.

2.7.2 Experimental setup

In the present work, a Nicolet 5DX Fourier Transform Infrared (FTIR) spectrometer with an attenuated total reflection (ATR) attachment (Twin Parallel Mirror Reflectance Attachment made by Harrick Scientific Corp.) was applied using a KRS-5 (Thalium Bromoiodide) crystal. First an IR background was obtained without EPDM specimens. Then a slice of EPDM specimen was placed on the crystal which was separated by 1mm and a predetermined pressure was applied on it. Some of the silicone fluid was transferred to the surface of the crystal, then it was monitored by the IR spectroscopy. After the test, the crystal was carefully cleaned by methanol. The specimens were cut into slices of 5.0x1.0x0.1cm. The wave numbers in the range 500-2000 cm^{-1} were used.

CHAPTER III

LOSS AND REGENERATION OF LMW FLUID

3.1 Introduction

One of the most important properties of ethylene propylene diene monomer (EPDM) is its inherent low surface energy which inhibits the spread of water droplets on the surface even in the presence of pollution. This reduces the development of leakage current and the flashover. The water repellency (hydrophobicity) of the surface in silicone rubber was attributed to the diffusion of low molecular weight (LMW) fluid from the bulk to the surface[43].

A study of the generation and the loss of the LMW fluid in EPDM has been conducted as a function of temperature in order to simulate the effects of the heat of the dry band discharges on the surface. Sufficient amount of LMW fluid on the surface and in the bulk of the material is required to maintain its hydrophobicity during the lifetime of the EPDM when used as insulators. In the present work the generation and the loss of LMW fluid in EPDM were determined after subjecting the specimens to different combinations of temperatures and durations of heating. The contact angle of EPDM was determined before and after different heat treatments and is correlated with the presence of the fluid. The time of heating at each temperature was varied from 0.5h to 11h. The temperature was varied from 23°C to 550°C. The fluid within the EPDM was extracted using analytical hexane. The decomposition of the alumina trihydrate filler at different temperatures was also studied. In the present study, the EPDM specimens contains 200

parts of alumina trihydrate (ATH) by weight per hundred (pph) parts of the EPDM rubber. The (ATH) is used as filler to improve the electrical performance and reduce the cost of the finished product[44-46].

3.2 Determination of optimum immersion time

3.2.1 Experimental conditions

EPDM specimens were cut from the weathersheds of a 46 kV outdoor insulator, which had been in service for 6 years. The dimensions of the specimens were about 1.0x1.0x0.5cm^3. Analytical hexane was used to extract the LMW fluid from EPDM. The ambient temperature was 23±3°C, and the humidity was 49±4% during this study. A high precision balance having a resolution of 0.01mg was employed to measure the weight. The measurement of the weight was done within 1min after removal from the liquid, and the specimens were put back into hexane thus maintaining the immersion condition. Typically two specimens were used for each condition.

3.2.2 Absorption of hexane

In order to ascertain the optimum time that is necessary to extract all the mobile fluid from the EPDM, the specimens were first immersed in hexane for up to 960h at 23±3°C. Fig.3.1 shows that in the first 5h, the weight of the specimens increased rapidly, due to a rapid absorption of hexane. Then the absorption rate began to slow down. From 5h to 90h, there was only a slight increase in the weight. Fig.3.1 shows that after 96h of immersion in hexane, the absorption reached saturation. From 96h to 960h, there was no

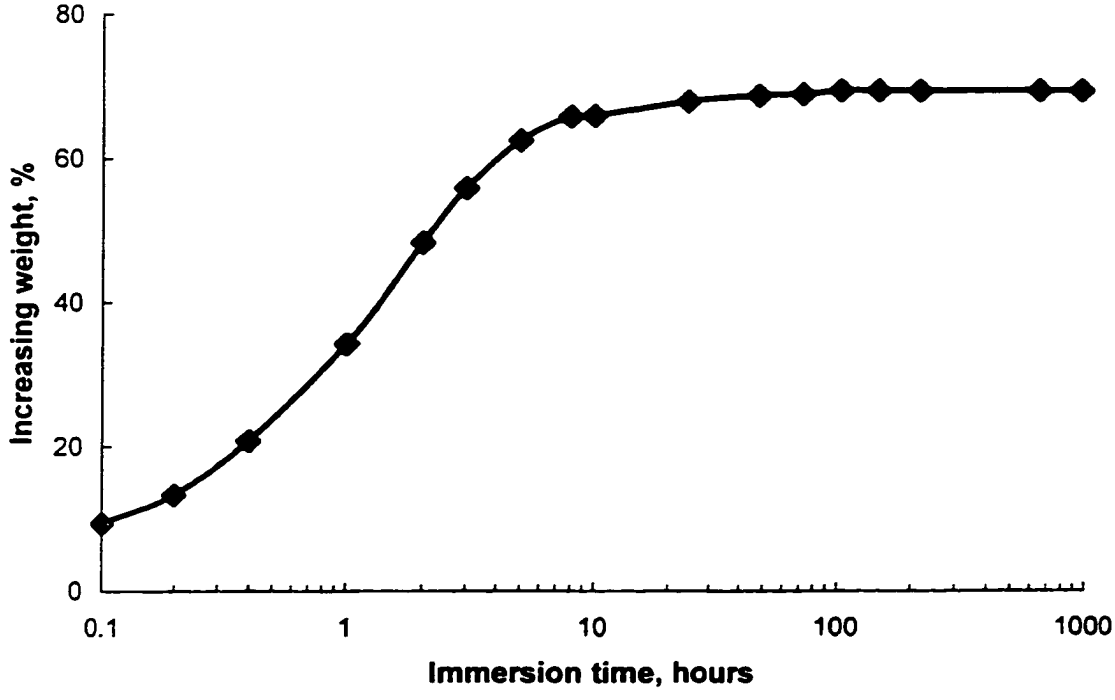

Figure 3.1 Percentage increase in weight of EPDM specimens as a function of immersion time in hexane. immersion, 23±3°C

further increase in the weight. Therefore, a period of 96h of immersion at 23±3°C was chosen for the immersion of EPDM in hexane to extract the LMW fluid from therein.

3.3 Determination of optimum evaporation time

After removing the specimens from hexane, sufficient time is required to allow a complete evaporation of the absorbed hexane. The specimens were left in air for up to 96 hours at 23±3°C and at a humidity of 49±4%. It is clear from Fig.3.2 that there was a rapid decrease in the weight within 2h due to the evaporation of hexane. After that, the evaporation rate slowed down. Fig.3.2 shows that 24h was sufficient for a complete evaporation of the absorbed hexane. Therefore an evaporation time of 24h at 23±3°C was chosen.

3.4 Determination of the amount of the mobile fluid in EPDM

In order to determine the amount of the mobile fluid, the virgin specimens were immersed in hexane and then allowed to completely evaporate in air. A study of the extraction of mobile LMW fluid as a function of immersion time in hexane in virgin specimens has been carried out. Two specimens were used for each condition. The dimensions of the specimens were 1.0x1.0x0.5cm^3. For each specimen a different immersion time in hexane was applied, followed by a complete evaporation in air. The weights before immersion and after a complete evaporation were measured. The weight difference is the amount of the fluid that has been extracted by hexane. Fig.3.3 shows the amount of the LMW fluid by percentage weight as a function of immersion time. It is shown that after 6h of immersion in hexane, 1.46% of the total weight of EPDM has been

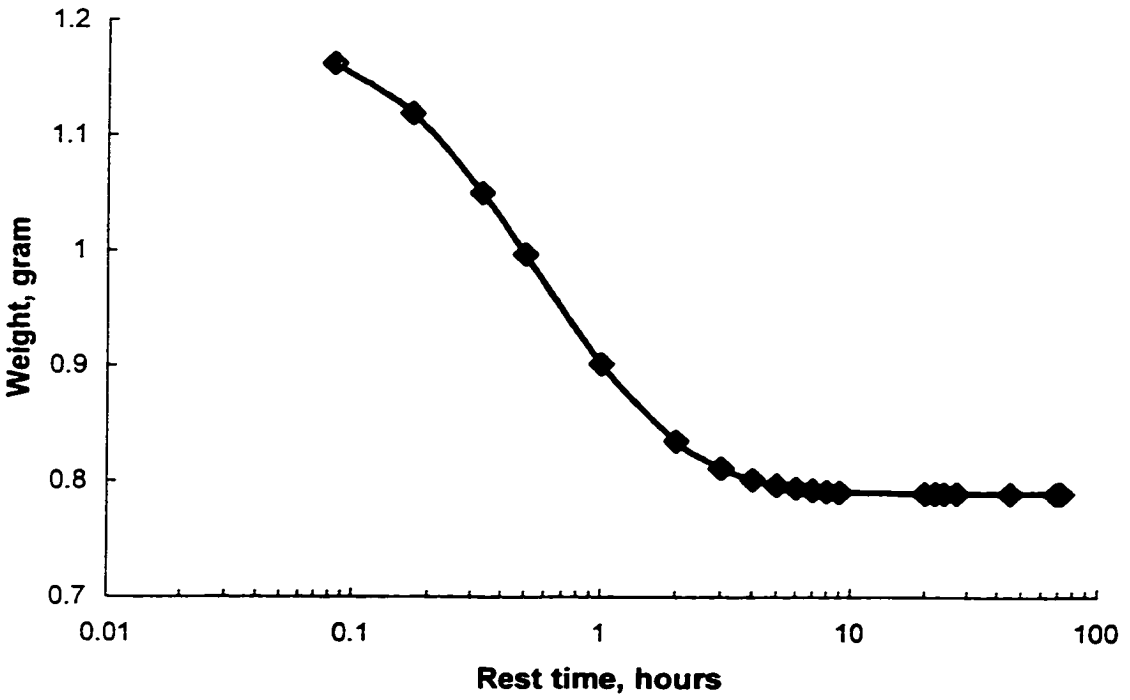

Figure3.2 Weight of EPDM specimens during evaporation in air at 23±3°C subsequent to immersion in hexane

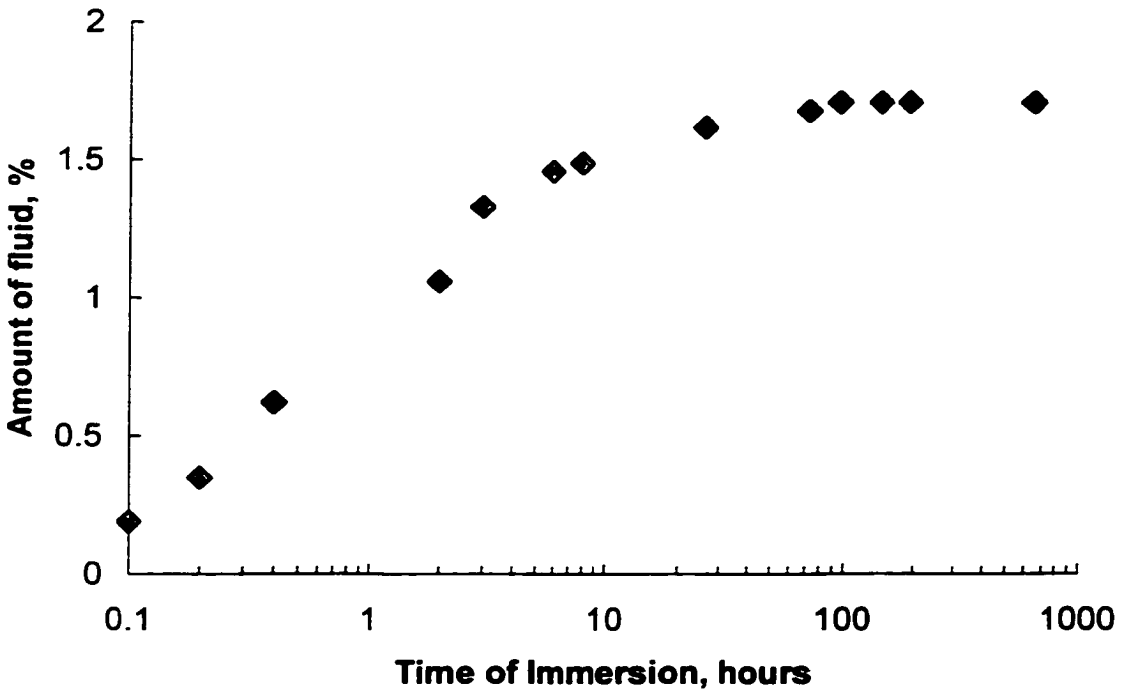

Figure 3.3 Percentage weight of mobile LMW fluid extratable from EPDM as a function of immersion time in hexane at 23±3°C

extracted as fluid. It is also observed from Fig.3.3 that after immersion at 23±3°C and followed with complete evaporation of the hexane in air for a further 96h, the maximum content of the mobile fluid is 1.72% after 96h of immersion and 1.72% after 600h of immersion in hexane. Amounts of LMW oil of 1.71% and 1.72% have been found in two other specimens that were immersed in the hexane for 144h and 192h, respectively.

3.5 Effect of the volume of the specimens on the level of the LMW fluid

The effect of the volume of the specimens on the amount of low molecular weight fluid was studied. In this experiment, the density of the EPDM specimens was determined from measurements of their weight and volume. The density of EPDM was determined to be 1.458±0.004 g/cm^3. Fig.3.4 shows that the content of the LMW oil is constant at 1.72±0.1% in the range of 0.83cm^3 to 14.41cm^3. Since the volume of all the specimens used in this study, except for the dependence of the amount of the fluid on the volume, was less than 2cm^3, Fig.3.4 clearly shows that the reported results are independent of the volume of EPDM.

3.6 Effect of the ambient humidity on the weight of the specimens

In order to investigate if there was an effect of the ambient humidity on the weight of the specimens, the weight of two specimens were measured as a function of time, at 23±3°C, and for a humidity of 49±4%. Fig.3.5 shows the weight of the specimens as a function of time. The maximum percentage change in the weight was found to be ± 0.025% which was considerably less than the variations in the levels of the LMW fluid found in this work as a function of the parameters investigated.

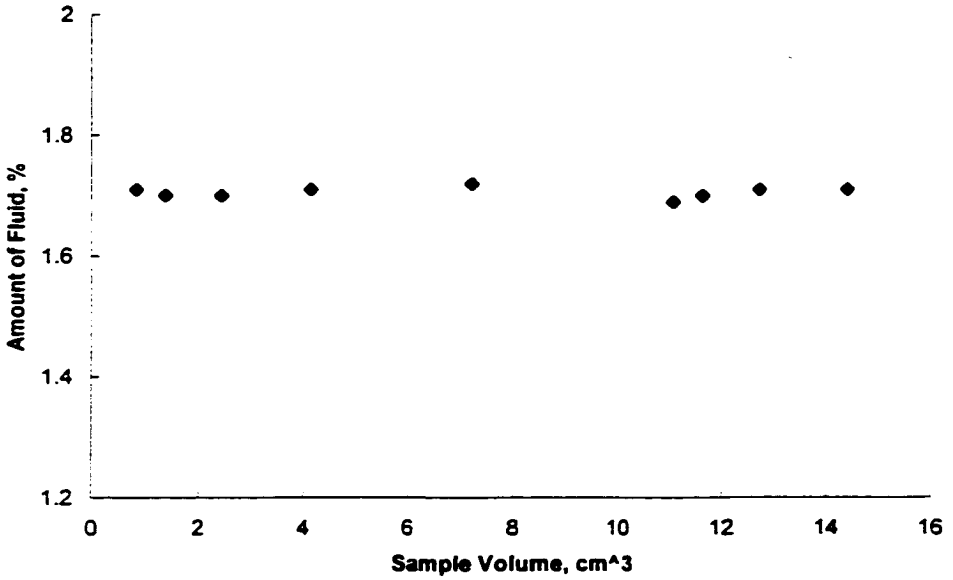

Figure3.4 The content of LMW fluid in EPDM specimens for different volumes

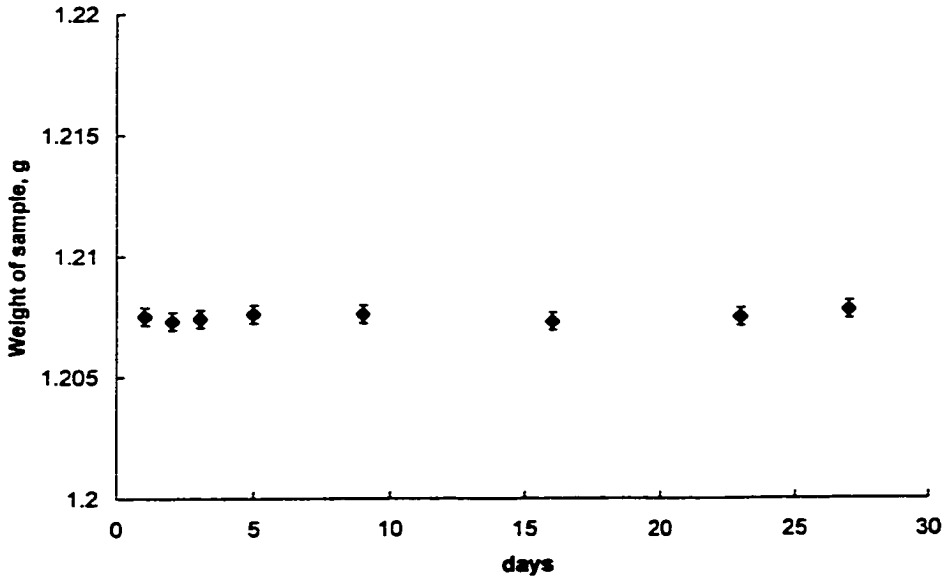

Figure 3.5 The weight of EPDM specimens as a function of time in air. Humidity, 49±4%

3.7 Loss and regeneration of LMW fluid

3.7.1 Regeneration of LMW fluid in specimens from which it had been previously removed

To investigate the effects of the heat generated by dry band arcings on the surface of EPDM, a series of experiments have been devised to simulate the condition. The specimens were subjected to temperatures of 50, 150, 240 and 380°C for different durations in the range of 0.5 to 11h in an attempt to simulate the heat produced by different levels of leakage currents and dry band arcings on insulators. The LMW fluid was first removed and then the specimens were placed in an electrical oven (60Hz). After heating for different durations, the samples were allowed to cool down and then immersed in analytical hexane for 96 h at 23±3°C. They were subsequently left in air at 23±3°C for 24h to allow a complete evaporation of the absorbed hexane. The weight difference before immersion in, and after complete evaporation of hexane is the amount of the fluid that has been extracted from the specimens. Fig.3.6 shows the amount of fluid in EPDM after heating for 1h. It can be seen that the production of fluid increased with increasing temperature for 1h of heating. At 50 and 150°C, small amounts of fluid of 0.13% and 0.14%, respectively were produced. At 240 and 380°C, there were significant increases in the amounts of fluid of 0.67% and 2.15%, respectively. The increase in the production of the fluid is due to the scissions of long molecular chains into short chains and the release of the trapped short chains from within the molecular structure [19,47,48]. These processes are enhanced with increasing temperatures. At 150°C and lower, the hydrolytic reaction is the main activity in the polymer [47]. At low temperatures the hydrolytic reaction is limited. Therefore, only a small amount of the fluid was produced

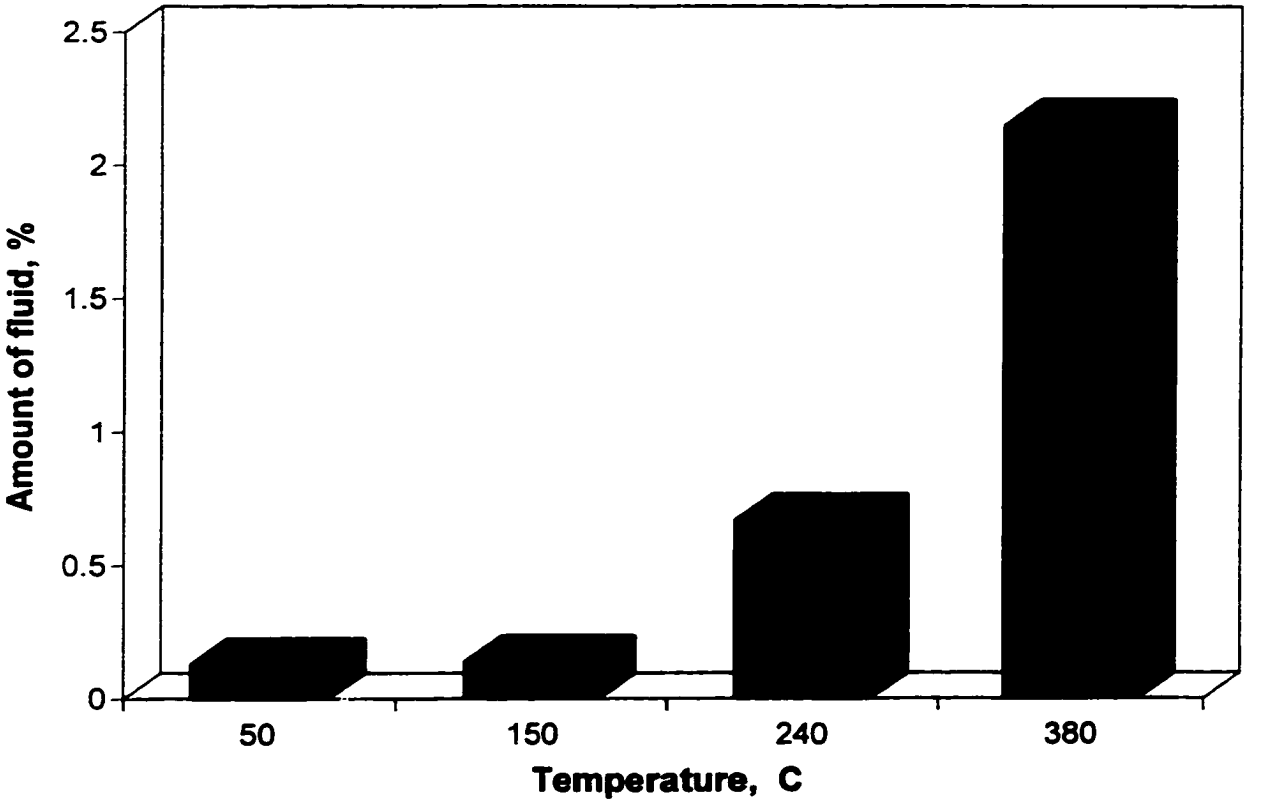

Figure 3.6 **Percentage weight of LMW fluid produced in EPDM as a function of temperature. Duration of heating 1h; specimens were devoid of fluid prior to heating**

at temperatures ≤150°C. At 240 and 380°C, the scission process is much more active. The scissions of long molecular chains increase significantly from oxidative reactions in the crosslinks [47]. Therefore the larger amount of the fluid found at 380°C is due to the oxidative reactions. Figs.3.7 and 3.8 show the amount of fluid that has been regenerated after the specimens were heated for 5 and 11 h, respectively.

From Figs.3.7 and 3.8, it can be seen that there was a significant decrease in the production of fluid at 380°C after 5 and 11h of heating compared to 1h (Fig.3.6). It is suggested that this could be due to the scissions of short molecular chains into volatile substances with increasing duration of heating which subsequently evaporated thus resulting in a reduction in the fluid remaining in the specimens. Because the loss and regeneration of LMW fluid take place concurrently during the heating process, it is suggested that at 380°C, the rate of loss of fluid due to its evaporation in the specimens, is faster than its rate of regeneration.

Figs.3.9 to 3.12 show the dependence of the fluid regenerated in the specimens as a function of the duration of heating at 50, 150, 240 and 380°C, respectively. In the specimens of Figs.3.9 to 3.12 the LMW fluid was first extracted using hexane. Fig.3.9 shows that the amount of the fluid produced after heating at 50°C for periods varying from 1 to 11h produced essentially the same amount of regenerated fluid of 0.135%±0.005%. Fig.3.10 shows that heating at 150°C resulted in a slight increase in the amount of the generated fluid from 0.14% to 0.18% after heating for 1h and 11h,

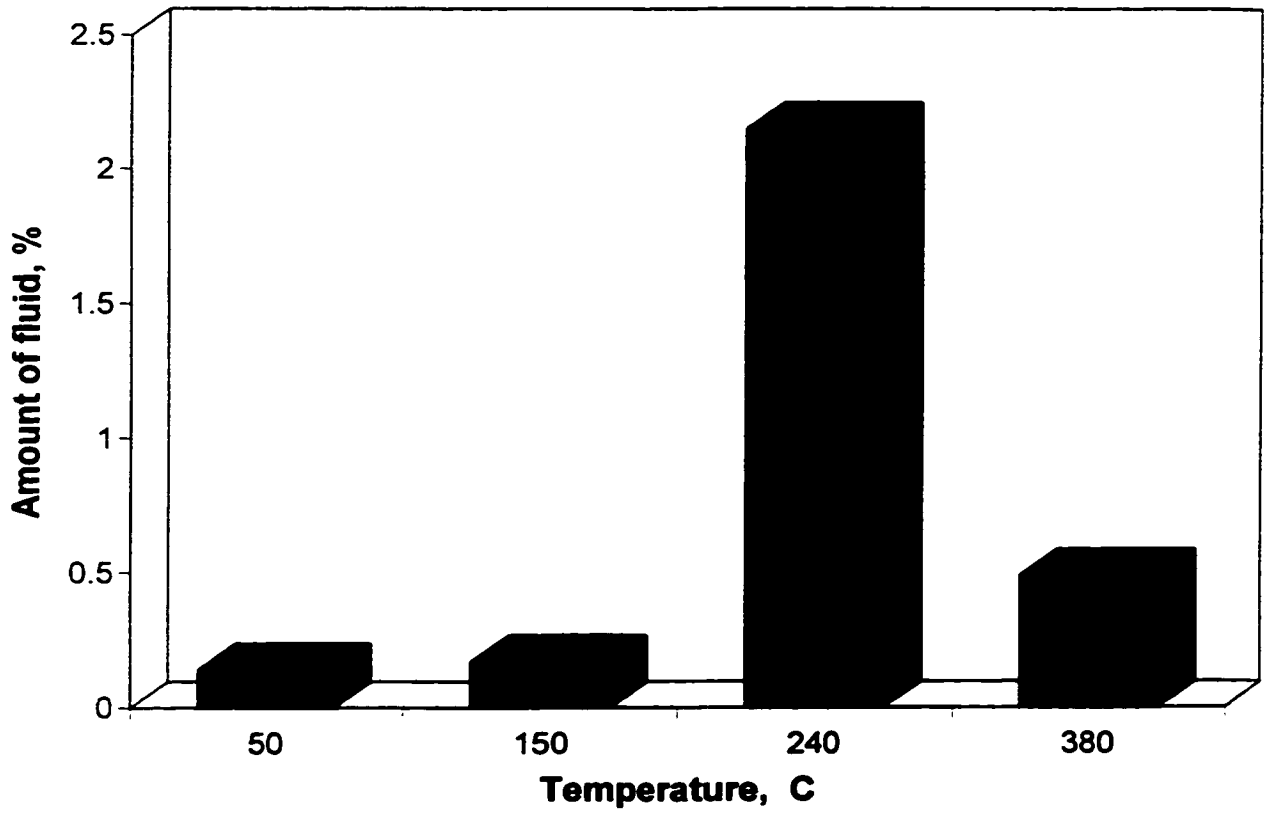

Figure 3.7 **Percentage weight of LMW fluid produced in EPDM as a function of temperature. Duration of heating 5h; specimens were devoid of fluid prior to heating**

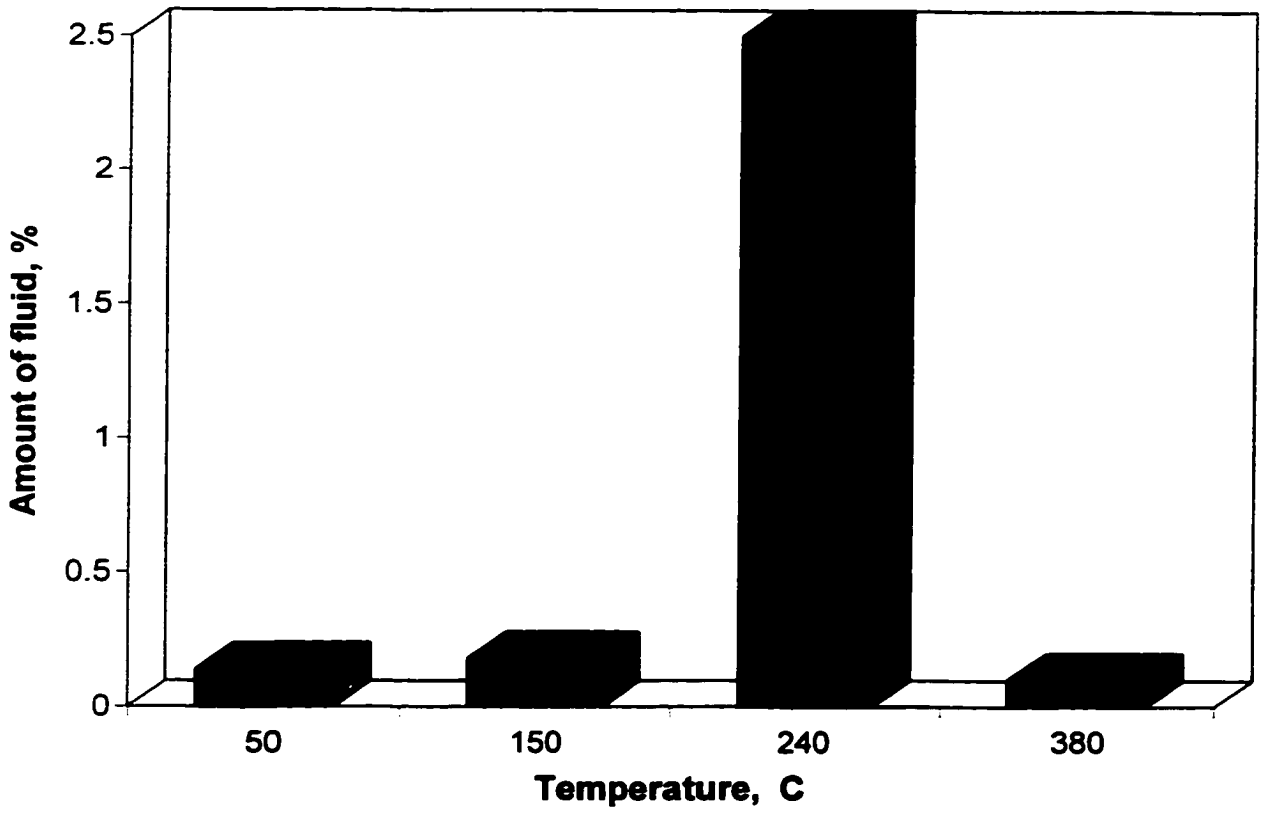

Figure 3.8 **Percentage weight of LMW fluid produced in EPDM as a function of temperature. Duration of heating 11h; specimens were devoid of fluid prior to heating**

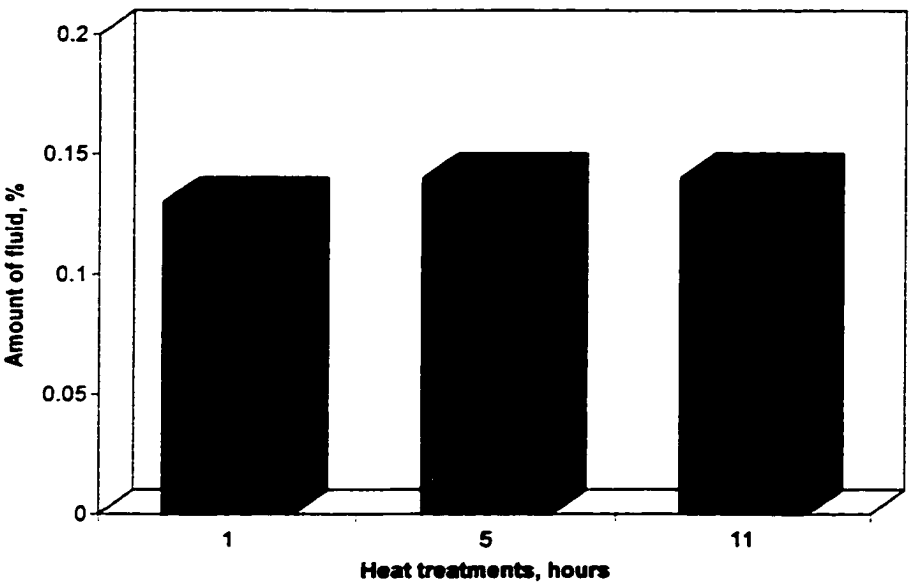

Figure 3.9 **Percentage weight of LMW fluid produced in EPDM as a function of duration at 50°C; specimens were devoid of fluid prior to heating**

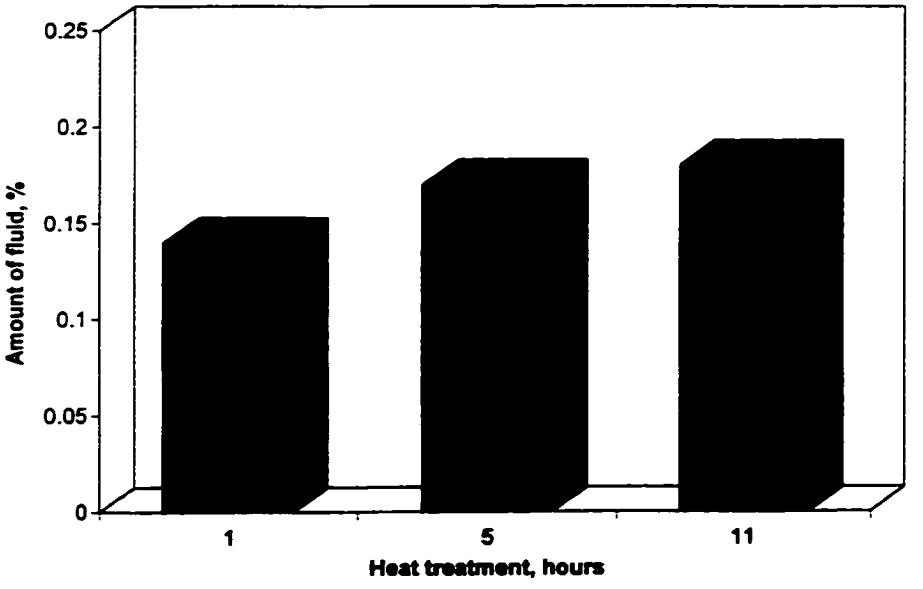

Figure 3.10 **Percentage weight of LMW fluid produced in EPDM as a function of duration at 150°C; specimens were devoid of fluid prior to heating**

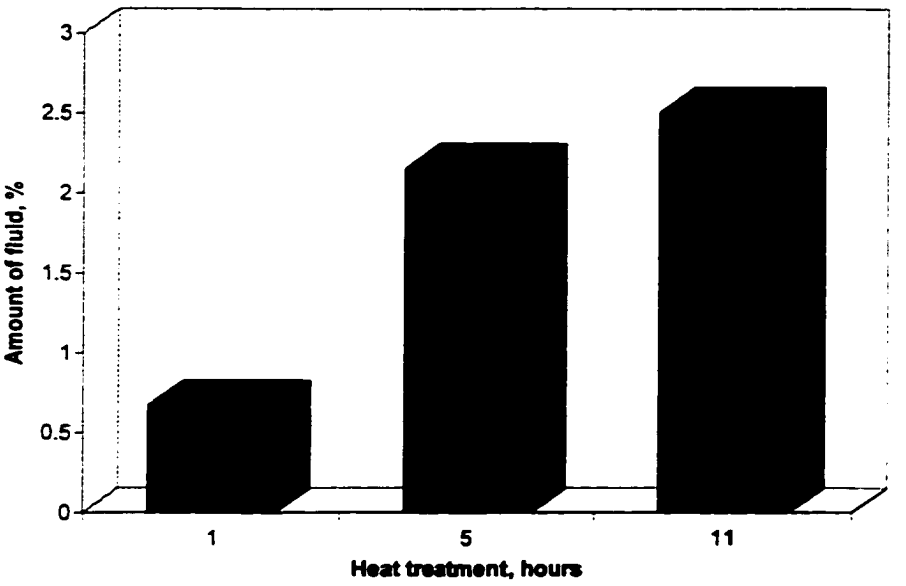

Figure 3.11 Percentage weight of LMW fluid produced in EPDM as a function of duration at 240°C; specimens were devoid of fluid prior to heating

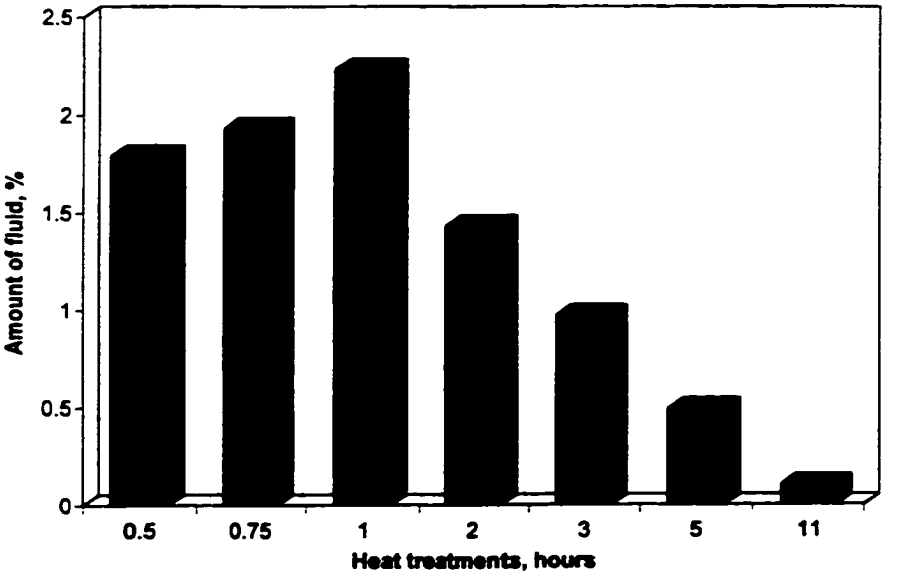

Figure 3.12 Percentage weight of LMW fluid produced in EPDM as a function of duration at 380°C; specimens were devoid of fluid prior to heating

respectively. Fig.3.11 shows a significant increase in the fluid from 0.67% to 2.5% after heating for 1 and 11h, respectively. Fig.3.12 shows that after 0.5h, 0.75h and 1h of heating at 380°C, the production of fluid was 1.79%, 1.93% and 2.23%, respectively. It will be observed from Fig.3.12 that the content of the fluid initially increased and then decreased with increasing durations of heating. After 2, 3, 5 and 11h heating at 380°C, the content of the fluid decreased to 1.43%, 0.97%, 0.49% and 0.1%, respectively. The initial increase in the regenerated fluid (Fig.3.12) was due to the enhanced scissions of the bonds and the release of the fluid from the bulk where it was regenerated. The loss of the fluid due to evaporation appears to be small, at short times (up to 1h) compared to the generated fluid. The decrease in the regenerated fluid is attributed to the evaporation of the volatile groups with increasing duration of heating (up to 11h) at 380°C (Fig.3.12).

Fig.3.13 shows a summary of the regeneration of the fluid in EPDM specimens, which were initially devoid of fluid as a function of time of heating at temperatures in the range 50-380°C. It will be observed that the most effective temperature for increasing the production of the LMW fluid within the range observed, is 240°C. At this temperature the net production of the fluid increases with increasing time of heating. At 380°C, the net production of the fluid decreases with time, and as stated above, is attributed to the increased evaporation of the generated fluid at the higher temperature.

3.7.2 Heat treatment of virgin samples

In order to compare the heating effects on virgin specimens and on those specimens from which the LMW fluid had been previously removed, virgin specimens were employed in

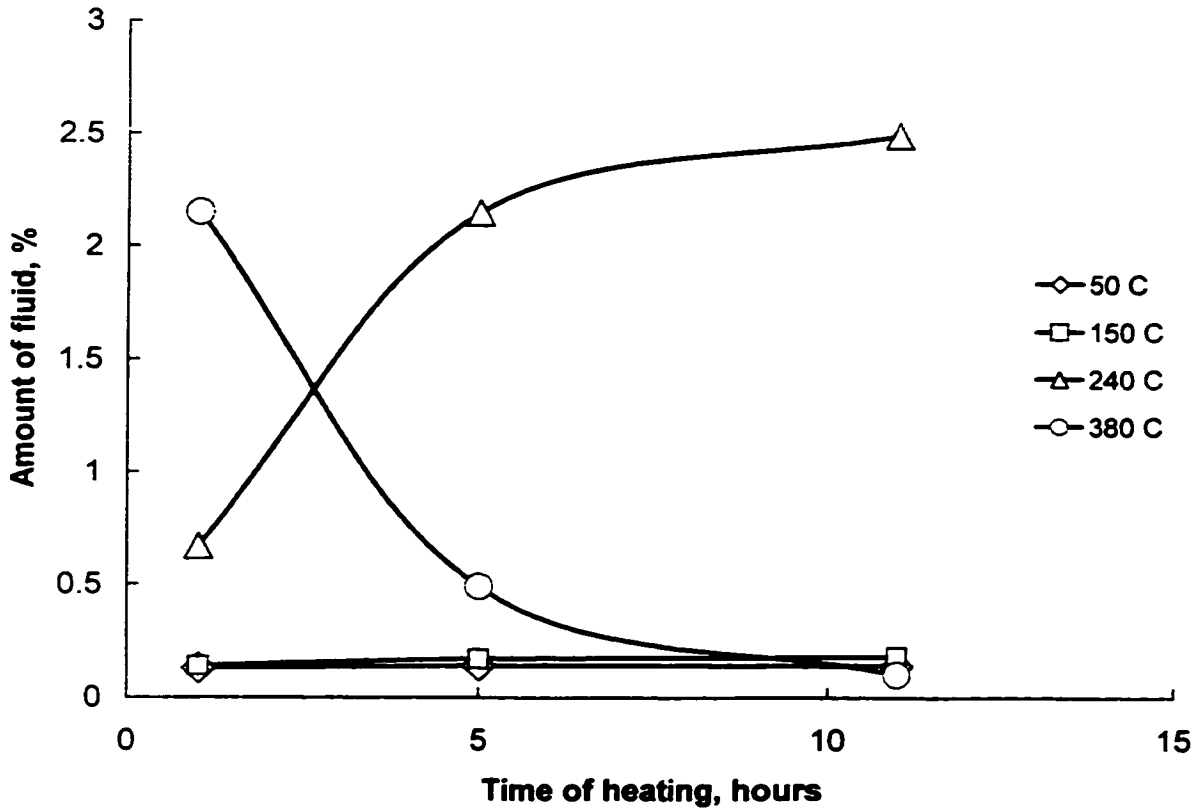

Figure 3.13 LMW fluid content in EPDM specimens as a function of heating time at different temperatures; specimens were devoid of fluid prior to heating

the following experiments. Figs.3.14, 3.15and 3.16 show the amount of LMW fluid in the virgin specimens, respectively, after heating for 1h, 5h and 11h at different combinations of oven temperatures. Figs.3.14 to 3.16 show the net amount of fluid due to the generation and the loss at different times and temperatures.

Fig.3.14 shows the measurements of the percentage weight of the LMW fluid in the specimens as a function of temperatures after 1h of heating. The weight of the virgin specimens was first measured before heating. After removal from the oven, the specimens were left in the air (for about 2min, at 50°C; 10min, at 240°C and 15min, at 380°C) to cool down to 23±3°C. The specimens were then immersed in hexane for 96h (Fig.3.1). Subsequently, they were left in air for a further 24h to allow the hexane to completely evaporate (Fig.3.2). The weight difference before immersion and after complete evaporation was the LMW fluid that was extracted. The content of the fluid in the virgin specimens was found to be (1.72±0.1)% which is depicted in Fig.3.14 at 23±3°C. It is shown in Fig.3.14 that after heating at 50 and 150°C for 1h, the content of the fluid was 1.72% and 1.68% respectively. Thus either the loss and generation of LMW fluid at temperature up to 150°C were both negligibly small or the generation of the new fluid was balanced by the loss due to evaporation. Fig.3.14 shows that heating for 1h at 240 and 380°C, an increase in the content of the fluid to 2.08% and 2.61%, respectively, was found. Figs.3.15 and 3.16 show the fluid content after heating virgin specimens for 5h and 11h, respectively. Fig.3.15 shows that after heating at 50, 150, 240 and 380°C for 5h, the content of the LMW fluid was 1.68%, 1.76%, 2.29% and 0.67%, respectively.

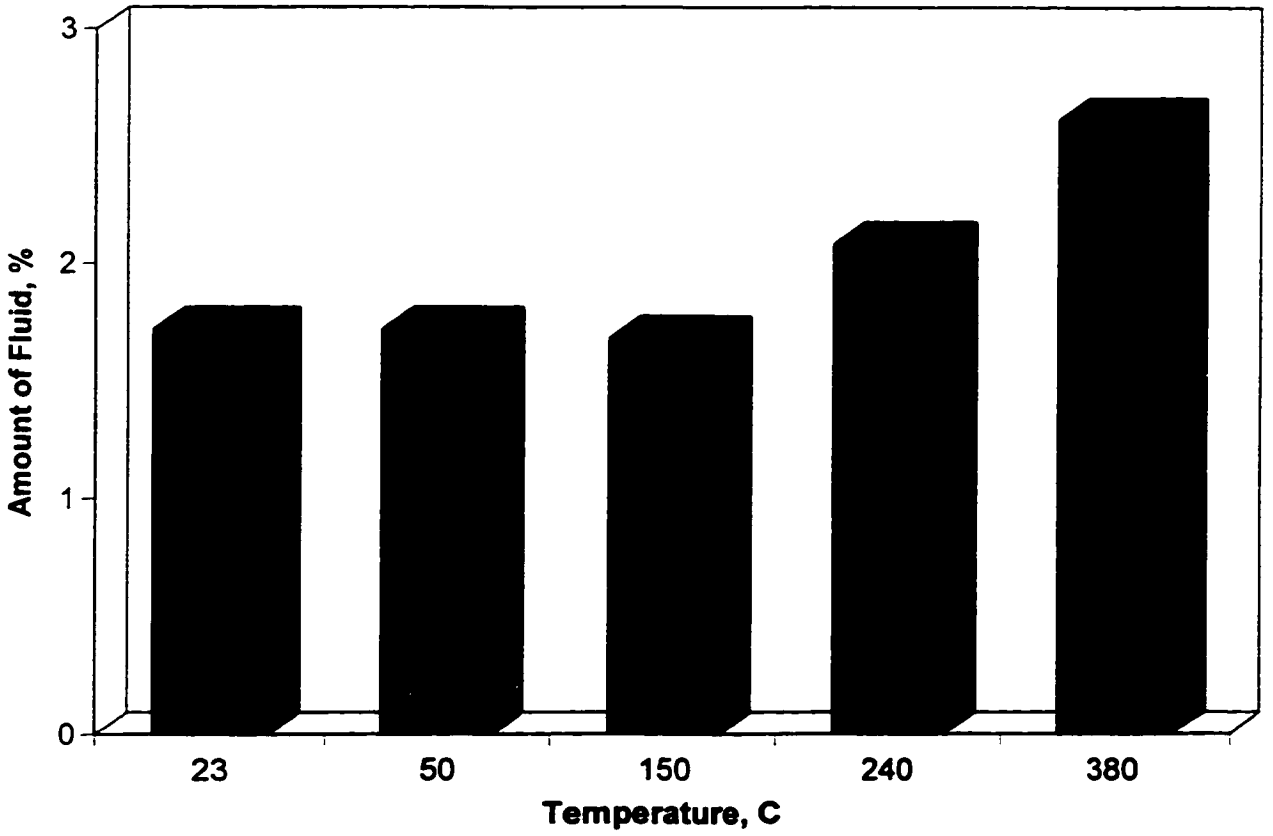

Figure 3.14 Percentage weight of LMW fluid in virgin EPDM after heating at different temperatures for 1h

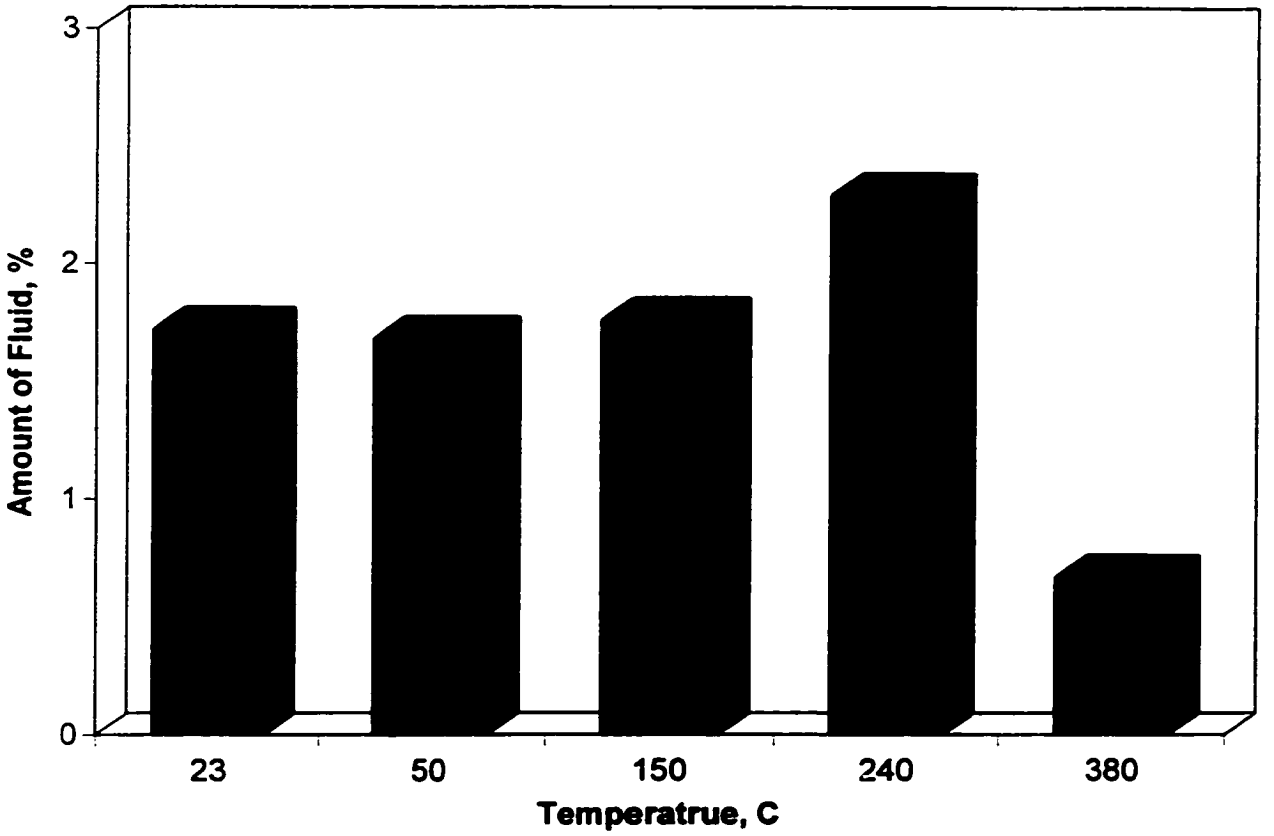

Figure 3.15 **Percentage weight of LMW fluid in virgin EPDM after heating at different temperatures for 5h**

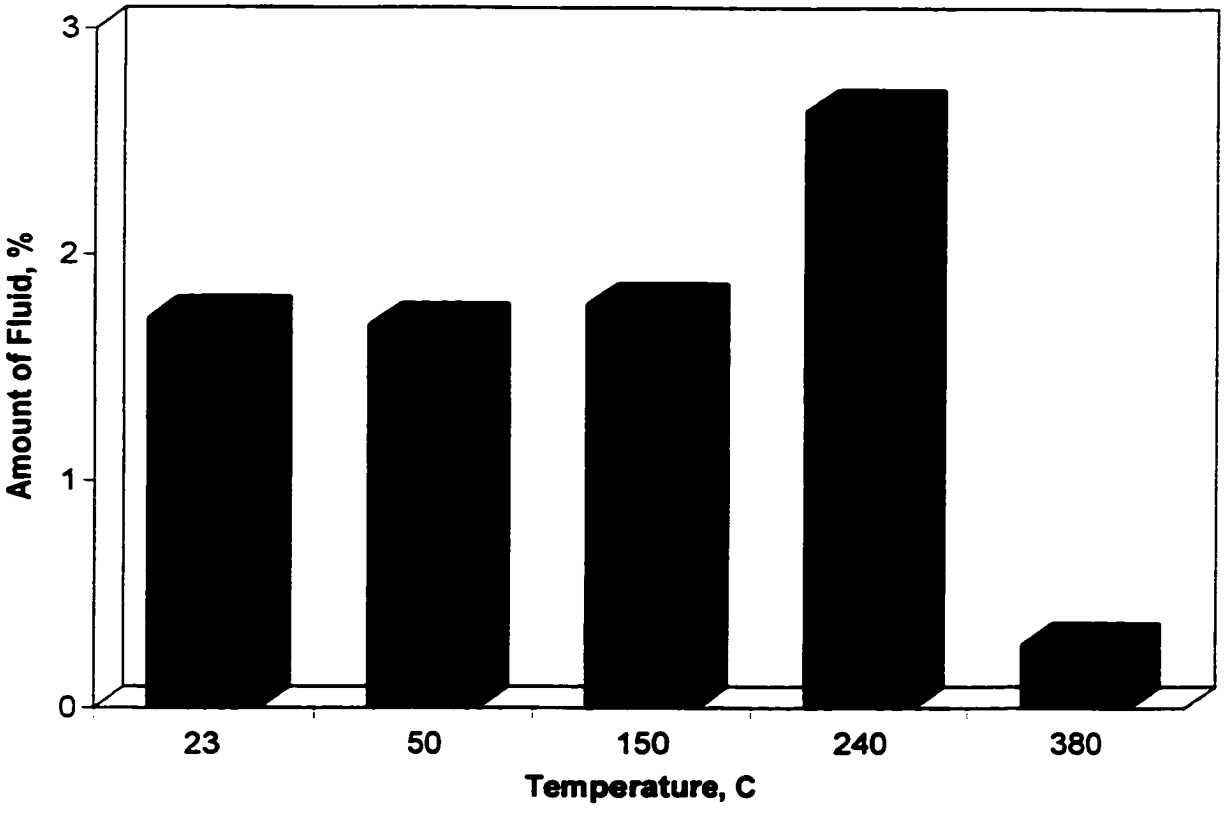

Figure 3.16 **Percentage weight of LMW fluid in virgin EPDM after heating at different temperatures for 11h**

Fig.3.16 shows that after heating for 11h at 50, 150, 240 and 380°C, the LMW fluid content was 1.69%, 1.78%, 2.64% and 0.28%, respectively.

Fig.3.17 shows the fluid content as a function of time of heating for up to 11h, in the temperature range 23 to 380°C. It is evident from Fig.3.17 that the amount of the fluid continued to increase at 240°C with increasing heating time up to 11h. At 380°C, the fluid content initially increased from 1.72 to 2.61% up to 1h and then steadily decreased. This suggests that the loss of the fluid possibly due to evaporation at 380°C, is higher than its regeneration for long duration (>1h) of heating(Fig.3.17).

Since it was found that the content of the LMW (1.72±0.1)% in virgin specimens of EPDM was independent of the sample volume (Fig.3.4). This value was subtracted from Fig.3.14, and the result is replotted in Fig.3.18. Comparing Fig.3.18 and Fig.3.6 shows that more LMW fluid was produced when the original fluid had already been removed (Fig.3.6) before heating than when it was not (Fig.3.14). This is either because more space was provided between the molecular chains for the regeneration process after removing the original fluid or because when the fluid had been left in (Fig.3.14) it evaporated during heating and therefore the net amount of the fluid was less. Therefore more fluid was found after heating in the specimens which were devoid of fluid (Fig.3.6) than in the virgin specimens (Fig.3.14 and 3.18).

A further investigation was carried out at 550°C. It was found that after heating for 1h the surface of the EPDM specimens melted and then disintegrated. A white residue was seen

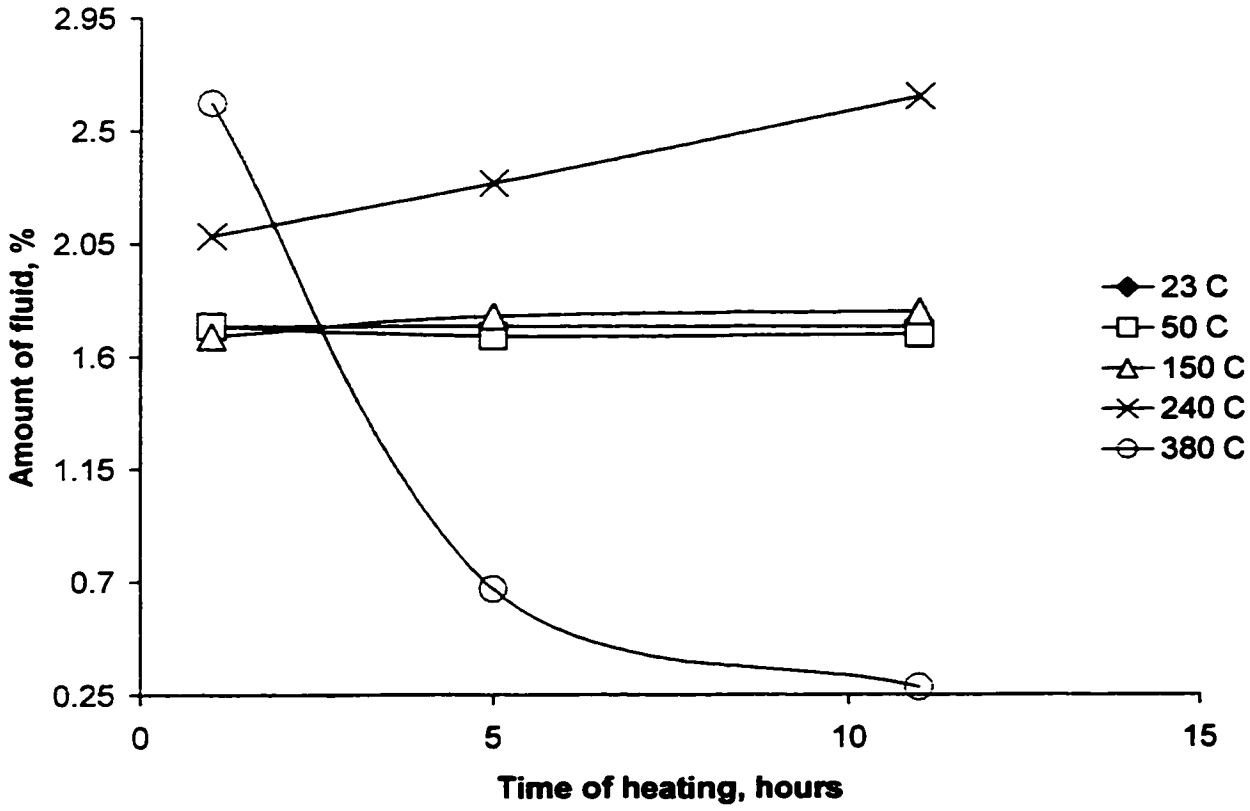

Figure 3.17 **LMW fluid content in virgin specimen of EPDM as a function of heating time at different temperatures**

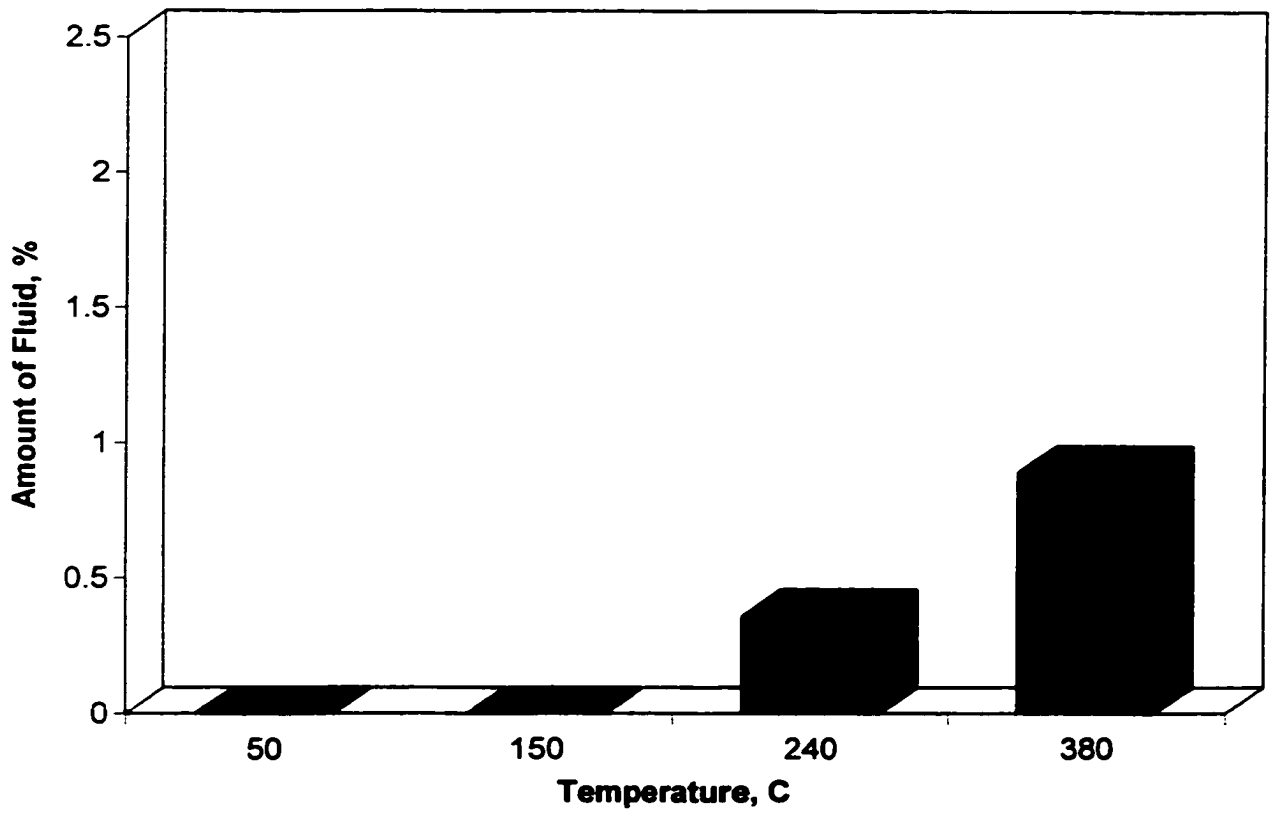

Figure 3.18 As for Fig.3.10 but subtracting the original amount of fluid present in the virgin specimen of 1.72%

to adhere to the container after cooling down. The color of the specimens changed from dark grey to white. The specimen was very brittle after heating, and it disintegrated into a white powder with even a light touch. It was obvious that 550°C was beyond the withstand capability of the EPDM rubber.

3.8 Laser beam treatment

3.8.1 Introduction

Another method of applying heat to the specimens was by using a laser beam. The surface of the specimens was irradiated with a high energy pulse from a laser beam. The heat generated by this method was intended to simulate the condition of intermittent dry band arcing in which the arc location varied continuously on the surface, due to its inherent instability on the surface of the insulator. An Argon laser system (model INNOVA 100-10) having 514nm, average output power 1.0W and different durations was used to vary the output energy impacting on the specimens surface. The energy range varied from 28.8 to 654J. The area of the laser spot was measured by taking a magnified (x10) photographs and measuring its size.

3.8.2 Content of LMW fluid

Fig.3.19 shows the production of the amount of the LMW fluid as a function of the laser beam energy. The mobile LMW fluid was first completely removed from the EPDM specimens before the laser beam treatment. It was found that the amount of the fluid varied in the range 0.28-0.49% with the varying laser energy from 28.8 to 654J. The laser beam did not penetrate the whole volume and did not cover the whole area of the

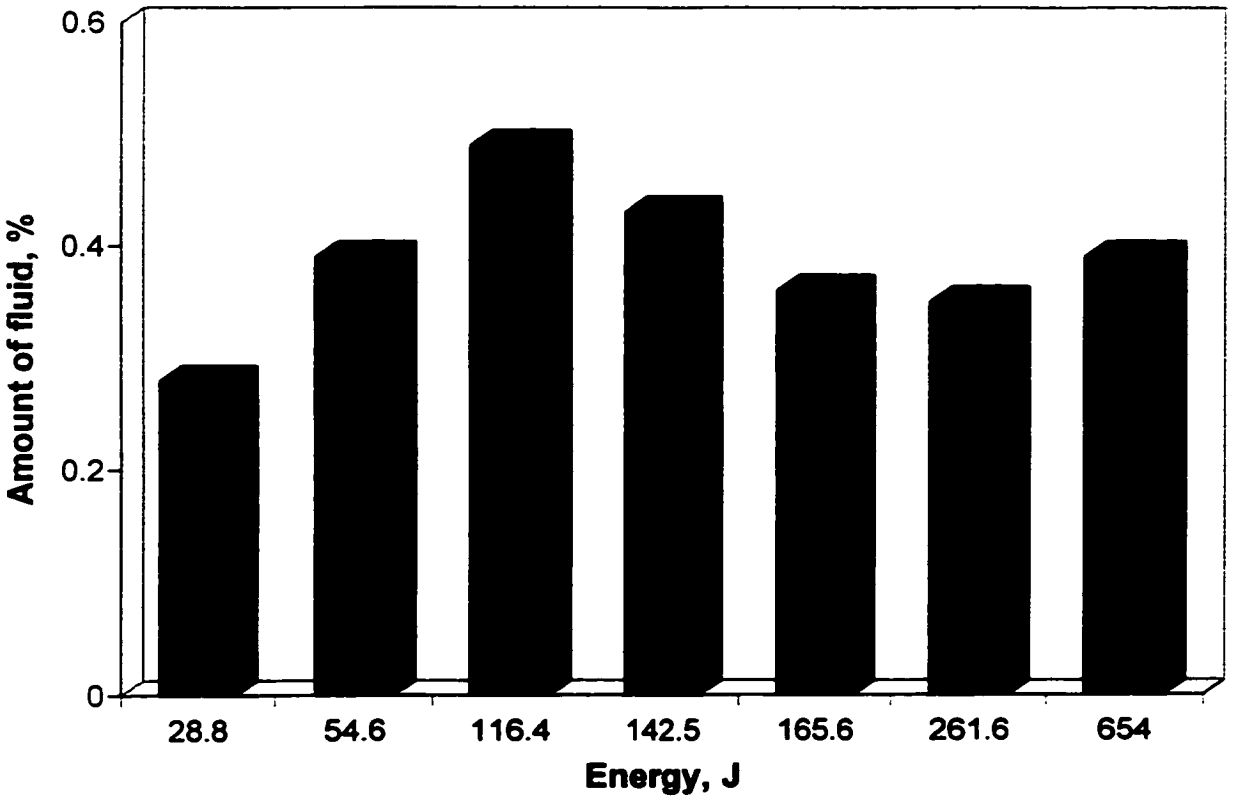

Figure 3.19 **Percentage weight of LMW fluid produced in EPDM as a function of laser energy applied to the surface. Specimens were devoid of fluid prior to laser application**

specimens. For each energy depicted in Fig.3.19 one shot was used. The area covered by the beam was about 0.149% ± 0.024% of the total area of the specimens. The energy was varied by adjusting the time of application and the power of the laser. The amount of the fluid produced may be described as independent of the beam energy at 0.385±0.105% (Fig.3.19). This experiment indicated that the LMW fluid can be reproduced using also heat generated by a laser beam.

Fig.3.20 shows the LMW fluid as a function of the laser energy produced in virgin specimens. In these specimens the fluid was not removed prior to subjecting them to irradiation by the laser beam. The fluid which was found after the laser beam treatment varied by only small amount in the range 1.7%-1.79% for the energy range 28.8-654J (Fig.3.20). The production of the fluid was negligibly small because of only small area of the specimen (0.126~0.173%) from the total area was subjected to heating by the laser beam.

Fig.3.21 shows that the net LMW fluid produced in virgin specimen after subtracting from Fig.3.20 the original amount of 1.72%. A comparison between Fig.3.19 and Fig.3.21 shows that more fluid was produced after laser bombardment in specimens where the fluid was first removed using hexane. This is also consistent with similar findings in specimens heated in an oven (Fig.3.18). The suggested reason for the phenomenon is the same as in the previous case in that more inter-molecular space was available in the specimen devoid of oil to enable the regenerated fluid to move freely into the hexane solution.

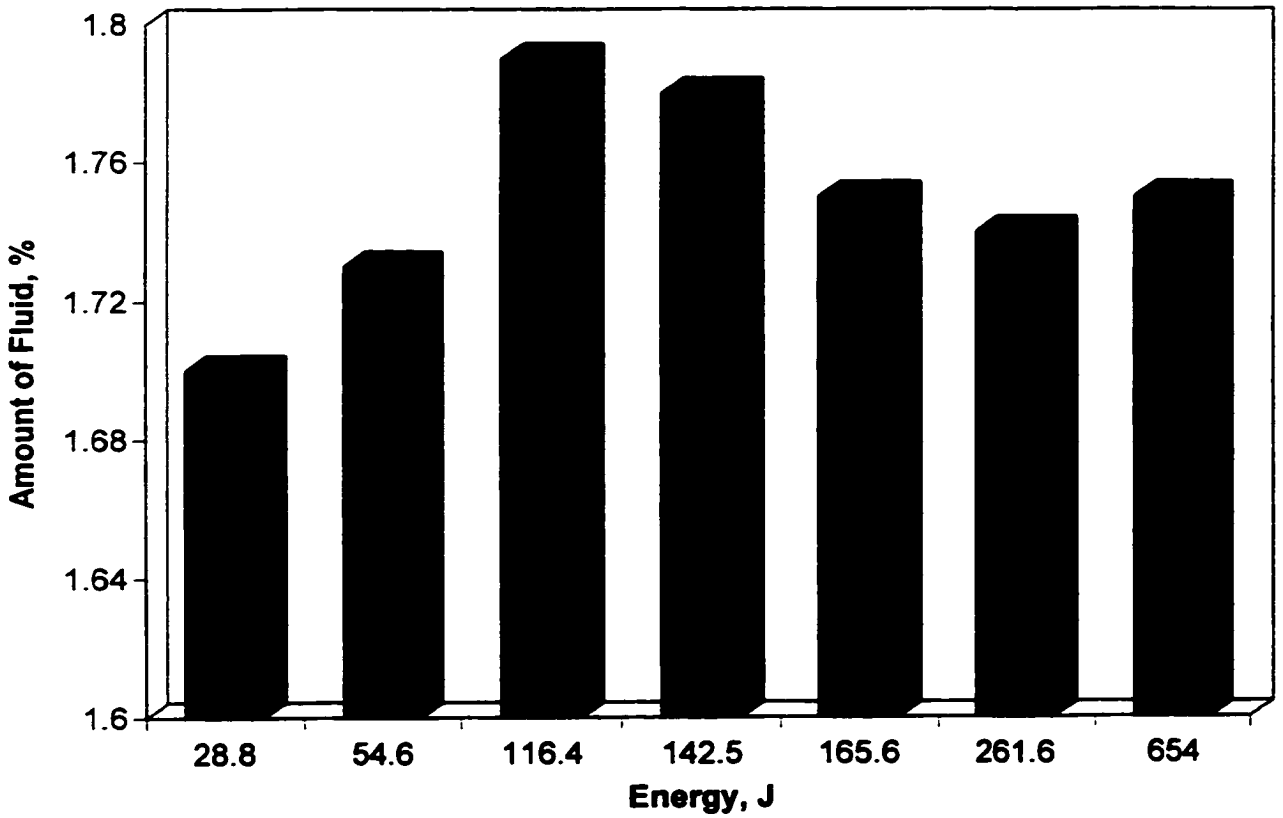

Figure 3.20 **Percentage weight of LMW fluid in virgin EPDM as a function of laser energy applied to the surface**

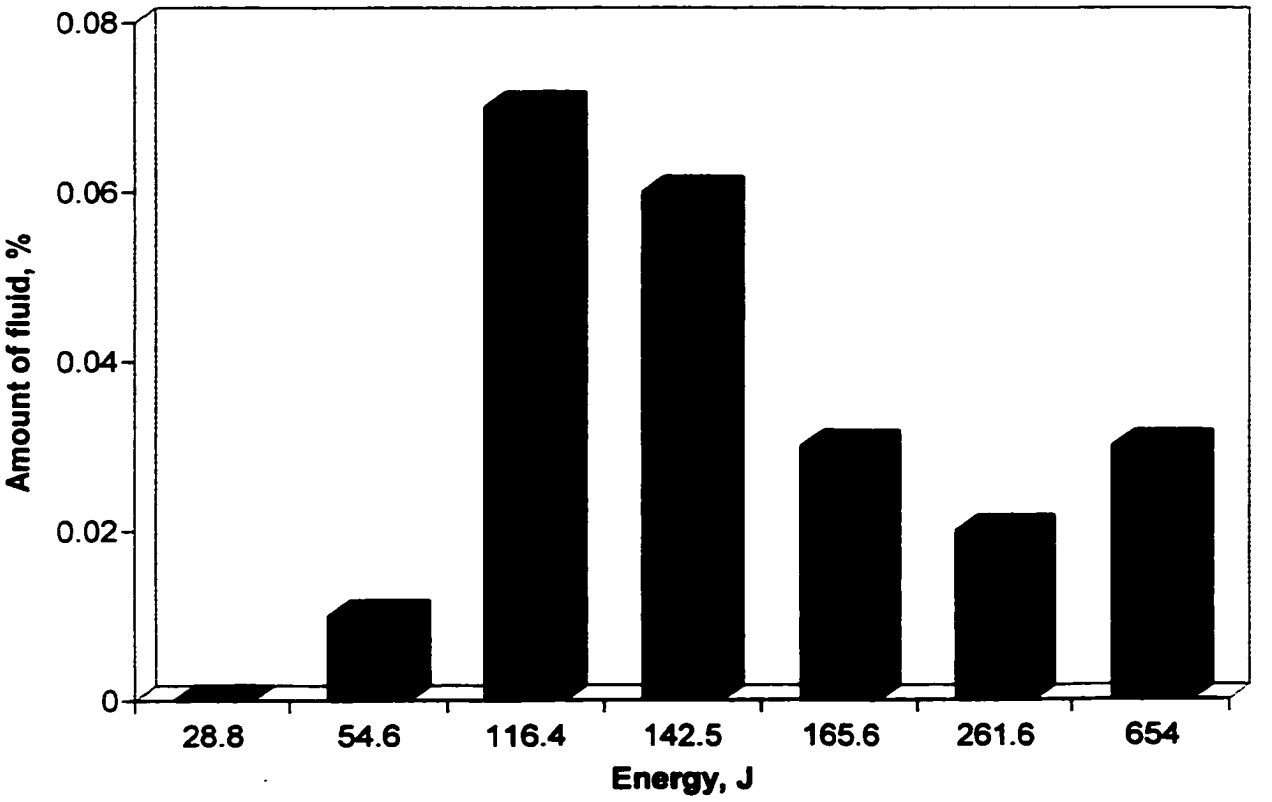

Figure 3.21 **As for Fig.3.16 but subtracting the original amount of fluid present in the virgin specimen of 1.72%**

Fig.3.22 shows the amount of fluid produced as a function of the number of the laser beam shots in EPDM specimens from which the fluid was previously removed. In each shot, the power was controlled at 1.05W, and a duration of 180s was applied. The surface area covered by each laser beam was about $0.149\pm0.024mm^2$ which was about $(0.149\pm0.024)\%$ of the total area of each specimen. Fig.3.22 shows that there is no correlation between the amount of fluid produced and the number of applications of the laser beam to the surface. The amount of fluid produced varied from 0.38% of the total volume of the specimens after one application of laser bombardment to 0.4% after 6 applications.

Fig.3.23 shows the effects of multiple laser beam shots applied to virgin EPDM specimens from which the fluid was not removal prior to laser treatment. The experimental conditions were the same as in Fig.3.22. Fig.3.23 shows that the total content of the LMW fluid after 1,2,3,4 and 6 shots were 1.78%, 1.89%, 1.82%, 1.83% and 1.85%, respectively. This suggests a very weak, or no correlation, between the amount of fluid produced and the number of applications of the laser beam to the EPDM.

3.9 Decomposition of alumina trihydrate (ATH) filler

3.9.1 Introduction

In order to achieve a desired performance and a long service life in outdoor usage, and also to reduce the cost, lower cost fillers are blended in during the manufacture process. Depending on the specific formulation, fillers and additives can comprise of the order of 20% to 80% by weight of the formulation. In the extreme case of 80% fillers and other

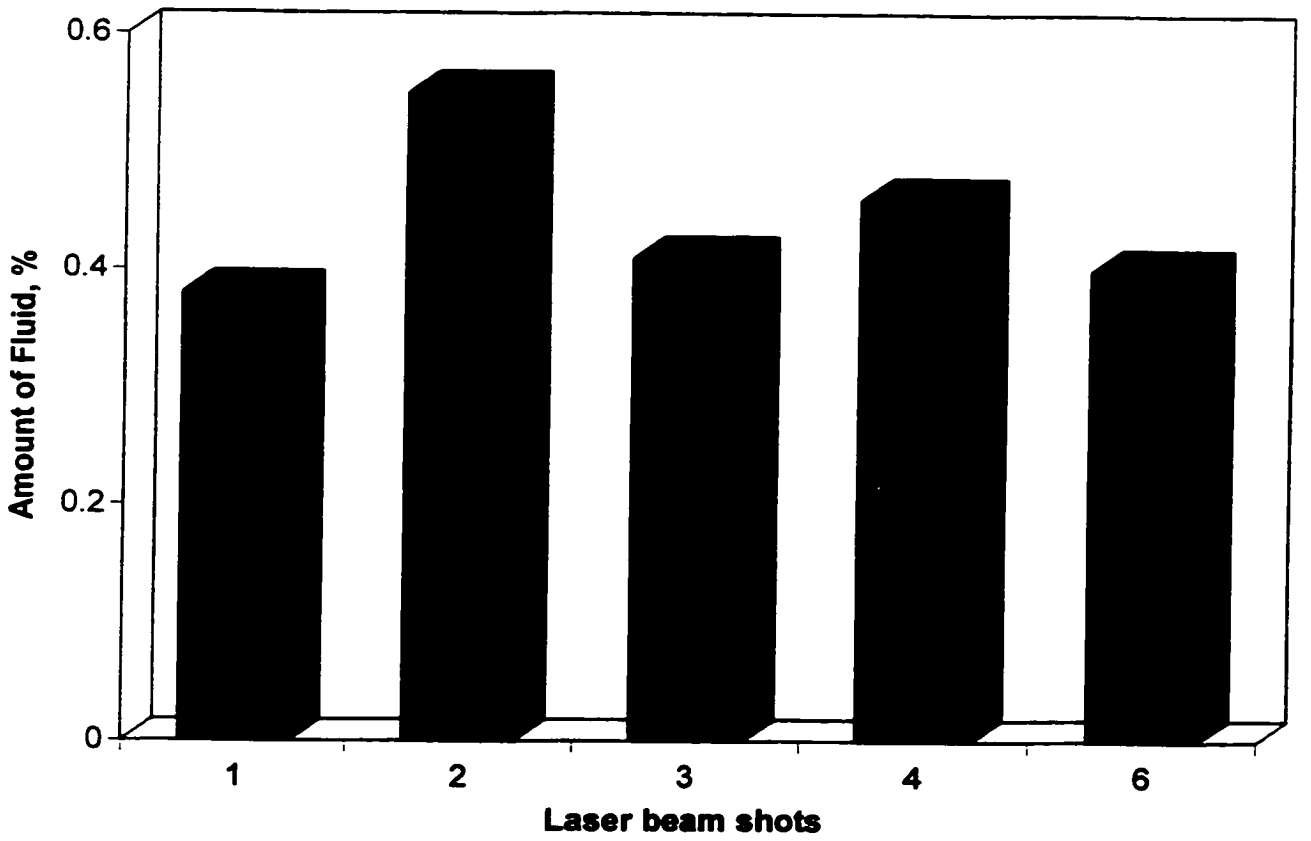

Figure 3.22 **Percentage weight of LMW fluid produced in EPDM as a function of laser beam shots. Specimens were devoid of fluid prior to bombardment**

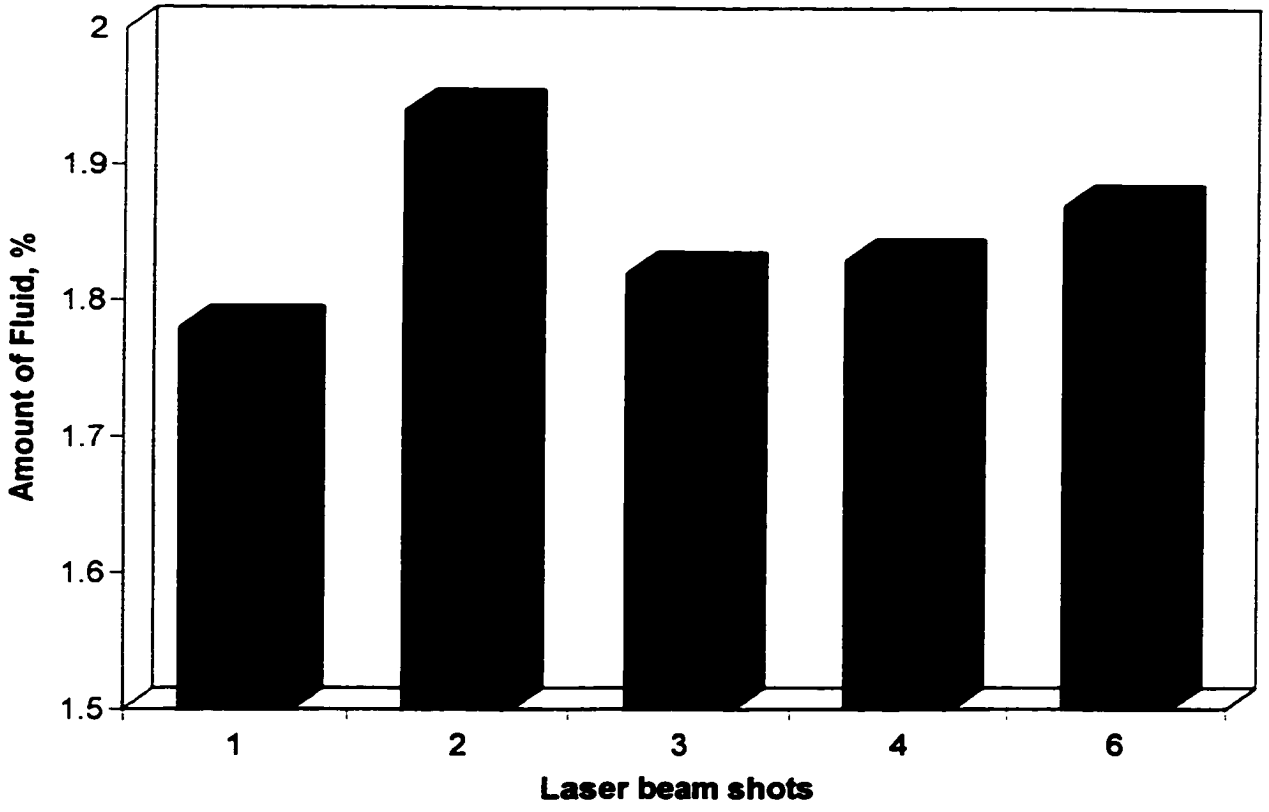

Figure 3.23 **Percentage weight of LMW fluid in virgin EPDM as a function of laser beam shots**

additives, only 20% by weight of the formulation is the base polymer. With such a range of base polymers and a variation in polymer grades, it is clear that polymer materials with the same base polymer are not identical. The combination of fillers and other additives works together as a system to reinforce the mechanical and/or electrical properties. Typical extending and reinforcing fillers include UV stabilizers, processing aids, cure agents, flame retardant, tracking and erosion resistors.

The EPDM samples used in the present work contained 200 parts of alumina trihydrate (ATH) filler per hundred (pph) of the polymer base by weight (200/300)*100=0.67%. The ATH is used to impart resistance to tracking and erosion. During the prolonged heating of EPDM specimens in the oven, at high temperatures, several processes exist simultaneously including regeneration and loss of LMW fluid, decomposition of the alumina trihydrate and evaporation of other volatile groups. Fig.3.24 shows the weight loss of specimens from which the LMW fluid was first extracted, after 1h heating at different temperatures. Fig.3.25 shows the weight loss of virgin specimens (fluid was not previously removed) after 1h heating at different temperatures. It can be seen from Fig.3.24 and 3.25 that the weight loss increases with the increasing temperatures. Fig.3.24 shows the percentage weight losses after heating for 1h at 50, 150, 240 and 380°C were 0.09%, 0.69%, 2.75% and 24.87%, respectively. It has been reported that heating at above 220°C causes the ATH to endothermically decompose into alumina and water[48-50].

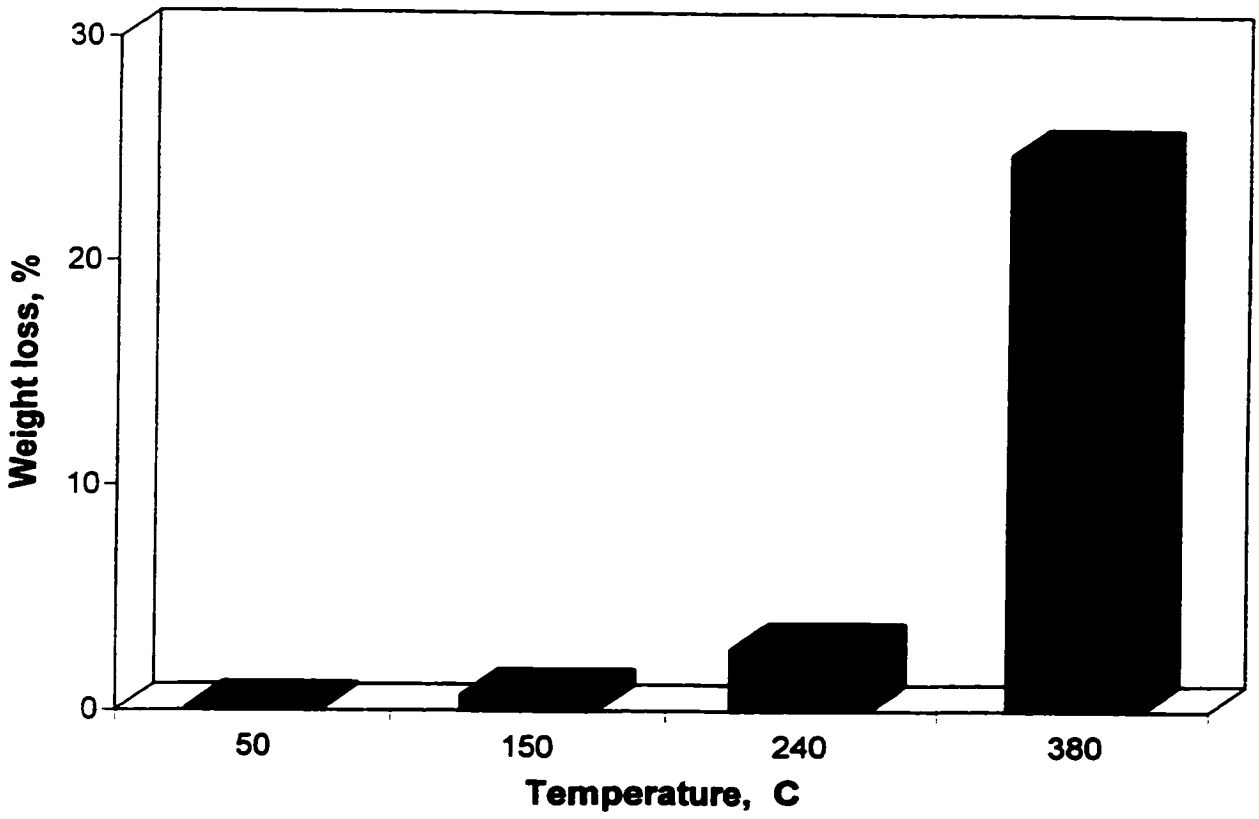

Figure 3.24 Percentage weight loss of EPDM subsequent to heating for 1h at different temperatures. specimens were completely devoid of fluid prior to heating

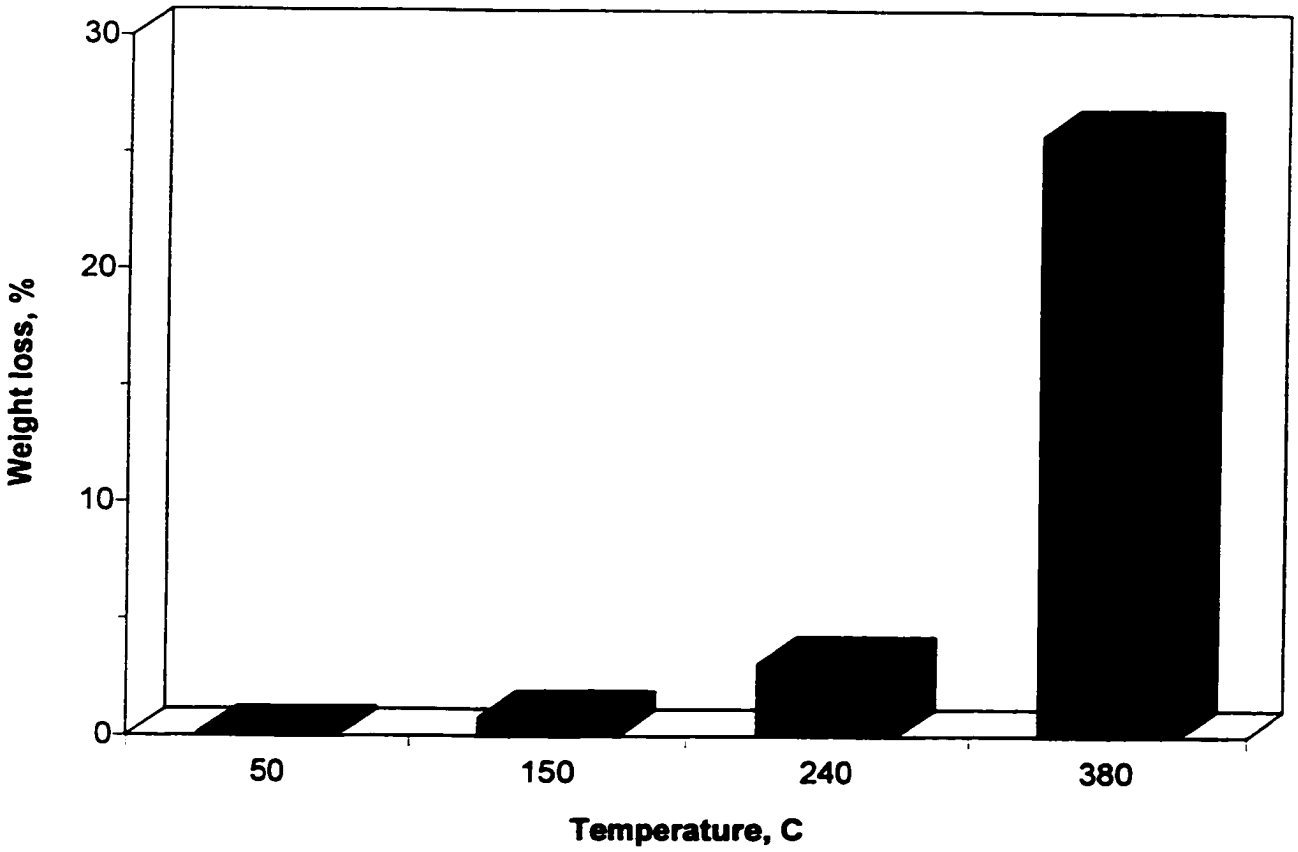

Figure 3.25 **Percentage weight loss of virgin EPDM subsequent to heating for 1h at different temperatures**

$$Al_2O_3\ 3H_2O \rightarrow Al_2O_3 + 3H_2O$$

The maximum theoretical loss of water in the ATH is 34.6%.

$$(3H_2O / Al_2O_3 \bullet 3H_2O = 54 / 155.96)$$

In the present study, the EPDM rubber used contained 200 pph ATH (66.7%). Therefore for a complete decomposition of the filler the theoretical weight loss is 23.2% (34.6%*66.7%). Our measured value was 24.8% at 380°C, which is in reasonable agreement with the theoretically predicted value. Fig.3.25 shows the weight losses in virgin samples were 0.11%, 0.78%, 3.1% and 25.78% after heating at 50, 150, 240 and 380°C, respectively. The slightly larger losses in the virgin specimens (Fig.3.25) compared to those when the LMW fluid was first removed (Fig.24) could be due to the larger losses of the LMW fluid from the virgin specimens.

CHAPTER IV

INVESTIGATION OF SURFACE HYDROPHOBICITY

4.1 Introduction

The main problem with porcelain and glass insulators is that the surface can easily be wetted. Therefore, leakage current may develop after accumulation of airborn contaminants, which leads to flashover and an outage in the power system. The flashover of insulators is a major practical limitation to achieve a reliable supply of electrical power and it could be very costly when purchasing of replacement power is necessary. A flashover in a substation might result in a destruction of an insulator, circuit breaker lock-out and potential damage to equipment. Therefore the wettablity of the insulator material is a critical factor during outdoor service of insulators.

The flashover of contaminated insulators has raised serious concerns for many years. Due to its complexity, the problem is still not well understood. There is still insufficient information available to explain the entire chemical and physical processes that would be involved in the flashover phenomena in contaminated and wetted insulators. Recently there has been much reported interest in the study of the surface effects of insulators and the relation to their electrical performance[51-57].

The wettability of a material is related to its surface free energy. Solid materials can be characterized either as having high-energy surface or low-energy surface. A material with a high energy surface is easily wetted and allows the spread over of water droplets on the

surface into a continuous film and therefore it is hydrophilic. For high voltage insulators, in order to minimize the leakage current and the consequent possibility of flashover, the surface must be of a low energy. This prevents the formation of a continuous water film on the surface, and therefore it is hydrophobic. Glass and porcelain have high-energy surface and are easily wetted. Some polymeric materials such as silicone rubber and EPDM have been recognized to have low-energy surface and thus possess good water repellency[58-60].

The contact angle is defined as the angle between the tangent to the water droplet on the surface and the horizontal plane. It gives an indication of the surface hydrophobicity. The measurement of the contact angle is relatively simple. The contact angle measurement provides an indication of the changes in the composition of the outer boundary of the surface. The measurement of the contact angle has been widely accepted to give a measure of the hydrophobicity of the surface [19-21,26,27,31,61-63].

In this chapter, the Young relationship between the contact angle and the surface free energy is given. The contribution of the changes in the molecular structure of the surface of EPDM rubber to the loss and recovery of hydrophobicity is presented. The measurements of the contact angle after subjecting the specimens to different levels of heat in an electrical oven and to laser beam bombardment are described.

4.2 Relationship between the contact angle and the surface tension

The contact angle is based on an equilibrium in a solid-liquid-air (three phases system). The angle occurs at the contact point of solid, liquid and air. If the system is at rest, a static contact angle is obtained. If the system is in motion, a dynamic contact angle is obtained[64]. In the present study the static contact angles were studied. The measurements of the contact angle were made in a stable and on a flat surface. Stable equilibrium would be obtained if the solid surface is smooth, homogeneous, planar, and nondeformable; the angle formed is the equilibrium contact angle. On the other hand, if the solid surface is rough or compositionally heterogeneous, the system may reside in one of many metastable states, the angle formed is a metastable contact angle [64,65].

In order to study the equilibrium phenomena, the solid, liquid and interfacial free energy, the concepts of energy of cohesion (W^c), energy of adhesion (W^a), and the free energy per unit area (γ) are now considered[31,32,66]. The surface tension (or surface free energy) per unit area, γ, is a measure of the attractive intermolecular forces between the solid surface and the liquid phase. It can be expressed as $\gamma=(\partial G/\partial A)_{T,P,N}$[66]; G is Gibbs free energy of the total system; A is the interfacial area; T is the temperature; P is the pressure; and N is the total number of moles of matter in the system.

The surface tension of a liquid or solid (γ) could be separated into two terms. For water, the surface tension consists of two components: $\gamma= \gamma^d + \gamma^p$, where superscript d is the London dispersion interaction and p is the hydrogen bonding. The fundamental problem associated with the contact angle equilibrium can be divided into two groups: those related to the structure and the constitution of the solid surface, and those related to the

mutual interactions of the three phases in the close vicinity of the contact line[67]. The mutual interactions phenomena is considered now. A schematic diagram of the system is shown in Fig.4.1. The contact angle is dependent on the solid surface free energy, and it is also related to the wettbility of the solid surface.

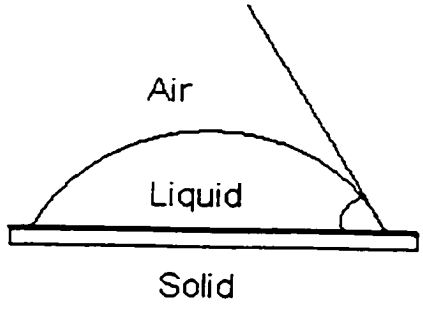

Fig.4.1 A schematic diagram of the system: A drop of liquid on a solid surface

4.2.1 Young equation for equilibrium contact angle

The Young equation for the equilibrium contact angle θ of a liquid l on a plane s in the saturated vapor of the respective liquid is expressed as [32]

$$\gamma_{lv}\cos\theta = \gamma_{sv} - \gamma_{sl}$$

Where γ_{lv} is the liquid surface tension (or surface free energy); γ_{sv} the solid surface tension in the presence of the vapor; and γ_{sl} the interfacial tension. The Young-Dupre equation for W_a in the presence of vapor becomes

$$W_a = \gamma_{lv}(1+\cos\theta)$$

Where W_a is the total energy of adhesion, which is the decrease of the Gibbs free energy change per unit area when an interface is formed from two individual surfaces. Simply it can be defined just as the energy required to separate reversibly the interface between two bulk phases from their equilibrium. It also can be expressed as [68]

$$W_a = \gamma_{sv} + \gamma_{lv} - \gamma_{sl}$$

or

$$\gamma_{sl} = \gamma_{sv} + \gamma_{lv} - W_a$$

For a liquid-solid system, it is only interacted by the dispersion forces only. The dispersion component of the energy of adhesion may be written according to the Young-Fowkes equation, as [68]

$$W^d_a = 2 (\gamma^d_{lv} \gamma^d_{sv})^{1/2}$$

In the presence of vapor, the equilibrium contact angle can be expressed as

$$\cos\theta = -1 + 2[(\gamma^d_{sv})^{1/2} (\gamma^d_{lv})^{1/2} / (\gamma_{lv})]$$

γ^d_{lv} and γ^d_{sv} stand for the London dispersion of the surface free energy of liquid-vapor and solid-vapor, respectively. The lower the surface energy, the larger is the contact angle. In this case, usually the contact angle is larger than 90° and the surface is hydrophobic. The hydrophobic and hydrophillic conditions are shown in Fig.4.2.

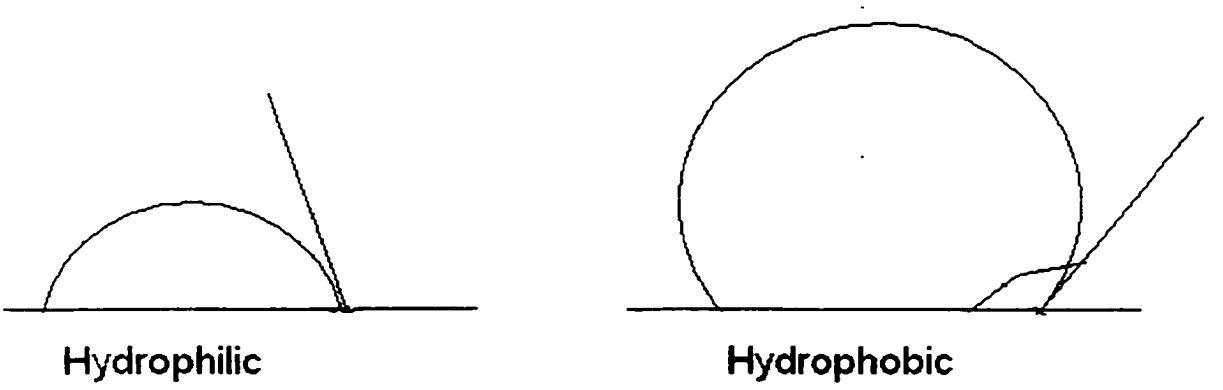

Fig.4.2 A diagram of hydrophilic and hydrophobic surface

4.3 The Contribution of Hydrophobic Groups to Contact Angle

Many synthetic polymers have intrinsically hydrophobic surface, i.e. they show a high contact angle of above 90°, usually on fluoro- and hydrocarbon-based polymers. Hydrocarbon is regarded as one of the hydrophobic groups. The low molecular weight fluid in EPDM has been identified in this study to be mainly made up of PDMS structure. The main compositions are hydrocarbon methyl groups (CH_3), silicon (Si) and oxygen (O). The reorientation or migration of the methyl groups can minimize the surface energy and is facilitated by the local motion of the polymer chains. Therefore, the reorganization of the polymer surface is especially rapid if the molecular mobility of the polymer chains is rapid [37].

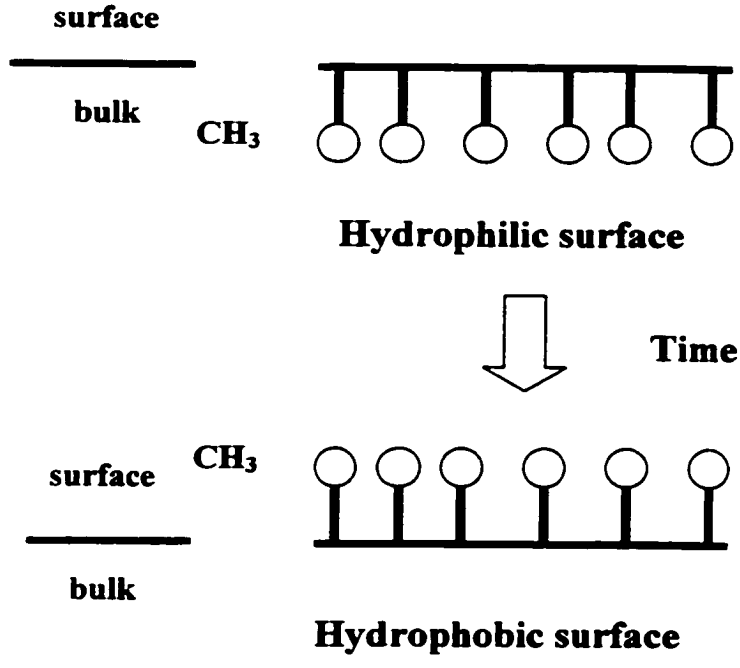

Fig.4.3 The reorientation of the CH_3 hydrophobic groups from the bulk to the surface. Resulting in the recovery of the surface from hydrophilic to hydrophobic.

4.4 Estimation of the surface free energy of the EPDM specimens

A method for measuring the surface energy of solids and for resolving the surface energy into contributions from dispersion and dipole-hydrogen bonding forces was studied. The surface energy of the virgin EPDM specimens was determined from the static contact angle measurements. Two liquids of water and methylene iodide, were used. The contact angles of water and methylene iodide were measured on EPDM specimens surface, and the surface energies was calculated using the harmonic-mean method.

The harmonic-mean equation is given as [29,65,69,70]

$$(1+\cos\theta_{H_2O})\gamma_{L1} = 4\left(\frac{\gamma_{L1D} * \gamma_{SD}}{\gamma_{L1D} + \gamma_{SD}} + \frac{\gamma_{L1P} * \gamma_{SP}}{\gamma_{L1P} + \gamma_{SP}}\right)$$

$$(1+\cos\theta_{MI})\gamma_{L2} = 4\left(\frac{\gamma_{L2D} * \gamma_{SD}}{\gamma_{L2D} + \gamma_{SD}} + \frac{\gamma_{L2P} * \gamma_{SP}}{\gamma_{L2P} + \gamma_{SP}}\right)$$

where θ_{H_2O} and θ_{MI} are the measured contact angles of droplets of water and methylene iodide. The subscripts 1 and 2 refer to the testing liquids of water and methylene iodide, respectively[64]. For water

$$\gamma_{L1} = 72.8 \text{ mJ/m}^2$$

$$\gamma_{L1D} = 22.1 \text{ mJ/m}^2$$

$$\gamma_{L1P} = 50.7 \text{ mJ/m}^2$$

For methylene iodide:

$$\gamma_{L2} = 50.8 \text{ mJ/m}^2$$

$$\gamma_{L2D} = 44.1 \text{ mJ/m}^2$$

$$\gamma_{L2P} = 6.7 \text{ mJ/m}^2$$

From (1) and (2) γ_{SH} and γ_{SD} can be found, and $\gamma_S = \gamma_S^d + \gamma_S^p$

The measurement of contact angle on the virgin EPDM specimen using water and methylene iodide as testing liquid was 99° and 56°, respectively. The dispersion and polar components of the EPDM surface tension (γ_S^d and γ_S^p) were calculated from the above two contact angles by solving the above Harmonic-Mean equations. The virgin EPDM specimens of 200 pph ATH were found to have a surface free energy of about $\gamma_S = 32.73 \times 10^{-3}$ J/m^2 ($\gamma_S^p = 2.78 \times 10^{-3}$ J/m^2 and $\gamma_S^d = 29.95 \times 10^{-3}$ J/m^2). This agrees with the literature value of $\gamma_S = 35.5 \times 10^{-3}$ J/m^2[66]. The calculation of the surface energy of EPDM specimens is given in Appendix A.

4.5 Experimental Conditions

In order to investigate the changes in the hydrophobicity of the surface after heat treatment in an electrical oven at different temperatures, the contact angle was monitored. The contact angle Θ was measured on a horizontal surface using a goniometer with sessile droplet of distilled water. The contact angle was defined as the angle between the tangent of the water droplet to the surface and the horizontal plane. The contact angle was measured over 6 locations for a given condition, and the average value is reported.

4.6 Measurement of the contact angles after immersion in hexane and evaporation in air

In order to have a detailed investigation of the contact angle θ and its relationship to the surface hydrophobicity, several studies were carried out. Fig.4.4 shows the contact angle as a function of immersion time in hexane at 23±3°C. The contact angles were measured immediately after the specimens were removed from hexane within 1 min and before substantial evaporation took place. It is clear from Fig.4.4 that the contact angle of the specimen dropped rapidly from 99° before immersion to 83° after 6 minutes of immersion in hexane. The contact angle continued to decrease with prolonged immersion in hexane. After 1h and 24h, the contact angles were 74° and 69°, respectively. When the immersion time reached 96h, θ dropped to 64.5°. Since the contact angle describes the surface hydrophobicity, its decrease indicates that the surface became hydrophillic. When the EPDM specimens were immersed in hexane, the mobile low molecular weight fluid on the surface and in the bulk was gradually extracted by hexane(Fig.3.3) and this left the surface devoid of fluid resulting in the observed reduction in θ (Fig.4.4).

Fig.4.5 shows the contact angle as a function of rest time in air at 23±3°C and after removal of the EPDM from the hexane. During this rest time, the hexane gradually evaporated from the surface and the bulk of the specimens which had been immersed for 96h. Fig.4.4 shows that the contact angles recovered rapidly. After 6min, the contact angle increased from 64.5° to 71°. After 1h and 4h, θ reached 85.5° and 87°, respectively. The contact angle remained constant at (87±2)° from 4h to 24h (Fig.4.5) of rest time

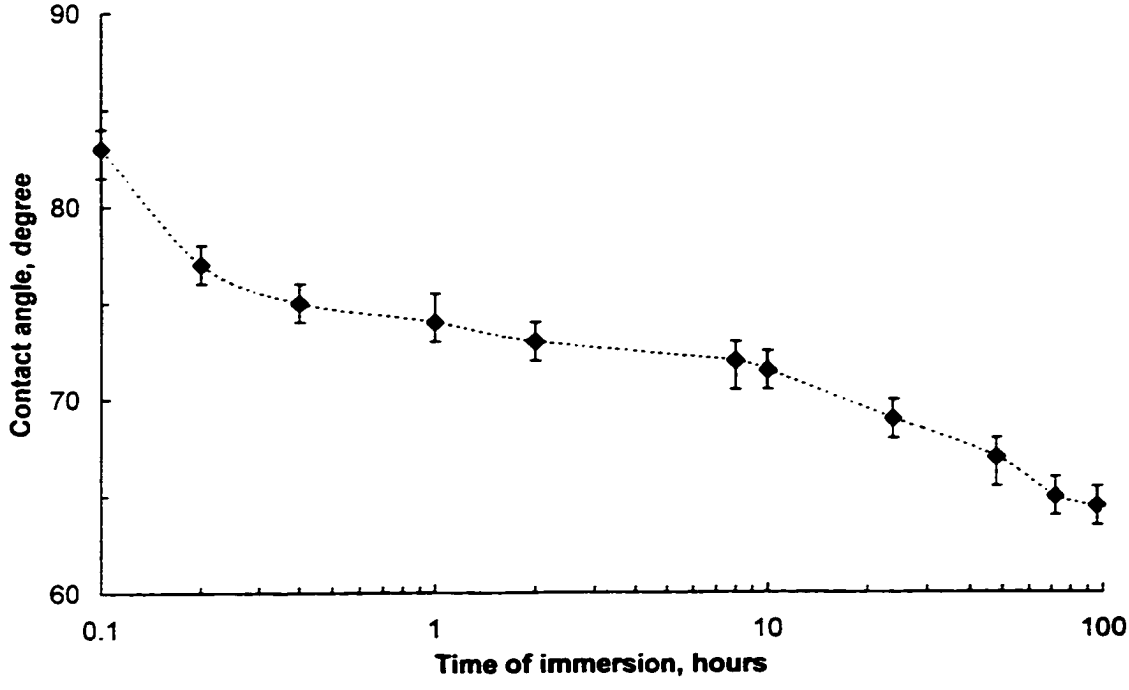

Figure 4.4 Contact angle on the surface of EPDM as a function of time of immersion in hexane

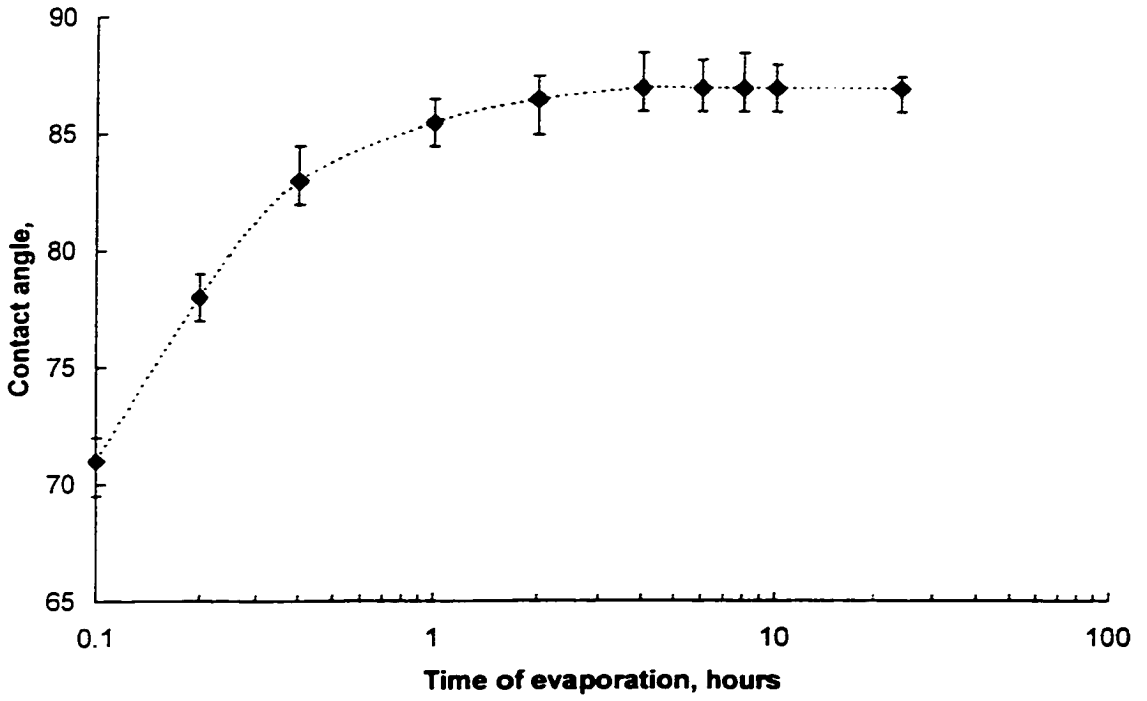

Figure 4.5 Contact angle on the surface of EPDM as a function of time after removal from hexane. EPDM was left in air at 23±3°C

when a complete evaporation of absorbed hexane had taken place (Fig.3.2). The value of 87° was below that of 99° of the virgin specimen.

The gradual recovery of the contact angle is due to the evaporation of hexane. After the complete removal of the LMW fluid from the EPDM specimens, it was noted that the surface of the EPDM specimens can still retain a certain hydrophobic property. For the contact angle, 87° is still considered as a high value when compared with glass and porcelain materials. This phenomenon was also observed by other researchers [10]. It is probably due to two factors: One is that there was still a small amount of the low molecular weight fluid remaining on the sample surface. It has been shown that even 0.01 mg of LMW fluid can provide very good water repellecy[23]. The second reason is probably that EPDM itself would contribute certain hydrophobicity property in the some way as say, high density polyethylene (θ=85°) which is devoid of fluid[71].

Fig.4.6 shows the contact angle as a function of immersion time in hexane after complete its complete evaporation in air for 24h. A virgin specimen was employed for each measurement. It will be seen from Fig.4.6 that the contact angle decreased as a function of immersion time and reached 87° after 96h of immersion in hexane and a rest time of 24h. A comparision of Figs.4.6 and 4.4 indicates that the contact angle was much lower (Fig.4.4) before substantial evaporation of the hexane took place. For example, after 96h of immersion in hexane, and for 1 minute of evaporation time that was necessary for completing the measurement θ was 64.5° (Fig.4.4) and after 24 h of rest time it was 87° (Fig.4.6). The reason for the higher values of θ in Fig.4.6 is due to the absence of hexane

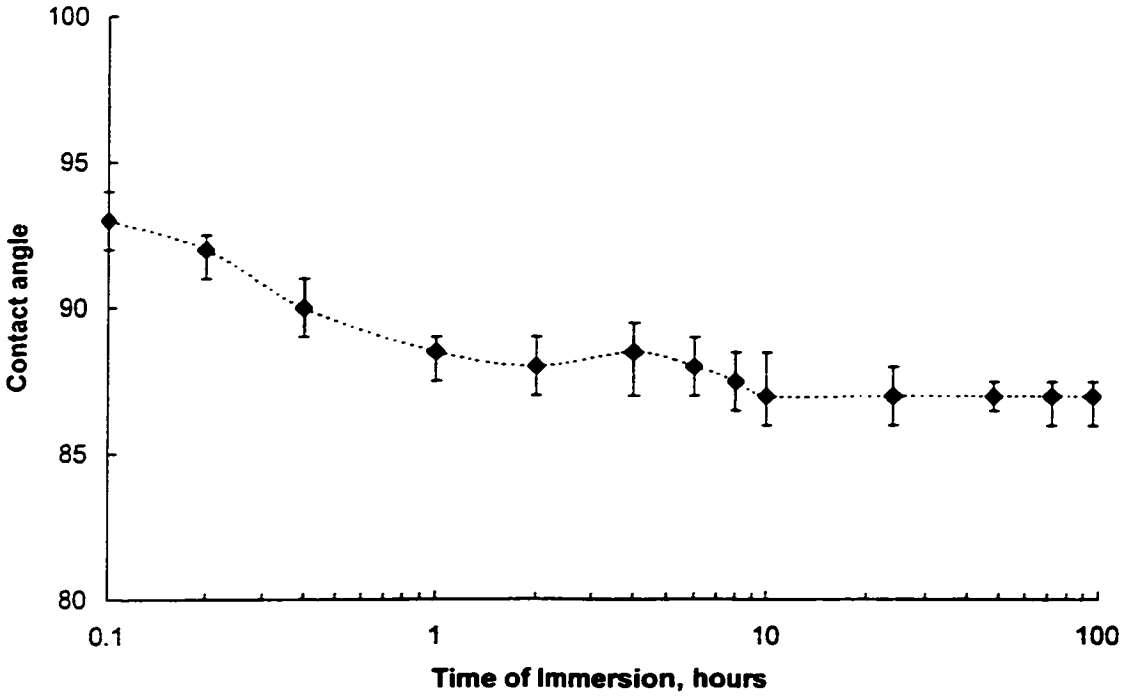

Figure 4.6 Contact angle on the surface of EPDM after different immersion times in hexane and its complete evaporation (24h) from the specimens in air

which is hydrophillic. Fig.4.6 shows that after 6min, 1h and 96h of immersion in hexane and following its complete evaporation for 24h, the contact angles were 93°, 88.5° and 87°, respectively. A reference to Fig.3.3 shows that after 6 mins. of immersion only a small proportion of the fluid ((0.19/1.72)*100=11%) was extracted and therefore θ is expected to be high at 93°. After 1h and 96h of immersion larger amounts of the fluid ((0.89/1.72)*100=51.7%; Fig.3.3) and (1.72/1.72)*100=100%; Fig.3.3), respectively were extracted and therefore the values of the contact angle were expected to be lower as indeed were observed (Fig.4.6).

4.7 Measurement of contact angles after heat treatments

4.7.1 Introduction

The effects of heating by an electrical oven (60Hz) and by laser beam bombardment on the production and loss of LMW fluid in the EPDM rubber were reported in Chapter III. The present study shows that the LMW fluid could be both regenerated during the heat treatment, and simultaneously lost by forming volatile groups and subsequent evaporation in air during the oven heating and laser treatment.

In this part of the study, the contact angle of the specimens after different levels of heating is reported. The measurements of the contact angle indicate a change in the surface hydrophobicity.

4.7.2 Measurement of the contact angles after heat treatment of specimens devoid of LMW fluid

Fig.4.7 shows the contact angle of EPDM specimens after heating at 50, 150, 240 and 380°C for 1h. The LMW fluid had been removed from these specimens prior to heating by immersion in hexane for 96h and allowing it to completely evaporate by leaving it in air for 24h at 23±3°C. The measurement of the contact angle were conducted at different times (2min, 50°C; 10min, 240°C; and 15min, 380°C) after removal from the oven to allow the specimens to cool down and were made at 23±3°C. Prior to heating and after the removal of the fluid the contact angle was 87±2°. The original contact angle in the aged specimens and before removing the mobile fluid was 99±3°.

Fig.4.7 shows that the contact angle decreased with increasing temperature from 23 to 50°C, and then increased steadily with further increasing temperature. The contact angles were 81°, 88°, 93° and 99°, respectively after heating the specimens for 1h at 50, 150, 240 and 380°C. The reason for the slight decrease of contact angle observed after heating at 50°C is not known at present time. Fig.3.6 shows that at 50°C there is a net production of LMW fluid albeit very small (0.13%) and the presence of this fluid should have either increased the contact angle or at least maintained its value at about 87°. The observed increase of the contact angle at higher temperature 150, 240 and 380°C (Fig.4.7) is attributed to the net production of fluid as shown in Fig.3.6.

Figs.4.8 and 4.9 show the measurements of the contact angle of EPDM specimens after heating for 5h and 11h, respectively. All other experimental conditions were the same as for Fig.4.7. After 5h of heating at 50, 150, 240, and 380°C, the contact angles were 82,

95, 98, 105°, respectively (Fig.4.8) and after 11h of heating, they were 85, 97, 103 and 116°, respectively(Fig.4.9). The contact angle appears to increase with increasing duration of heating from 1 to11h (Fig.4.10) for all temperatures. A reference to Fig.3.9 indicates that the amount of fluid present in the specimens after heating at 380°C decreased with increasing duration of heating from 1 to 11h. It appears that there is no direct correlation between the contact angle and the amount of fluid present in the bulk of the specimen. This is because it is sufficient for only a very thin film of fluid to affect the surface property and therefore the hydrophobicity. Additionally the orientation of the methyl groups affects the hydrophobicity irrespective of the amount of the fluid present in the material[72,73].

4.7.3 Factors influencing the contact angle

It is clear from Figs.4.8 and 4.9 that the EPDM surface still retained high values of θ, and therefore very good hydrophobicity, after heating at 380°C for 5 and 11h. A reference to Figs.3.7 and 3.8 shows that there was a large decrease of the net production of LMW fluid after heating at 380°C for these durations. Some special phenomena during the heating at 380°C were noted. The color of the specimens turned from dark gray to light gray and/or white. The specimens shrinked after heating to about 2/3 of the original dimensions. The surface of the specimens was not smooth when compared to the specimens which were heated at 50, 150 and 240°C. After heating at 380°C for 5h, and especially for 11h, bubbles could be seen on the specimens surface, and some part of the specimens where the bubbles appeared became brittle. Some fragments dropped off from the specimens randomly. It was clear that the surface of the specimens had been

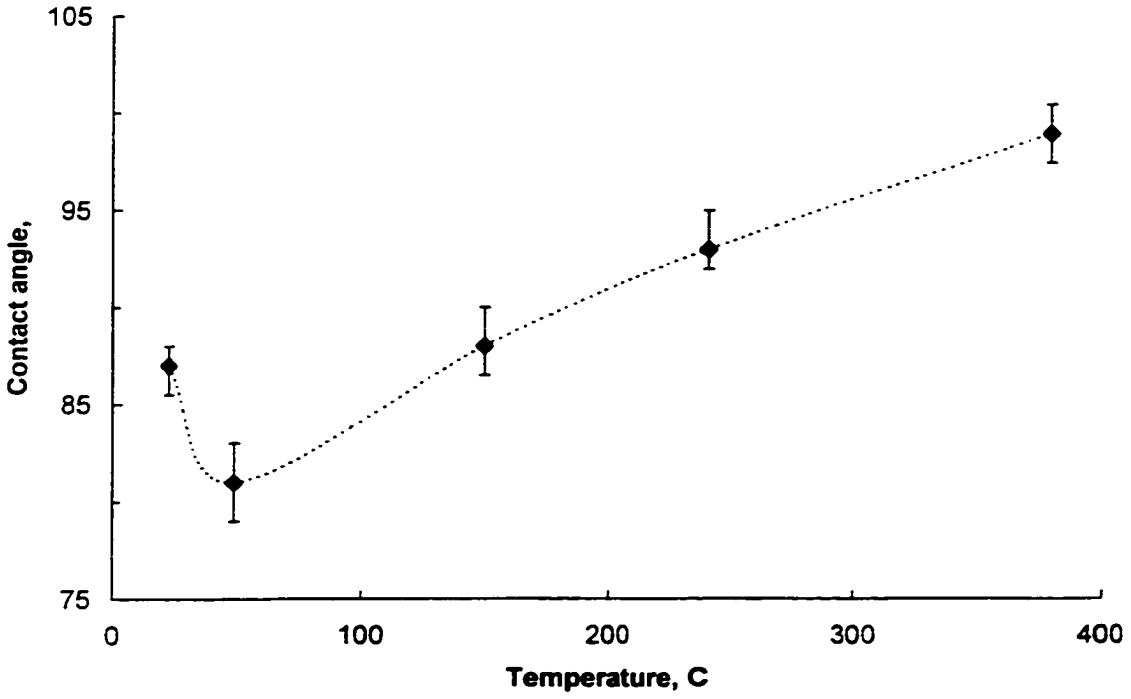

Figure 4.7 Contact angle on EPDM subsequent to heating at different temperatures for 1h. Specimens were devoid of fluid prior to heating

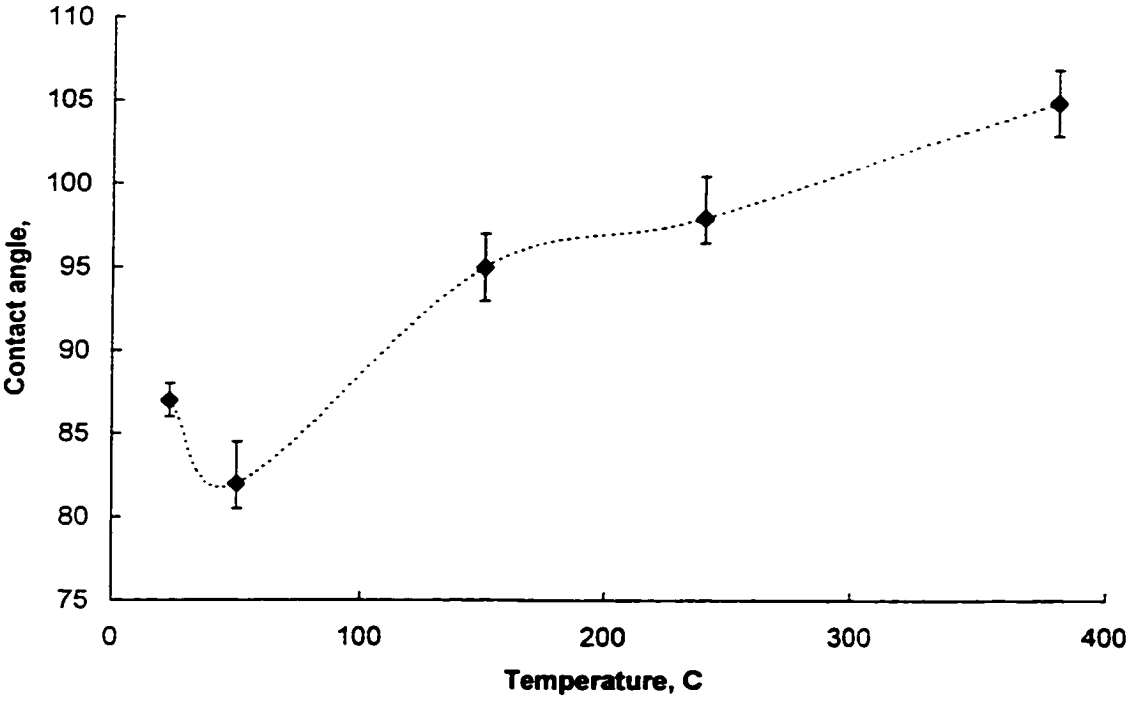

Figure 4.8 Contact angle on EPDM subsequent to heating at different temperatures for 5h. Specimens were devoid of fluid prior to heating

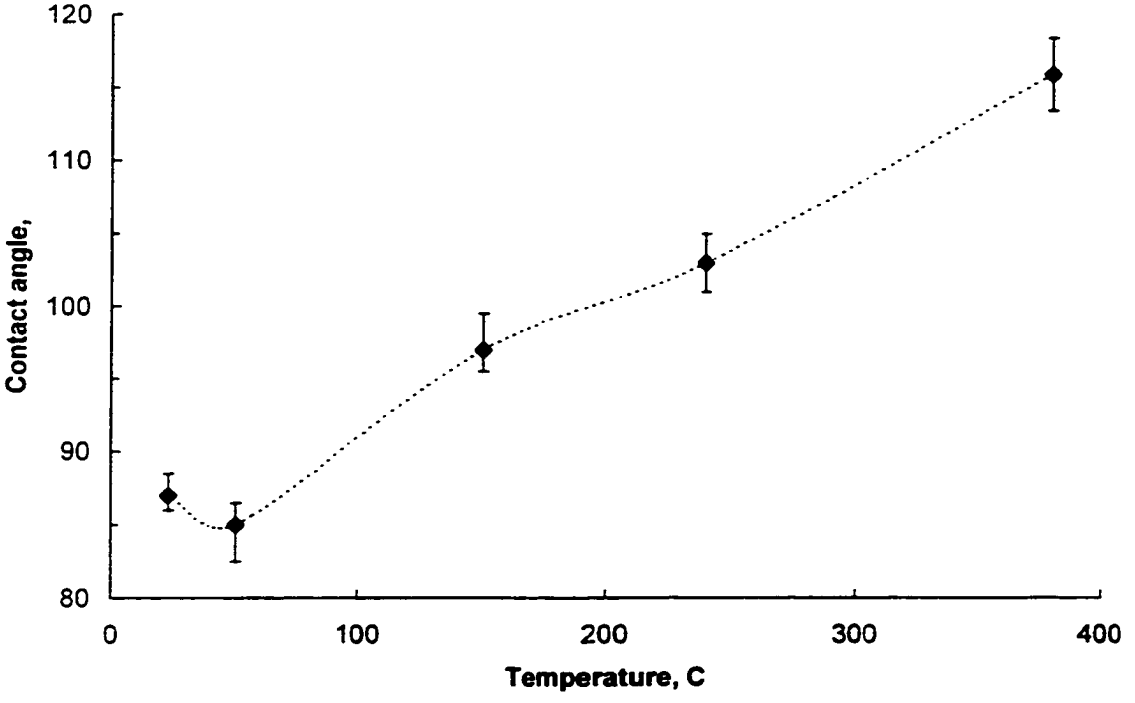

Figure 4.9 Contact angle on EPDM subsequent to heating at different temperatures for 11h. Specimens were devoid of fluid prior to heating

deformed after heating at 380°C. The surface condition observed after heating at 380°C for 5 and 11h could be described as metastable states. The contact angle formed is a metastable contact angle. As was mentioned in chapter 4.2, the angle formed in a smooth and nondeformable surface is a static contact angle. Wu has defined metastable angle[64].

Fig.4.10 shows the dependence of the contact angle as a function of time of heating the specimens which were devoid of the LMW fluid. It will be observed that the contact angle increases with time of heating for all temperature except for 50°C when it initially decreased for up to 1h and then steadily increased. Fig.4.10 gives a summary of the results depicted in Fig.4.7 to 4.9.

4.8 Measurement of the contact angles on virgin samples after heat treatment

Virgin specimens were heated in an electric oven at 50, 150, 240 and 380°C for 1, 5 and 11h, respectively. After heating, the specimens were allowed to cool down in air and the contact angle was measured at 23±3°C.

Fig.4.11 shows the contact angle of virgin specimens as a function of temperature after heating for 1h. The contact angle of the virgin specimen before heating was 99°. It can be seen from Fig.4.11 that the contact angle decreased to 85° after heating at 50°C, then it increased to 87°, 96° and 99°, respectively, at 150, 240 and 380°C. These results may have significant relevance to EPDM insulators which may be subjected to occasional ambient temperature of the order of 50°C in some regions of the world. The increase of

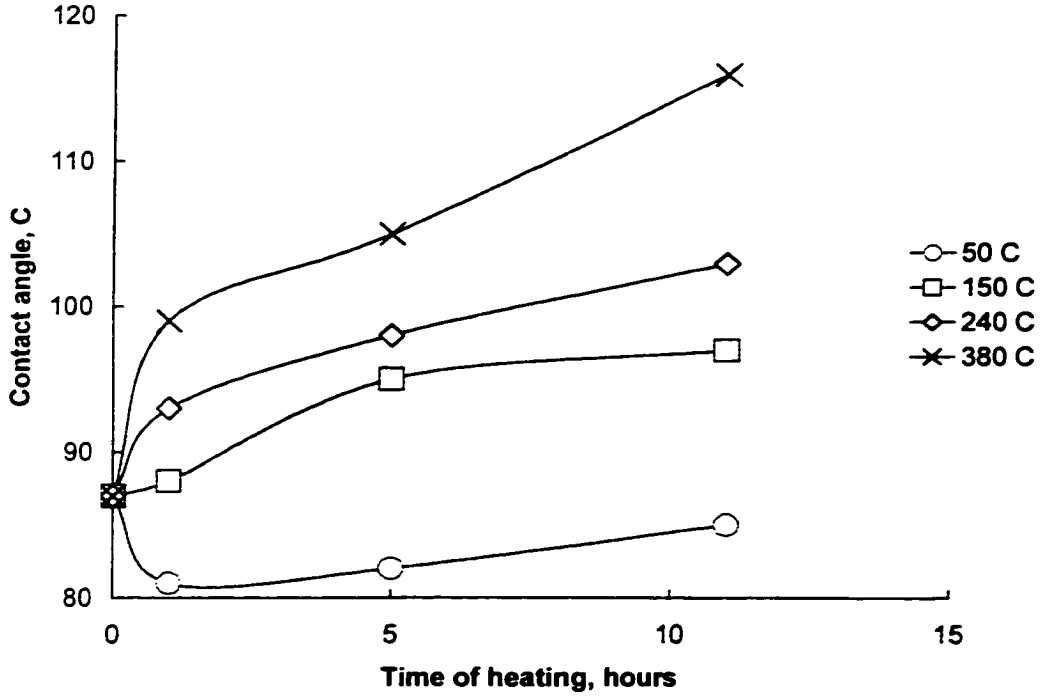

Figure 4.10 Dependence of the contact angles on duration of heating in the electrical oven at various temperatures. Material, EPDM; contact angle was measured at 23±3°C; specimens were devoid of LMW fluid before heating

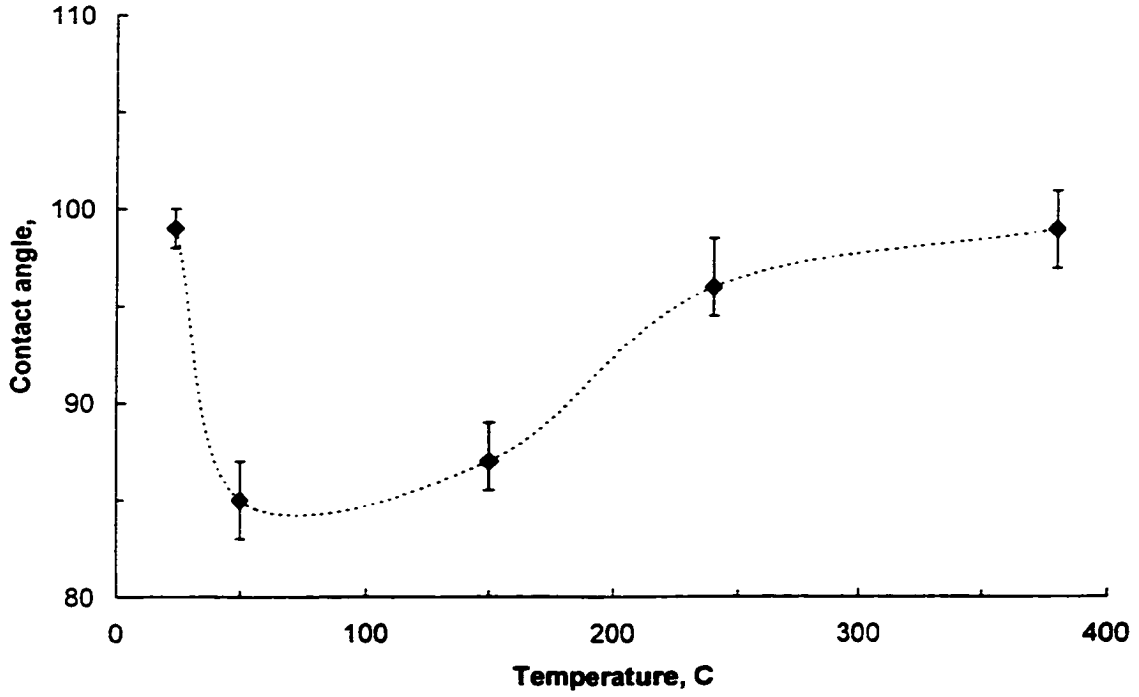

Figure 4.11 Contact angle on virgin EPDM subsequent to heating at different temperatures for 1h

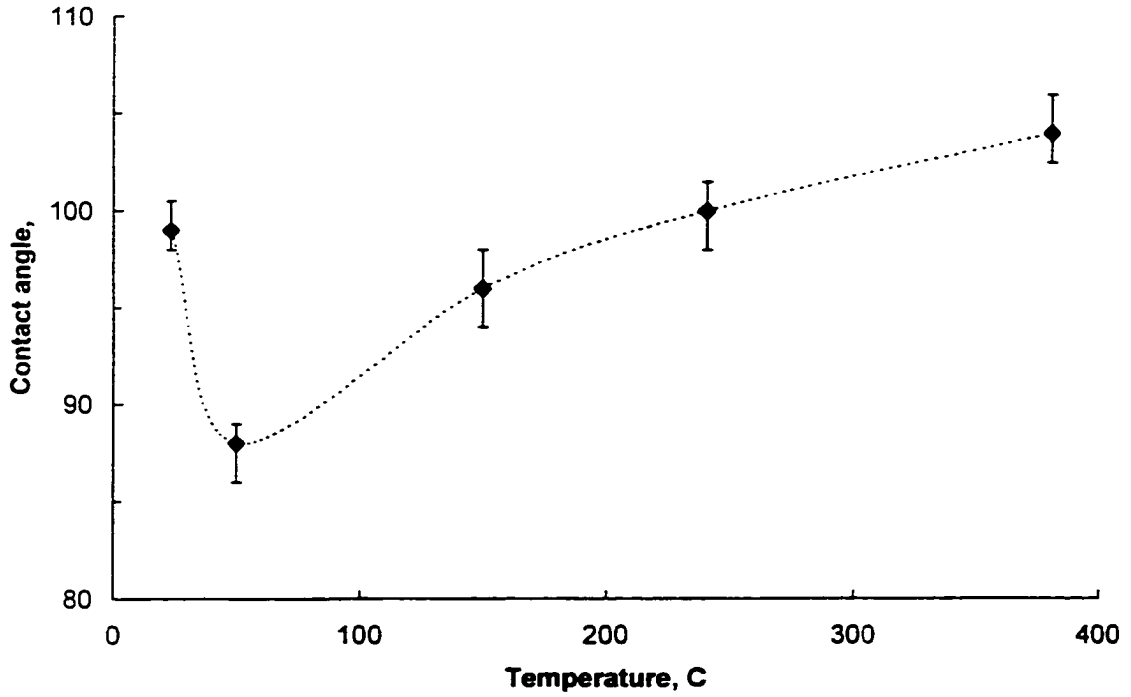

Figure 4.12 Contact angle on virgin EPDM subsequent to heating at different temperatures for 5h

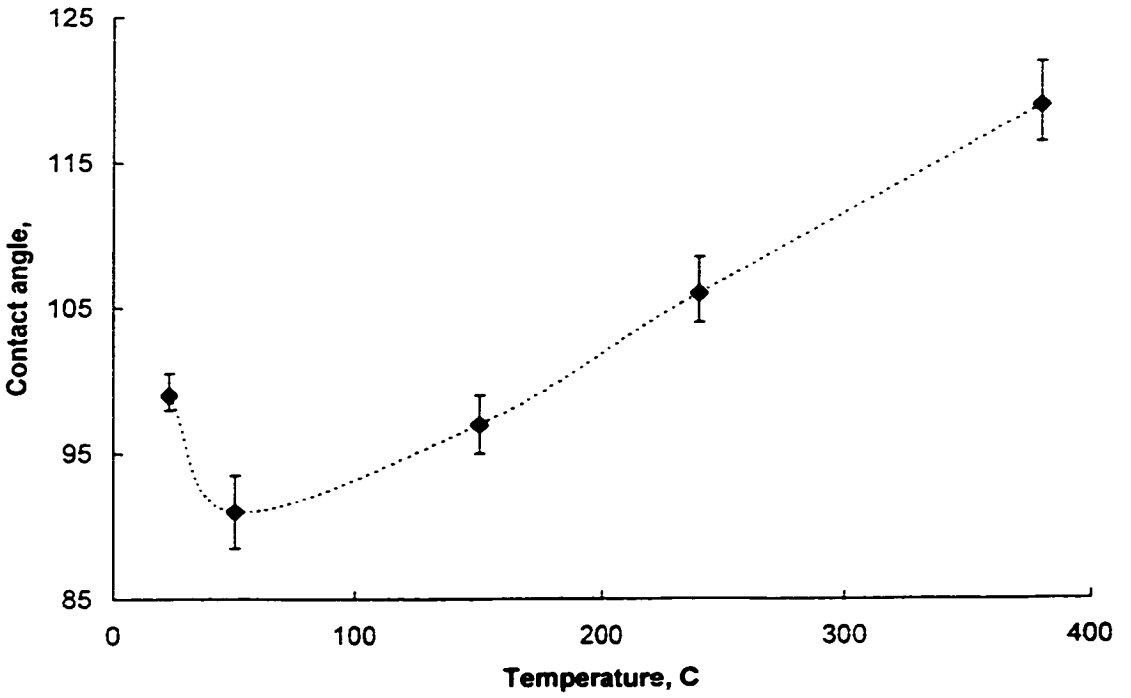

Figure 4.13 Contact angle on virgin EPDM subsequent to heating at different temperatures for 11h

the contact angle at higher temperatures is due to more production of LMW fluid by bond-breaking of the long EPDM molecular chains into shorter and mobile chains. The reduction of the contact angle after heating virgin specimens for 1 to 11h at 50°C (Figs.4.11 to 4.13) is consistent with similar findings after heating at the same temperature specimens from which the LMW fluid had been removed (Figs.4.7 to 4.9).

Fig.4.12 and 4.13 show the contact angle of EPDM after heating at 50,150, 240 and 380°C for 5 and 11h, respectively. The experimental conditions were the same as in Fig.4.11. After heating for 5 and 11h at 50°C the contact angle decreased from 99° to 88° and 91°, respectively. Then it increased to 96°, 100° and 104°, respectively, at 150, 240 and 380°C after 5h of heating (Fig.4.12). After heating for 11h the contact angles were 97°, 106° and 119° at 150, 240 and 380°C, respectively. After 5 and 11h of heating at 380°C on virgin specimens, a large contact angles were measured. This was despite the large reduction of the LMW fluid in the specimens after heating at this temperature (Figs.3.7, 3.8, 3.11 and 3.12). The same phenomenon was observed in the specimens in which LMW had been previously devoid before heating(Figs.4.7 to 4.9). Fig.4.14 shows a summary of the dependence of θ on the heating time, on virgin specimens, at various temperatures. θ is seen to increase with increasing duration of heating from 1h to 11h for all temperatures.

4.9 Contact angle after heating and removal of LMW fluid

All specimens of Fig.4.12 which had been virgin and then were heated for 5h at different temperatures were subsequently immersed in hexane for 96h, and then left in air for 24h

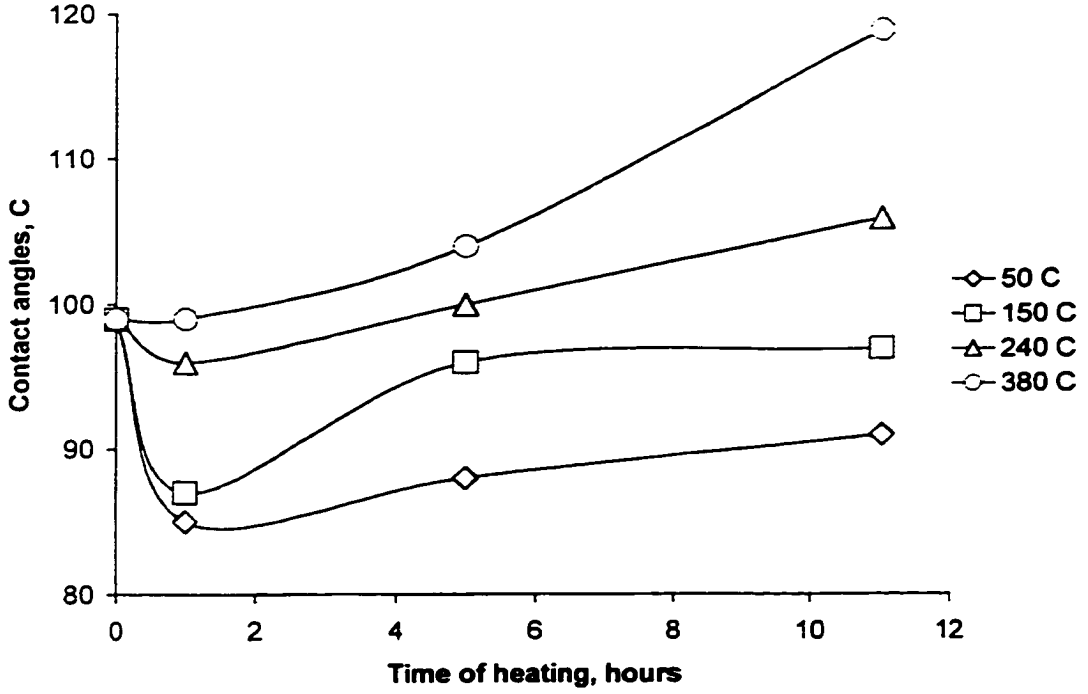

Figure 4.14 Dependence of the contact angles on duration of heating in the electrical oven at various temperatures. Material, virgin EPDM; contact was measured at 23±3°C

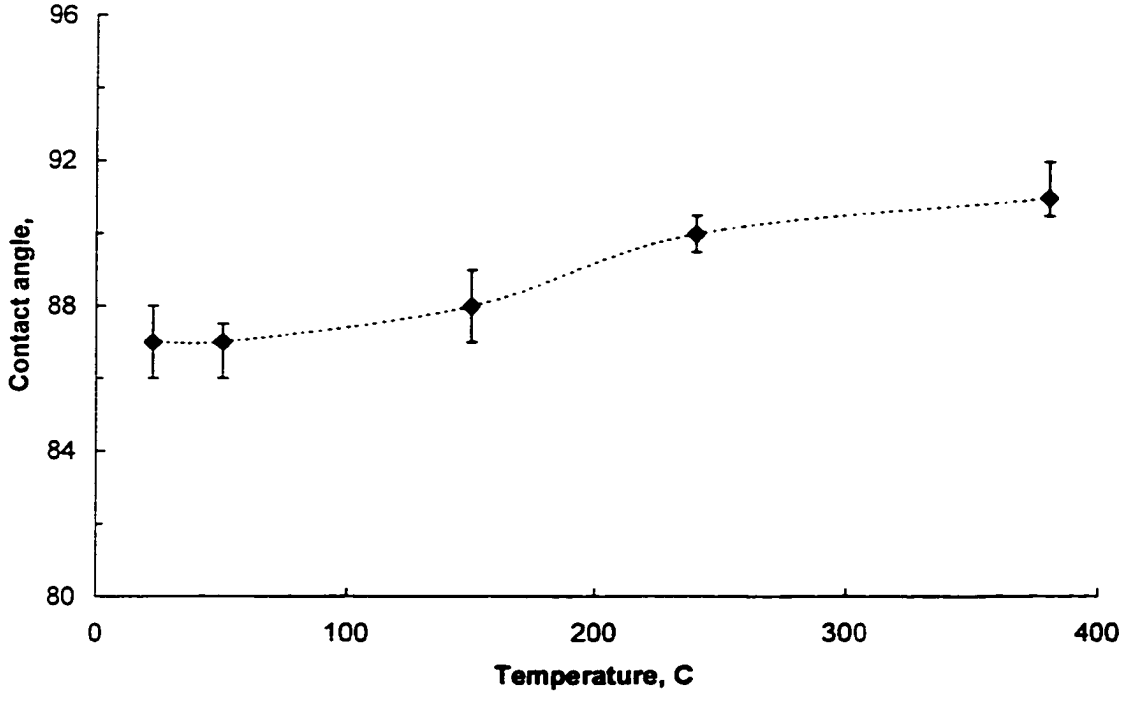

Figure 4.15 Contact angle on specimens of Fig.4.12 after removal of LMW fluid by immersion in hexane (96h) and rest in air (24h)

for complete evaporation of hexane. The contact angles were measured again in these same specimens from which the LMW fluid had been removed. The measured angles are plotted in Fig.4.15 against temperature. The contact angles after heating for 5h at 50, 150, 240 and 380°C and removal of the LMW fluid were found to be 87, 88, 90, and 91°, respectively(Fig.4.15). Prior to heating in the oven but after removal of the fluid θ=87°(Fig.4.10). Comparing Fig. 4.15 with 4.12, it shows that the contact angles had substantially decreased after extracting the LMW fluid. Fig.4.12 shows the corresponding contact angles before extracting the fluid were 99, 88, 96, 100, and 104°, respectively, after heating for 5h at 23, 50, 150, 240 and 380°C. Fig.4.15 clearly demonstrates that when the LMW fluid is removed the contact angle decreased respectively to 87, 87, 88, 90 and 91°C.

4.10 Measurement of the contact angles after laser beam bombardment

The effect of the application of argon laser beam to the EPDM specimens on the quantity of the LMW fluid was reported in chapter III. The heat provided by this method was intended to simulate the effects of intermittent dry band arcing to the specimens. The arc location may vary continuously on the surface of specimens and lasts a very short duration at a given location. The average output power of the laser system was1.0W. The energy range varied from 28.8 to 654J by adjusting the duration of the laser. The laser beam was applied only once as a single pulse to the surface for a given level of energy.

Fig.4.16 shows the measurements of the contact angles on virgin specimens as a function of laser beam energy. The measurements were taken at the perifery of the spot and not on

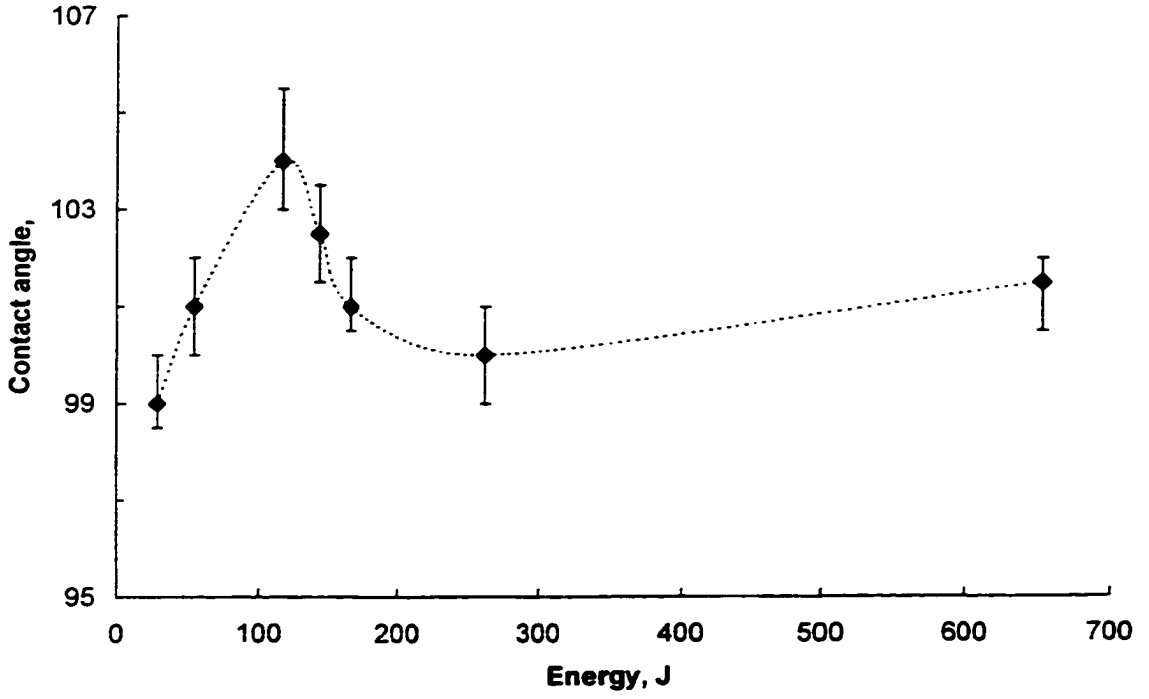

Figure 4.16 Contact angle on virgin EPDM subsequent to laser beam bombardment at different energies

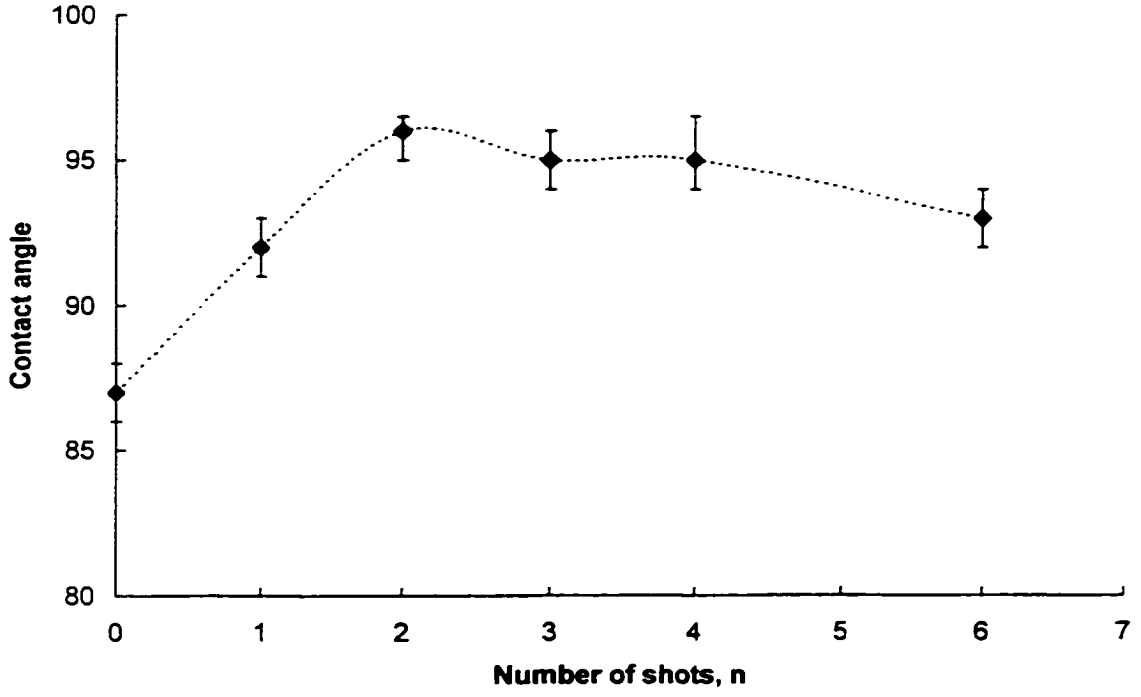

Figure 4.17 Contact angle on EPDM subsequent to different numbers of laser beam application. Specimens were devoid of LMW fluid prior to laser application

the spot because of surface distortion therein. The contact angle after applying different energy levels of the laser beam was relatively constant in the range of 99° to 104° (Fig.4.16). This is unlike the contact angle of the specimens after heating in the electrical oven (Figs.4.11 to 4.13), where larger variations were observed. A marked spot having an area of about ($0.075\pm0.005mm^2$) was created after the bombardment. The spot area was measured from photographs of the spots having a magnification of 10 times.

Fig.4.17 shows the measurements of the contact angle as a function of the number of applications of the laser beam. The LMW fluid was removed from these specimens prior to the application of the laser beam. The energy in each application was 1.05Wx180s=189J. Fig.4.17 shows that after the laser beam bombardment, the contact angle varied from 92° to 96°. It was noted that before the laser beam bombardment, the contact angle value of specimens was 87°. After 1 shot of laser beam, it increased to 92°. The contact angle increased to 96° after 2 shots. After 4 and 6 shots, the contact angle was 95° and 93°, respectively. The small variation of the contact angle depicted in Fig.4.17 after application of the laser energy is consistent with the small variation in the value of the LMW fluid produced (Fig.3.18). The area outside the spot when the laser energy fell was not heated significantly and therefore the changes in the contact angle (Fig.4.17) and the production of the LMW fluid (Fig.3.18) were very slight.

Fig.4.18 shows the measurement of the contact angle as a function of the number of applications of laser beam on virgin EPDM. For each shot, the energy was 1.05Wx180s=189J as in Fig.4.17. The contact angle of the virgin specimens was 99°.

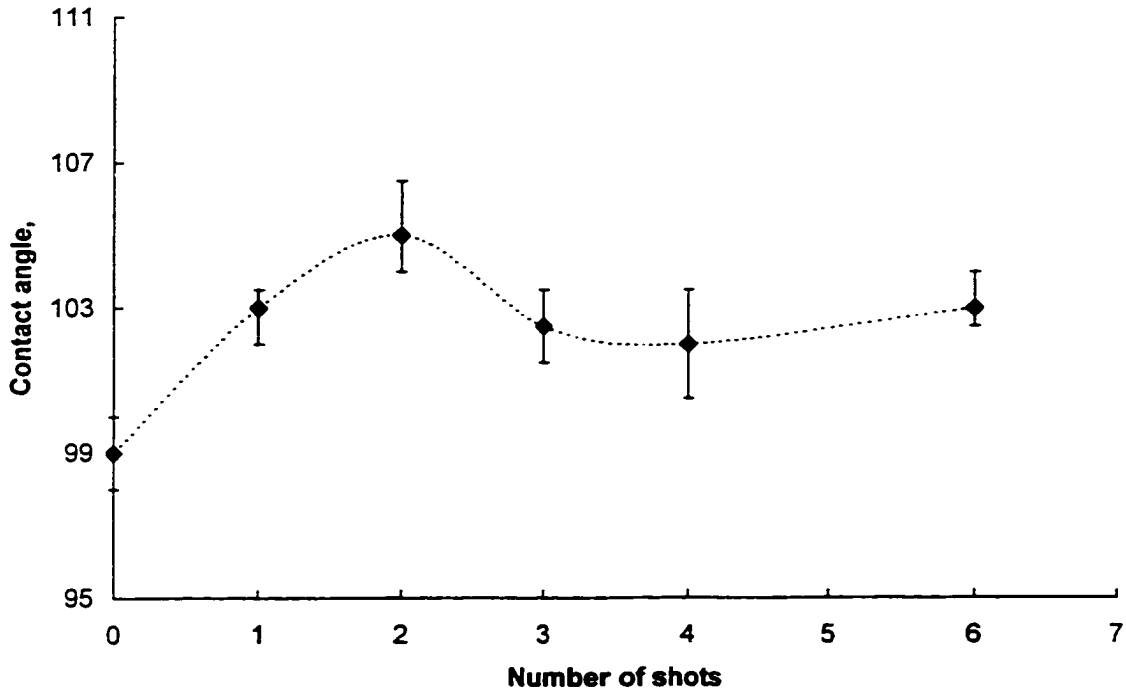

Figure 4.18 Contact angle on virgin EPDM subsequent to different numbers of laser beam application

After one application of laser beam, θ increased to 103°. After 2, 3, 4 and 6 shots, the contact angles were 105°, 102.5°, 102° and 103°, respectively. This shows that only small variations of the contact angle were observed after applications of laser beam energy to virgin specimens of EPDM. Fig.4.18 also demonstrates that the presence of LMW fluid in the insulating material increased the contact angle to values above those found when the fluid had been removed (Fig.4.17).

CHAPTER V
SURFACE CHEMICAL ANALYSIS

5.1 Introduction

The performance of outdoor insulators is largely influenced by the material surface properties, which are determined by the inherent properties of the material. Therefore chemical surface investigation can be used to evaluate and if necessary improve the performance of polymeric insulators [74-75]. The molecular bonding is the way in which atoms are held together because of the mutual attractions. In the present work, attenuated total reflection (ATR) Fourier Transform Infrared (FTIR) has been investigated to study the molecular bonding, which is a good method of examining the molecular structure. Different structures, or different molecules, absorb electromagnetic radiation at specific wavelengths. The spectra provide an evidence of the presence of certain specific atoms or groups of atoms, therefore it can be used as elemental analysis for chemical composition of the material [76-78]. In the nuclear magnetic resonance (NMR) study, the spectrograph gives a detailed information on the atomic nuclei oscillation, which can be used to identify unknown groups. That method is based on measuring the specific radio frequencies that are emitted by the nuclei and the rate at which the realignment of the molecules occur [79]. The SEM uses the secondary electrons produced by the scanning beam to give an imagine of the surface of the specimen being scanned [80].

This thesis presents a study on the presence of low molecular weight (LMW) fluid in EPDM and a surface chemical investigation to identify the fluid. The maintenance of the water repellency of the surface of EPDM, after a temporary loss of its hydrophobicity, is

due to the diffusion of LMW fluid from the bulk to the surface. The LMW fluid could be regenerated by the scissions of long molecular chains. This chapter reports on 1. the photo-micrographs of the fracture of the surface of EPDM following irradiation by a laser beam using Scanning Electron Microscopy (SEM), 2. the identification of the LMW fluid using Nuclear Magnetic Resonance (NMR), 3. the chain length of the siloxane and its concentration using Gas Chromatograph in combination with a quadruple mass spectrometer (GC-MS) and 4. the molecular bonds using ATR attached Fourier transform infrared spectroscopy (FTIR-ATR)

5.2 Scanning electron microscope (SEM) analysis

In the present study, specimens of EPDM were cut from the weathersheds of 46 kV outdoor insulator and were subjected to either heating in an electrical oven or to a laser beam irradiation. The physical changes on the surface after heating in the oven and also after the laser irradiation were investigated with the aid of a scanning electron microscope (SEM). The electron beam was accelerated using 15 kV which penetrated into the surface of EPDM to a depth of about 10 μm. In the SEM study, (JEOL 5800-LV), a 15 keV electron beam was used at a pressure of 10^{-4} to 10^{-3} Pa. Fig.5.1 shows SEM photograph (magnification 75) of the EPDM specimen after two applications of laser irradiation with an energy of 189J lasting 180s each. The damage on the surface can be seen. A larger magnification (500) shows visible cracks on the target area where the laser irradiation impacted (Fig.5.2). The damage to the surface resulted from the high temperature of the surface. The increased temperature created a low molecular weight fluid in the material, as was recently reported [20-21]. The bombardment with the laser

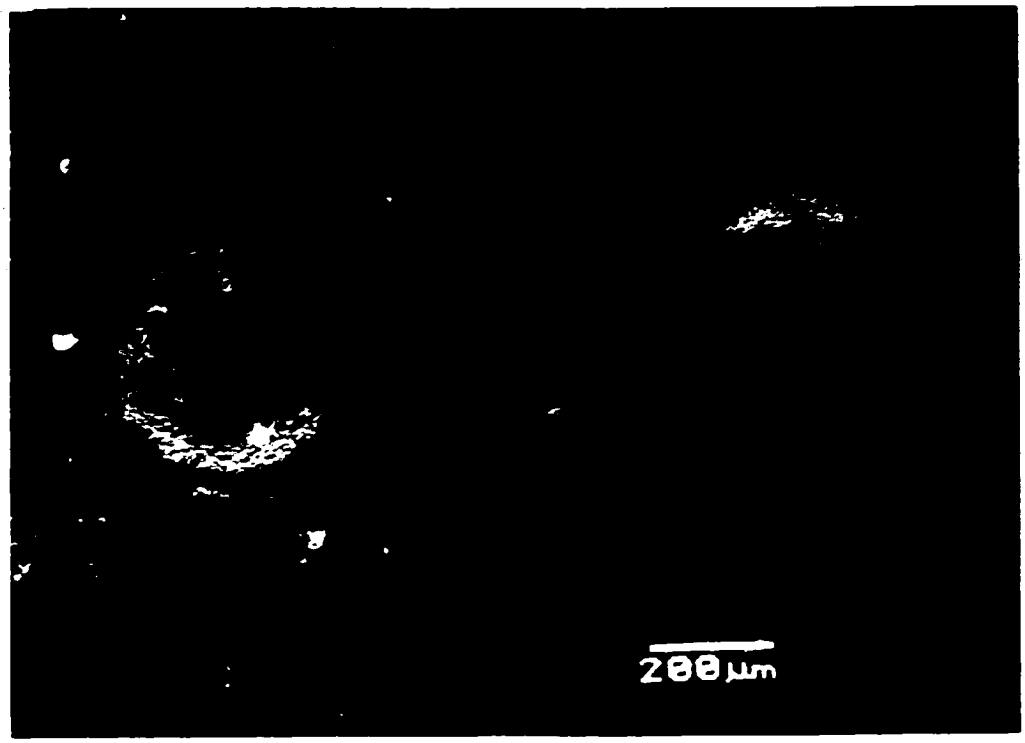

Figure 5.1 SEM photograph of EPDM specimens irradiated with a laser beam. Energy of the beam 189J. Number of shots, 2; magnification x75

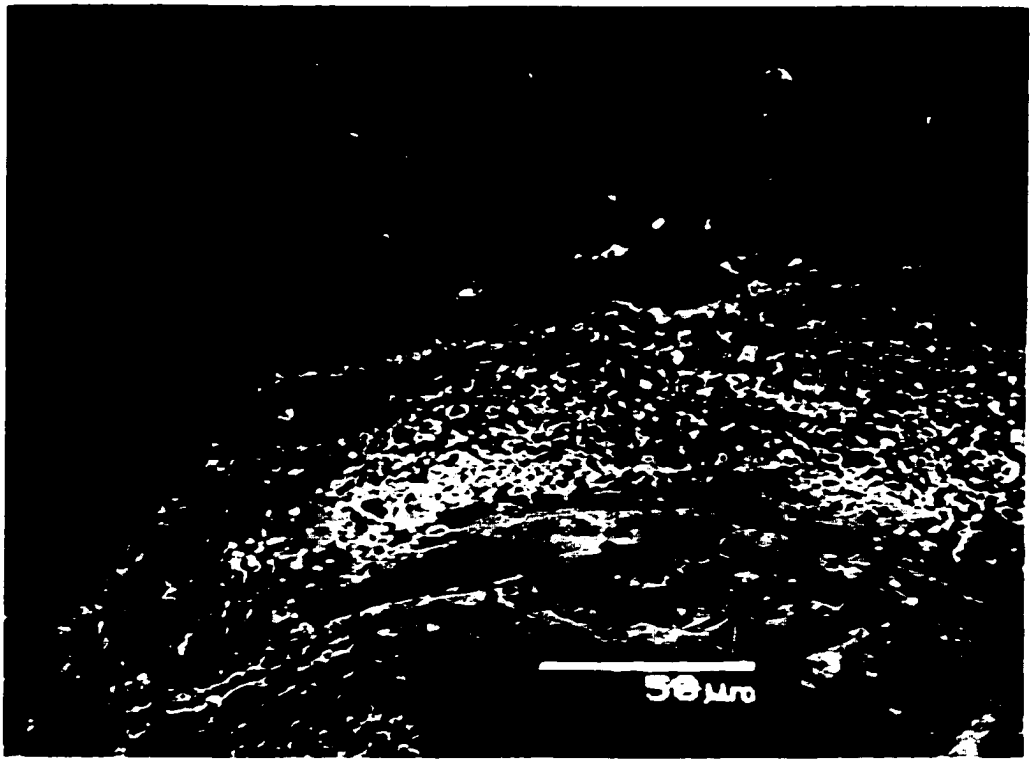

Figure 5.2 **SEM photograph within the irradiated area showing visible damage to the surface; magnification x500**

beam simulated the condition of intermittent dry-band arcing where the arc location continuously varies on the insulator surface. SEM photographs (not shown) of the specimens which were heated in the oven for 1h at temperatures of up to 380°C did not show significant changes on the surface from the virgin specimens.

5.3 Identification of LMW fluid by nuclear magnetic resonance (NMR)

In the present work, a nuclear magnetic resonance (NMR) technique was used to identify the LMW fluid extracted from the EPDM. The NMR spectrum was obtained by placing samples in a homogeneous magnetic field and applying electromagnetic energy at suitable frequency until a resonance frequency was obtained. Fig. 5.3 shows the spectra for analytical hexane. Fig. 5.4 shows the spectra for silicone fluid (20 centipoise viscosty). Fig. 5.5 shows the spectra for a mixture of hexane and the LMW fluid, which was extracted from EPDM. Fig. 5.6 shows the identification of LMW fluid by the comparing Fig. 5.5 to Figs.5.3 to 5.4. It was noted that though the chemical shifts were very small they were clearly demonstrated. The peaks in the spectra were the functional groups in the sample and they were integrated, so that the height of each step was proportional to the area under the corresponding spectral line. In the NMR spectrum, the area of each line was proportional to the number of nuclei contributing to it.

5.4 Identification of the mobile fluid in EPDM using GC-MS spectrometer

The fluid which has been extracted from EPDM was identified as composed of siloxane molecules which is a silicone fluid. Fig.5.7 shows the GC-MS spectrum for the siloxane molecules. Siloxane molecules units of n=3 to n=6 (-$[Si(CH_3)_2\text{-}O]_n$-) and cyclo-siloxane

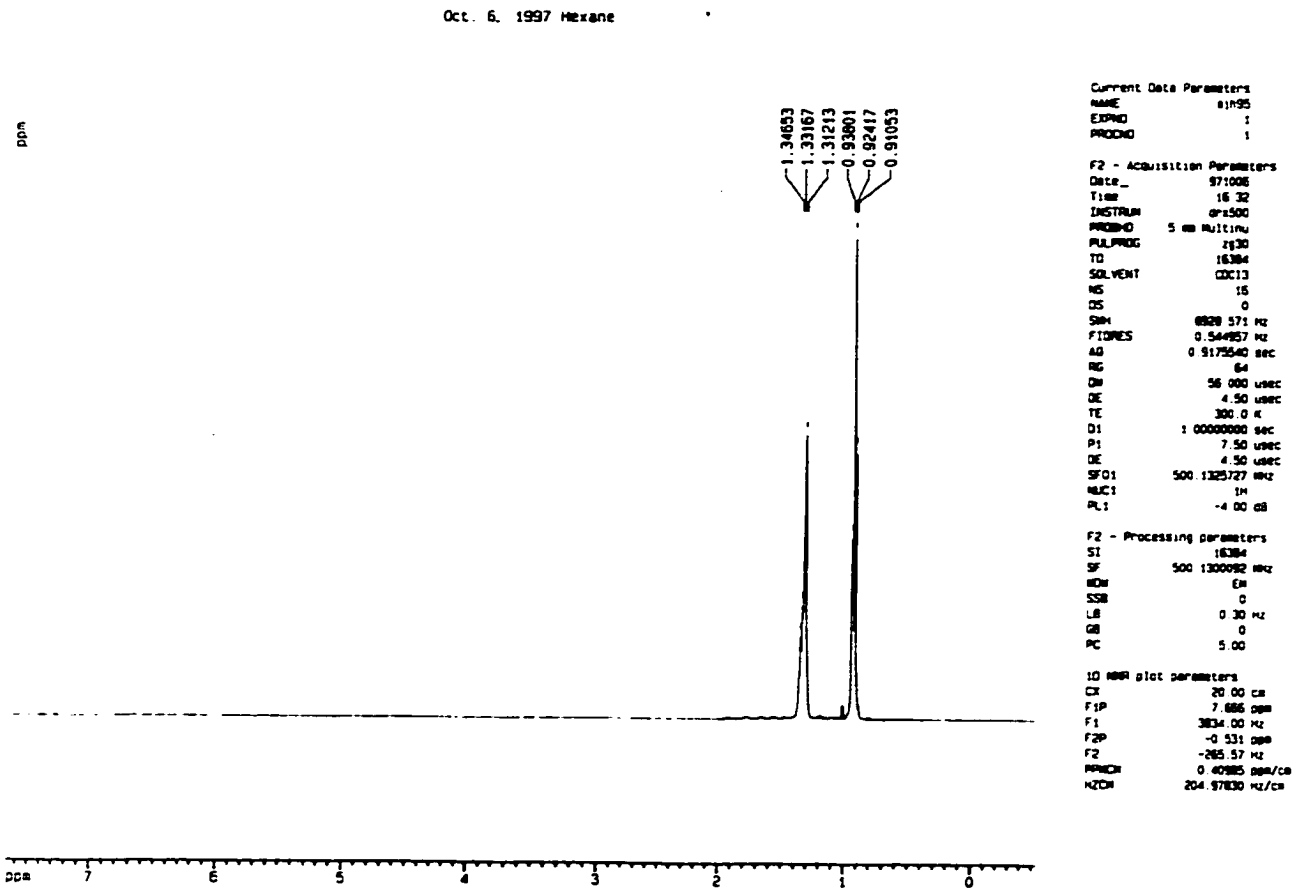

Figure 5.3 **NMR spectra for analytical hexane**

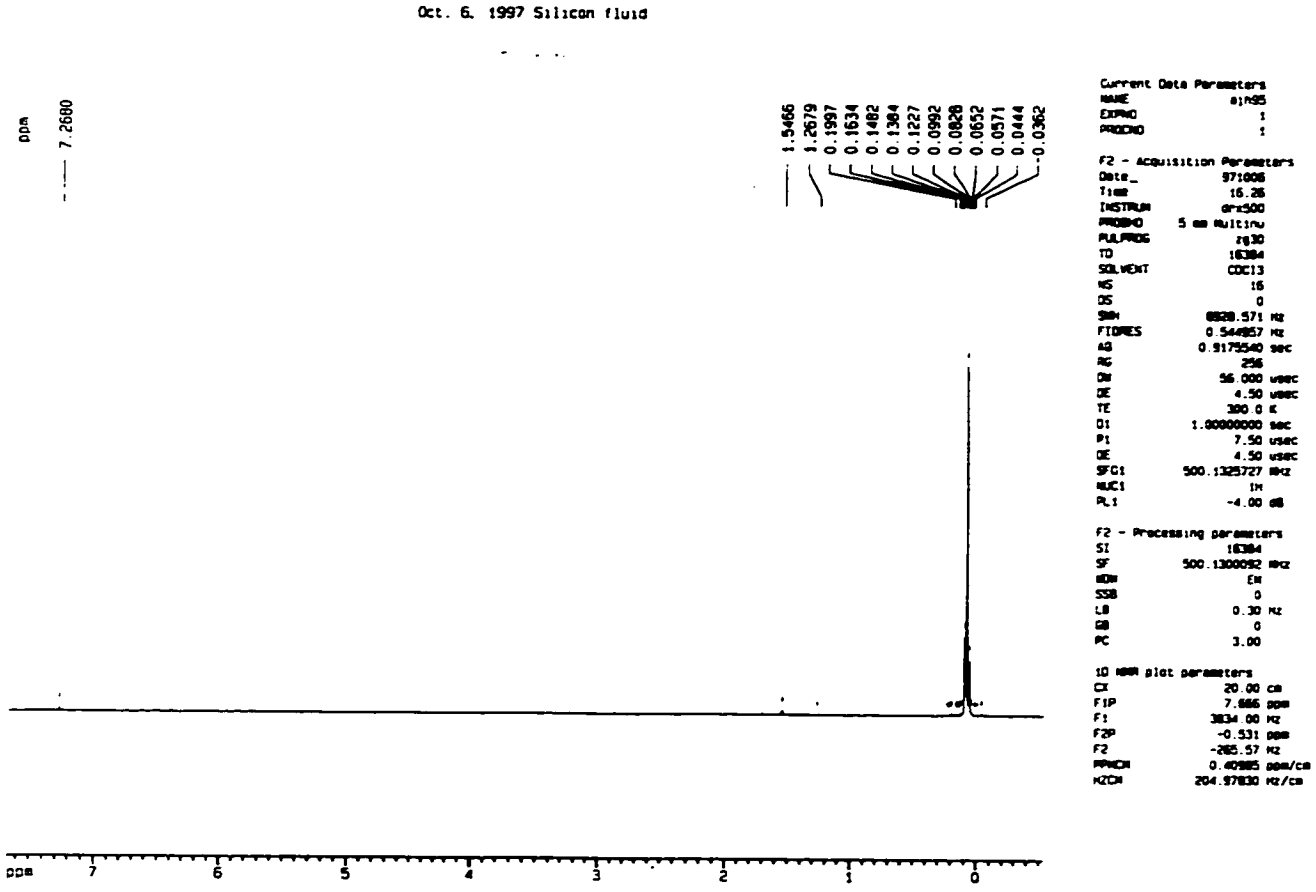

Figure 5.4 NMR spectra for silicone fluid (20 centipoise viscosty)

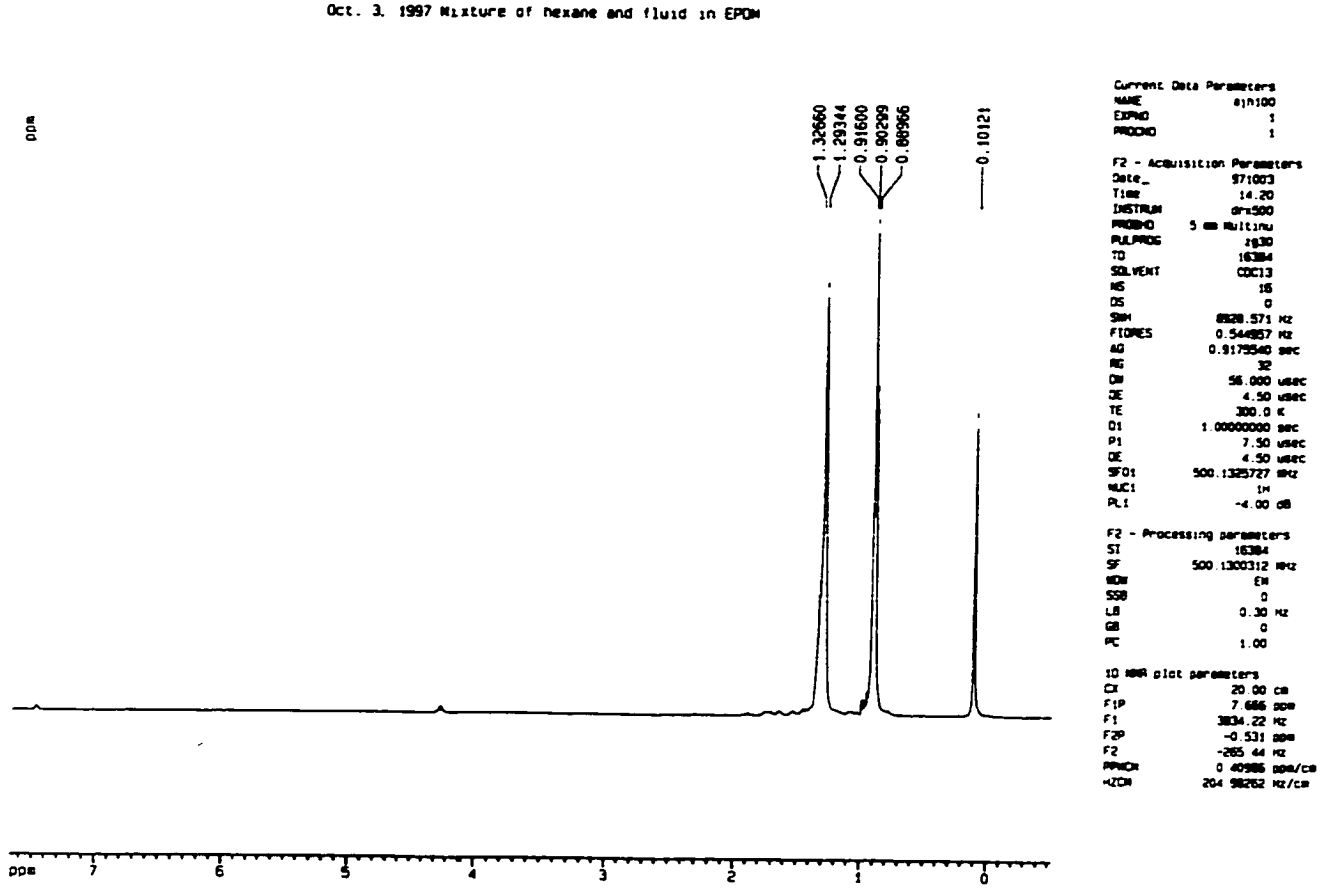

Figure 5.5 NMR spectra for a mixture of hexane and the LMW which was extracted from the EPDM specimens

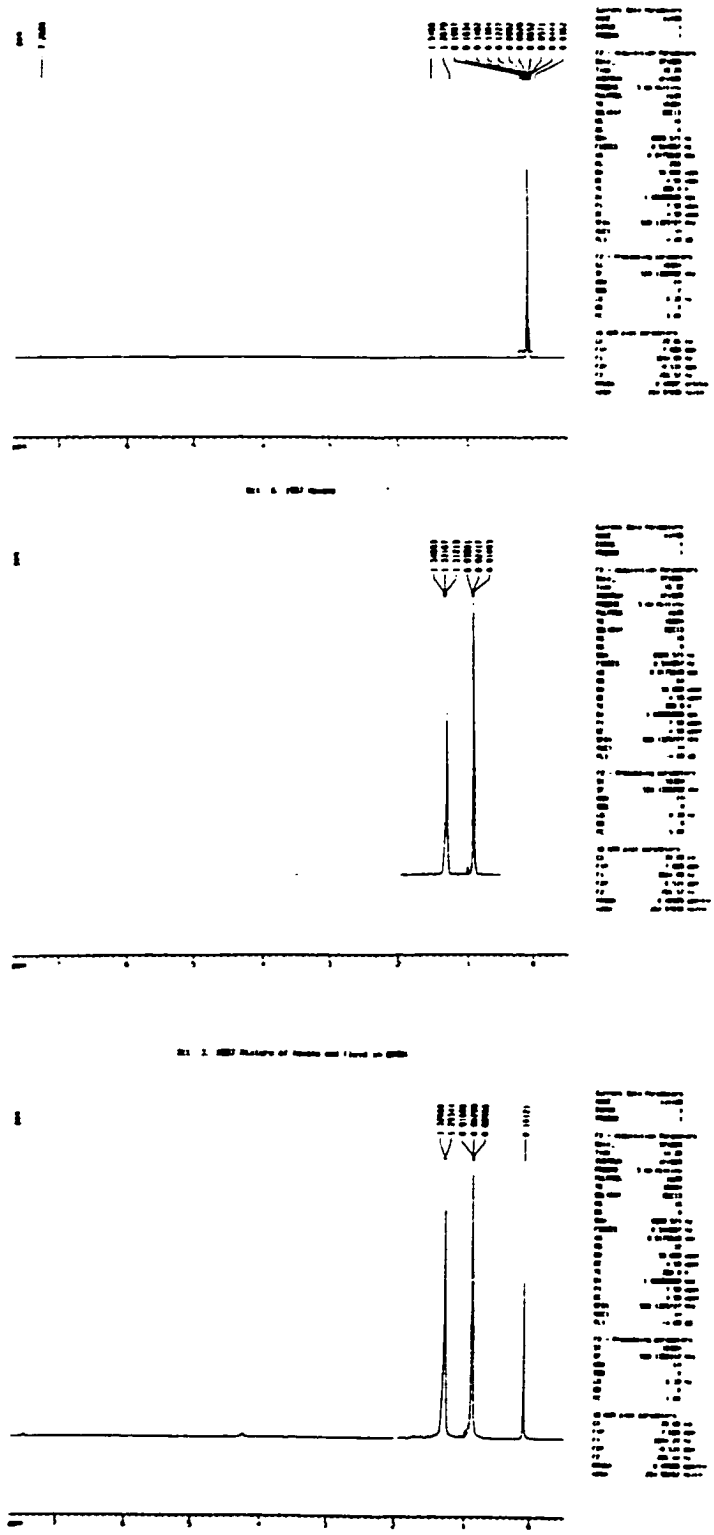

Figure 5.6 **NMR spectra of hexane, silicone fluid (20 centipoise), and a mixture of the LMW fluid extracted from EPDM in hexane**

With units of n=6 to n=12 were identified in the spectrum. The largest concentration was of cyclo-siloxane having n=8 (mass range 592 g/mole). It was observed that both linear and cyclic structures existed in the silicone fluid. Both structures contribute to the hydrophobic performance of EPDM. It was suggested that cyclic structures could be more effective than the linear ones [7]. In Fig.5.7, n is the unit of linear structure and n^+ is the unit of cyclic structure. The GC spectrum of the siloxane molecules provides a good indication of the LMW units that migrate to the surface to provide the hydrophobic property. Fig.5.8 shows the linear chemical structure of LMW components with units of n=1 (siloxane), n=3 (trisiloxane, octamethyl) and cycli structure of n^+=6 units (cyclo-hexasiloxane, dodecamethyl). The presence of LMW siloxane fragments (Fig.5.7) suggests that they could migrate as a fluid to the surface and thus provide the hydrophobic property. It has been recently suggested that even with extremely low LMW fluid content of less than 0.01%, a hydrophobicity transfer may take place[30].

5.5 Generation and diffusion of the LMW fluid from the bulk to the surface

EPDM specimens having the dimension of 1mmx10mmx50mm were examined using a FTIR-ATR spectrometer (Nicolet 5DX) incorporating Thalium Bromoiodide KRS-5 crystal. Figs.5.9 and 5.10 show the transmission IR spectra after heat treatment of EPDM specimens. Absorption was due to the presence of the infrarad silicone fluid on the surface of the EPDM. The peaks in presence of the infrarad in (IR) spectra represent the characteristics absorption bands. Absorption at 1270-1255 cm^{-1} (band 1) is due to CH deformation in the Si-CH_3 groups. Absorption at 1100-1000 cm^{-1} (band 2) is due to the Si-O bond in Si-O-Si. Absorption at 840-790 cm^{-1} (band 3) is characteristic of Si-alkyl

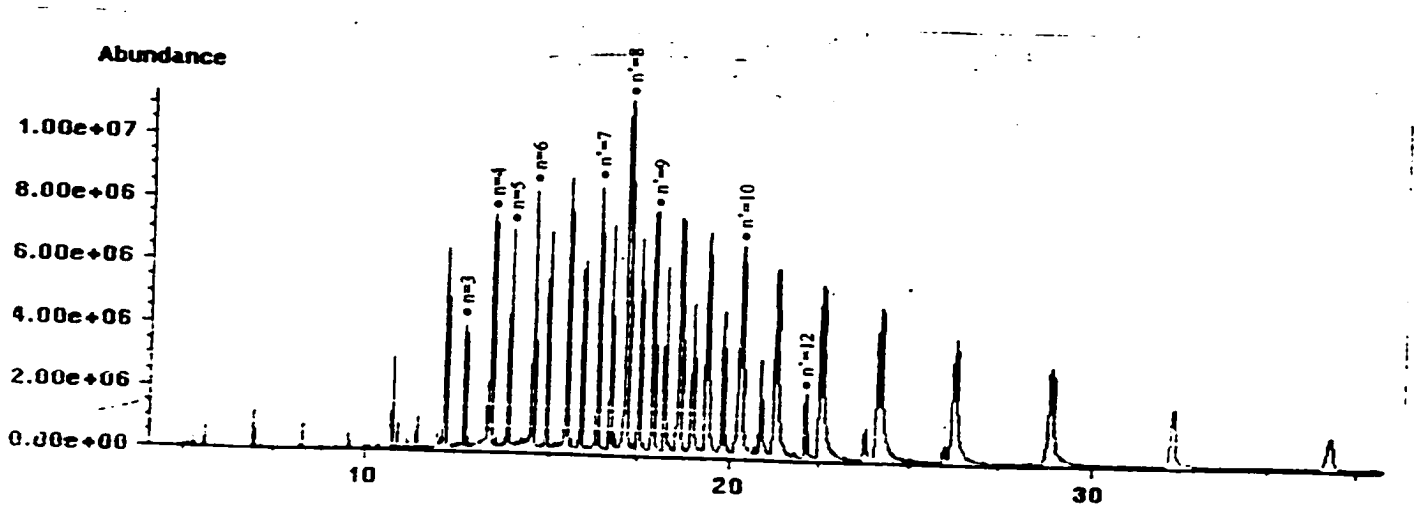

Figure 5.7 Gas chromatography and mass spectrometry (GC-MS) spectrum of the fluid extracted from EPDM

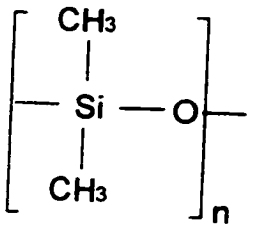

Siloxane

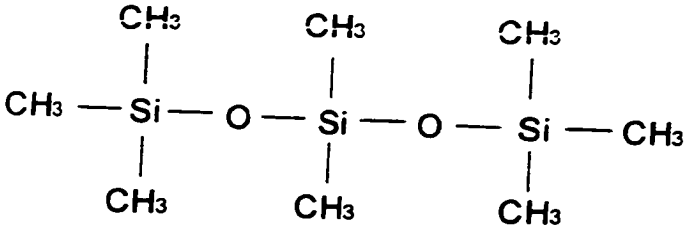

Trisiloxane, octamethyl

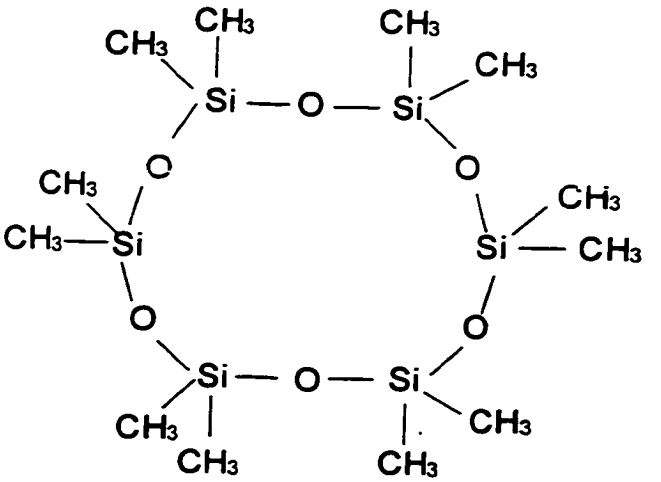

cyclohexasiloxane, dodecamethyl

Figure 5.8 Chemical structure of n=1, n=3 and n^{+}=6 units of siloxane identified using GC-MS spectrum in the fluid extracted from EPDM

groups as $Si(CH_3)_3$ and $Si(CH_3)_2$. The EPDM specimens contained 200 parts of alumina trihydrate (ATH) per weight of the base polymer.

Fig.5.9 shows the infrared spectra in the transmission mode after heating the specimens for 1h at 380°C (curve A), 240°C (curve B), and 150°C (curve C). The untreated specimen is also shown (curve D). After heating, the specimen were then immersed in hexane for a brief time of 10 min to remove the fluid from the surface and subsequently allowing the diffusion of the LMW fluid to take place from the bulk to the surface as well as the evaporation of hexane from the surface by leaving the specimen in air at 23±3°C for 50 min. It will be observed from Fig.5.9 that the transmitted spectra decreased for bands 1 to 3, with increasing temperature 23°C (curve D), to 380°C (curve A). This was due to a larger absorption of the IR radiation by the larger amount of fluid generated with increasing temperature. The IR spectra thus confirms the increased production with increasing temperature of the LMW fluid which was recently reported in EPDM [20-21]. In that work, the increased production of the LMW fluid was determined quantitatively using a sensitive balance.

In Fig.5.10 the experimental conditions were identical to those depicted in Fig.5.9 except that the specimens were left in air for 4h, thereby allowing more diffusion of the LMW fluid of the LMW fluid to the surface to take place. Fig.10 shows that there was a smaller variation in the amount of the fluid of the fluid on the surface (bands 1 to 3) of the four specimens after allowing a long time for the fluid to diffuse from the bulk to the surface.

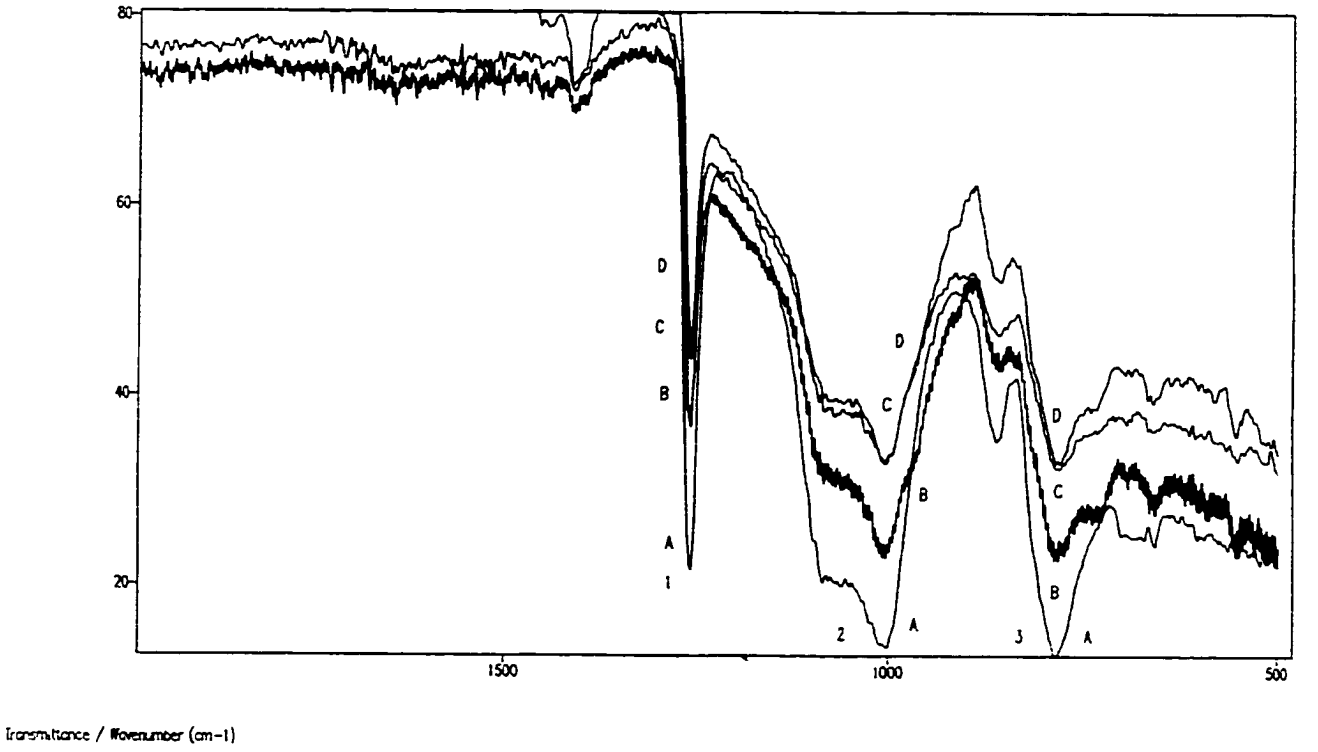

Figure 5.9 **IR spectra in the transmission mode after heating EPDM specimens for 1h at different temperatures, then removing the LMW fluid from the surface by immersion in hexane for 10 min and subsequently allowing the fluid to diffuse back from the bulk by leaving the specimen in air at 23±3°C for 50 min. A, 380°C; B, 240°C; C, 150°C; D, (23°C) virgin**

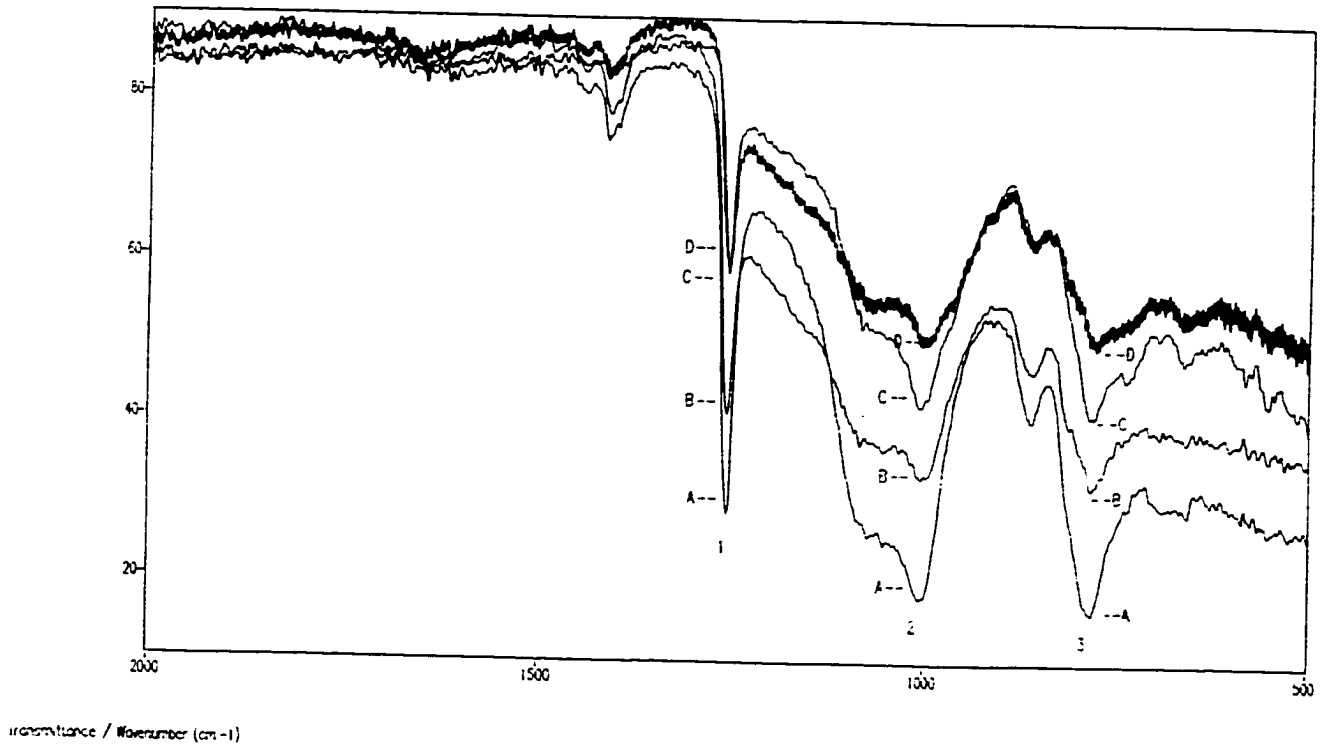

Figure 5.10 **As for Fig.5.9 except that the diffusion time in air is 4h**

CHAPTER VI

CONCLUSIONS AND SUGGESTIONS FOR FURTURE RESEARCH

6.1 Conclusions

1. The amount of the mobile fluid in the virgin EPDM which has been applied in the present study is 1.72±0.1%. The content of the LMW fluid is independent of the volume of the specimens in the range of 0.83cm^3 to 14.41cm^3. (CHAPTER III)

2. The LMW fluid could be regenerated by the scissions of long molecular weight chains into short and/or the release of the trapped short chains after the application of heating in an electrical oven. This simulates the heat produced by different levels of leakage currents and dry band arcing on the insulator. In the specimens from which the fluid was removed prior to heating, the amount of the fluid produced after heating at 50°C for periods varying from 1 to11h produced essentially the same amount of regenerated fluid of 0.135%±0.005%. Heating at 150°C resulted in a slight increase in the amount of the generated fluid from 0.14% to 0.18% after heating for 1h and 11h, respectively. A significant increase in the fluid from 0.67% to 2.5% after heating for 1 and 11h at 240 has been observed. The content of the fluid initially increased at 380°C for periods varying from 0.5 to 1h and then decreased with increasing durations of heating. After 2, 3, 5 and 11h of heating at 380°C, the content of the fluid decreased to 1.43%, 0.97%, 0.49% and 0.1%, respectively. The initial increase in the regenerated fluid was due to the enhanced scissions of the bonds and the release of the fluid from

the bulk where it was regenerated. The loss of the fluid due to evaporation appears to be small, at short times (up to 1h) compared to the generated fluid. The decrease in the regenerated fluid is attributed to the evaporation of the volatile groups with increasing duration of heating (up to 11h) at 380°C. The most effective temperature for increasing the production of the LMW fluid within the range observed, is 240°C. At this temperature the net production of the fluid increases with increasing time of heating. At 380°C, the net production of the fluid decreases with time, and as stated above, is attributed to the increased evaporation of generated fluid at higher temperature.

3. More LMW fluid was produced when the original fluid had already been removed before heating than when it was not. This is either because more space was provided between the molecular chains for the regeneration process after removing the original fluid, or because when the fluid had been left in the specimen, it evaporated during heating and therefore the net amount of the fluid was less.

4. After heating the EPDM specimen at 550°C for 1h, the sample was very brittle and disintegrated into a white powder. The temperature was beyond the withstand capability of the EPDM rubber.

5. The production of the fluid in a virgin EPDM specimen was negligibly small after a laser beam irradiation for one shot in the energy range 28.8-654J. This was

because of only small area of the specimen (0.07~ 0.08%) form the total area was subjected to heating by the laser beam. The production of the amount of the LMW fluid, varied in the range 0.28-0.49% at the above energy range, after one shot of laser beam irradiation in the EPDM specimen that LMW fluid was previously removed. More fluid was produced after laser irradiation in specimens where the fluid was first removed using hexane. This is also consistent with similar findings in specimens heated in an oven. On both virgin specimens and specimen that LMW fluid was prior removed, there is no correlation between the amount of fluid produced and the number of applications of the laser beam bombardment to the surface.

6. ATH filler is added to the EPDM rubber to impart tracking and erosion resistance. Heating the EPDM specimens at 380°C for 1h resulted in complete decomposition of alumina trihydrate into alumina and water. The weight loss is 24.8% on the specimen that LMW fluid was prior devoid, which is in reasonable agreement with the theoretical value of 23.2%.

7. The contact angle of EPDM specimens decreased rapidly from 99°before immersion to 83° after 6 minutes of immersion in hexane. The contact angle continued to decrease with prolonged immersion in hexane. It dropped to 64.5° after 96h immersion, which indicated that the surface had become hydrophilic.

When the EPDM specimens were immersed in hexane, the mobile low molecular weight fluid on the surface and in the bulk was gradually extracted by hexane and this left the surface devoid of fluid resulting in the observed reduction in θ. The contact angle increased from 64.5° to 71° after 6min evaporation in air. The contact angle remained constant at (87±2)° from 4h to 24h of rest time when a complete evaporation of absorbed hexane had taken place. The gradually recovery of the contact angle in this case was due to the evaporation of hexane.

8. The contact angles increased with increasing duration of heating from 1 to 11h for all temperatures. This is because it is sufficient for only a very thin film of fluid to affect the surface property and therefore the hydrophobicity. Additionally the orientation of the methyl groups affects the hydrophobicity in addition to the amount of the fluid present in the material. The surface of the specimens was deformed after heating at 380°C. The surface condition observed after heating at 380°C for 5 and 11h could be described as a metastable state. The contact angle formed is a metastable contact angle.

9. The contact angles measured on the EPDM specimens after laser beam irradiation were relatively constant in the range of 99° to 104°. The small variation of the contact angle on the EPDM specimens after the application of laser beam irradiation is consistent with the small variation in the value of the LMW fluid produced. The area outside the spot where the laser energy fell, was not heated

significantly and therefore the changes in the contact angle and the production of the LMW fluid were very slight.

10. SEM photographs have demonstrated the physical changes on the surface after laser irradiation. A large magnification shows visible cracks on the target area where the laser irradiation impacted. SEM photographs of the specimens which were heated in the oven for 1h at temperatures of up to 380°C did not show significant changes from the virgin specimens.

11. The LMW fluid in the EPDM specimens was identified to be silicone fluid by using NMR spectrum. GC-MS spectrum shows that the fluid extracted from EPDM was identified as composed of siloxane molecules which is a silicone fluid. Siloxane molecules units of n=3 to n=6 ($-[Si(CH_3)_2-O]_n-$) and cyclo-siloxane with units of n=6 to n=12 were identified in the spectrum. The largest concentration was of cyclo-siloxane having n=8 (mass range 592g/mole). The peaks in presence of the infrarad in (IR) spectra represent the characteristics absorption bands. Absorption at 1270-1255 cm^{-1} (band 1) is due to CH deformation in the $Si-CH_3$ groups. Absorption at 1100-1000 cm^{-1} (band 2) is due to the Si-O bond in Si-O-Si. Absorption at 840-790 cm^{-1} (band 3) is characteristic of Si-alkyl groups as $Si(CH_3)_3$ and $Si(CH_3)_2$.

6.2 Suggestions for future research

The low molecular weight fluid in the EPDM has been extensively investigated. However, there are many aspects which may affect the performance of EPDM and further research is suggested to improve the performance of EPDM.

1. The size and loading level of ATH particles may lead to different performance of EPDM. Aggregation of this kind of filler is often seen in polymeric insulators. It is suggested to study this aspect in a future work to improve the performance of EPDM.

2. Effects from wind and salt on the low molecular weight fluid in the EPDM. Outdoor wind can give the water droplet kinetic energy. The kinetic energy may transfer to the surface. The reorientation of CH_3 might happen at the surface, therefore the loss of hydrophobicity is suspected. Arcing might result to the ionization of NaCl to Cl^- and Na^+, Cl^- attaches to Si which is aided by the arcing energy. Therefore more hydrolysis reactions might happen at this condition.

3. Life time of the EPDM speicimens. However the life time can not be solely estimated by the thermal degradation. The diffusion of the low molecular weight fluid provides the recovery of hydrophobicity on the degraded surface. Several other laboratory techniques should be applied to estimate the life time of EPDM insulators.

APPENDIX A

DETERMINATION OF γ_S

$$(1+\cos\theta_1)\gamma_1 = 4\left(\frac{\gamma_1^{\,d}\gamma_s^{d}}{\gamma_1^{\,d}+\gamma_s^{d}}+\frac{\gamma_1^{\,p}\gamma_s^{p}}{\gamma_1^{\,p}+\gamma_s^{p}}\right) \leftarrow \text{Harmonic-mean, equation}$$

$\gamma_1 = \gamma_{water} = 72.8 \leftarrow$ Liquid1, water

$\gamma_1^{\,d} = \gamma_{water}^{d} = 22.1 \leftarrow$

$\gamma_1^{\,p} = \gamma_{water}^{p} = 50.7 \leftarrow$

$$(1+\cos\theta_1)\times 72.8 = 4\left(\frac{22.1\times\gamma_s^{d}}{22.1+\gamma_s^{d}}+\frac{50.7\times\gamma_s^{p}}{50.7+\gamma_s^{p}}\right)$$

$$(1+\cos\theta_2)\gamma_2 = 4\left(\frac{\gamma_2^{\,d}\gamma_s^{d}}{\gamma_2^{\,d}+\gamma_s^{d}}+\frac{\gamma_2^{\,p}\gamma_s^{p}}{\gamma_2^{\,p}+\gamma_s^{p}}\right) \leftarrow \text{Harmonic-mean, equation}$$

$\gamma_2 = \gamma_{MI} = 50.8 \leftarrow$ Liquid2, MI

$\gamma_2^{\,d} = \gamma_{MI}^{d} = 44.1 \leftarrow$

$\gamma_2^{\,p} = \gamma_{MI}^{p} = 6.7 \leftarrow$

$$(1+\cos\theta_2)\times 50.8 = 4\left(\frac{44.1\times\gamma_s^{d}}{44.1+\gamma_s^{d}}+\frac{6.7\times\gamma_s^{p}}{6.7+\gamma_s^{p}}\right)$$

Let $\gamma_s^{d} = D, \gamma_s^{p} = P, \rightarrow$ d : London, dispersion; p : hydrogen, bonding

$$(1+\cos\theta_1)\times 72.8 = 4\left(\frac{22.1\times D}{22.1+D}+\frac{50.7\times P}{50.7+P}\right)$$

$$(1+\cos\theta_2)\times 50.8 = 4\left(\frac{44.1\times D}{44.1+D}+\frac{6.7\times P}{6.7+P}\right)$$

$C_1 = (1+\cos\theta_1)\times 72.8 \div 4$

$C_2 = (1+\cos\theta_2)\times 50.8 \div 4$

$$C_1 = \frac{22.1 \times D}{22.1 + D} + \frac{50.7 \times P}{50.7 + P}$$

$$C_2 = \frac{44.1 \times D}{44.1 + D} + \frac{6.7 \times P}{6.7 + P}$$

$$C_1 = \frac{1}{\left(\frac{1}{D}\right) + \left(\frac{1}{22.1}\right)} + \frac{1}{\left(\frac{1}{P}\right) + \left(\frac{1}{50.7}\right)}$$

$$C_2 = \frac{1}{\left(\frac{1}{D}\right) + \left(\frac{1}{44.1}\right)} + \frac{1}{\left(\frac{1}{P}\right) + \left(\frac{1}{6.7}\right)}$$

$$C_1 = \frac{1}{X_1 + a_1} + \frac{1}{X_2 + a_2} \rightarrow X_1 = \frac{1}{C_1 - \frac{1}{X_2 + a_2}} - a_1;$$

$$C_2 = \frac{1}{X_1 + a_3} + \frac{1}{X_2 + a_4} \rightarrow X_1 = \frac{1}{C_2 - \frac{1}{X_2 + a_4}} - a_3;$$

$$X_1 = X_1 \Rightarrow \frac{1}{C_1 - \frac{1}{X_2 + a_2}} - a_1 = \frac{1}{C_2 - \frac{1}{X_2 + a_4}} - a_3$$

$$\frac{(1 - a_1c_1)X_2 + (a_2 - a_1a_2c_1 + a_1)}{c_1X_2 + (a_2c_1 - 1)} = \frac{(1 - a_3c_2)X_2 + (a_4 - a_3a_4c_2 + a_3)}{c_2X_2 + (c_2a_4 - 1)};$$

Let $b_1 = a_2 - a_1a_2c_1 + a_1; b_2 = 1 - a_1c_1; b_3 = a_4 - a_3a_4c_2 + a_3; b_4 = 1 - a_3c_2; b_5 = a_2c_1 - 1; b_6 = c_2a_4 - 1; b_7 = c_1; b_8 = c_2$

$$\frac{B_2X_2 + B_1}{B_7X_2 + B_5} = \frac{B_4X_2 + B_3}{B_8X_2 + B_6} \Rightarrow (B_2B_8 - B_4B_7)X_2^2 + (B_2B_6 + B_1B_8 - B_4B_5 - B_3B_7)X_2 + (B_1B_6 - B_3B_5) = 0 \Rightarrow$$

$$\text{Final} \Rightarrow X_2 = \frac{-(B_2B_6 + B_1B_8 - B_4B_5 - B_3B_7) \pm \sqrt{(B_2B_6 + B_1B_8 - B_4B_5 - B_3B_7)^2 - 4 \times (B_2B_8 - B_4B_7) \times (B_1B_6 - B_3}}{2 \times (B_2B_8 - B_4B_7)}$$

Solution here:

θ1	99	
θ2	56	
y1	-0.156434436	y1=cosθ1
y2	0.559192917	y2=cosθ2
c1	0.015352893	c1=(1+y1)*72.8/4
c2	0.01980175	c2=(1+y2)*50.8/4
a1	45.24886878	costant a1=1/22.1
a2	19.72386588	costant a2=1/50.7
a3	22.67573696	costant a3=1/44.1
a4	149.2537313	costant a4=1/6.7
b1	51.27054427	b1=a2-a1*a2*c1+a1
b2	0.305298947	b2=1-a1*c1
b3	104.911666	b3=a4-a3*a4*c2+a3
b4	0.550980724	b4=1-a3*c2
b5	-0.697181592	b5=a2*c1-1
b6	1.955485082	b6=c2*a4-1
b7	0.015352893	b7=c1
b8	0.01980175	b8=c2
y3	0.385690048	y3=b2*b6+b1*b8-b4*b5-b3*b7
y4	0.148756813	y4=y3*y3
y5	-0.002413695	y5=b2*b8-b4*b7
y6	173.4012668	y6=b1*b6-b3*b5
y7	-0.00482739	y7=2*y5
y8	1.822907765	y8=y4-4*y5*y6
y9	1.350151016	y9*y9=y8
x2	359.58172	x2=1/P x1=1/D
Solid(P)	0.002781009	
x1	33.38914255	y10 379.3055859 y10=x2+a2
		y11 0.002636397 y11=1/y10
		y12 0.012716497 y12=c1-y11
Solid(D)	0.029949856	y13 78.63801133 y13=1/y12
Total	0.032730865	Solid(P)+Solid(D)

BIBLIOGRAPHY

[1] S. Simmons, M. Shah, J. Mackevich and R.J. Chang, "Silicone Elastomer consideration", IEEE Electrical Insulation Magazine, Vol.13, pp.25-31, 1997

[2] O.E.Gouda, "Flashover of Over-head H.V.T.L. Insulators under Desert Pollution Conditions", CEIDP, pp.605-611, 1990

[3] B.F.Hampton, "Flashover mechanism of polluted insulation", Proc. IEE, Vol.111, pp.985-990, 1964

[4] A. E.Vlastos and S. M.Gubanski, "Surface structural, changes of naturally aged silicone and EPDM composite insulators", IEEE Trans. on PD., Vol.6, No.1, pp.888-895, 1991

[5] A. E.Vlastos and E. Sherif, "Natural, aging of EPDM composite insulators", IEEE Trans. on PD., Vol.5, No.1, pp.406-414, 1990

[6] D.J.Parr and R.M.Scarisbrick, "Performance of synthetic insulating materials under polluted conditions", Proc. IEE, Vol.112, pp.1625-1632, 1965

[7] H.R.Baker and R.N.Bolster, "Surface electrical leakage on insulators and coatings in the presence of moisture condensation", IEEE Trans. on EI, Vol.11, No.3, pp.76-80, 1976

[8] T. Zhao and R.A. Bernstorf, "Aging tests of polymeric housing materials for non-ceramic insulators", IEEE Electrical Insulation Magazine, Vol.14, No.2, pp.26-33, 1998

[9] J. Mackevich and M. Shah, "Comparison of porcelain and polymer electrical insulation", IEEE Electrical Insulation Magazine, Vol.13, No.3, pp.5-11, 1997

[10] J. Mackevich and S. Simmons, "Material considerations", IEEE Electrical Insulation Magazine, Vol.13, No.4, pp.10-16, 1997

[11] IEEE Working Group report, "Application of insulators in a contaminated environment", IEEE Trans. on PAS, Vol.PAS-98, pp.1676-1695, 1979

[12] R.G.Houlgate and D.A.Swift, "Composite Rod Insulators for AC Power lines: Electrical Performance of Various Designs at a Coastal Testing Station", IEEE Trans. on Power Delivery, Vol.5, pp.1944-1952, 1990

[13] R. J.Arhart, "The chemistry of ethylene propylene insulation I, II", E.I.Du Pont de Nemours and Company, Inc., Electrical Insulation magazine, Vol. 9, No.6, pp.11-13, pp.31-34, 1993

[14] L.E.Lipinski and J.Michaiski, "Wettability of the EPDM elastomers as an aspect of selfwashability of high voltage insulator", paper SPT accepted for presentation at the IEEE Stockholm Power Tech Conference, pp.304-309, 1995

[15] J.Kindersberger and M.Kuhl, "Effect of hydrophobicity on insulator performance", 6th International Symposium on HV Eng., paper 12.01, 1989

[16] D.K.Das-Gupta, "Polyethylene: Structure, Morpholohy, Molecular motion and dielectric behavior", IEEE, Electrical Insulation Magazine, Vol.10, No.3, pp.5-11, 1994

[17] M.Brown, "Compounding of ethylene-propylene polymers for electrical applications", Electrical Insulation magazine, Vol.10, No.1, pp.16-22, 1994

[18] H. Deng and R. Hackam, "Impact of weather conditions and formulations on LMW silicone fluid content in RTV silicone rubber coatings", Conf. Record of CEIDP, pp.437-440, 1996

[19] S. H.Kim, "Electrical performance and surface analysis of RTV silicone rubber coatings for H.V. outdoor insulators", Ph.D dissertation in University of Windsor, Ontario, Canada, 1992

[20] L.Cao and R.Hackam, "LMW fluids in EPDM", 1997 CEIDP Conference, 97CH36046, Vol. II, pp.423-426, 1997

[21] L.Cao and R.Hackam, "Effects of heating to the presence of fluid in EPDM", Proc. of ISEI Conference, Vol.II, pp.360-364 , 1998

[22] T. Sorqvist and A. E.Vlastos, "Hydrophobicity and leakage current statistics of polymeric insulators long-term exposed to coastal contamination", Record of IEEE ISEI, pp.335-340, 1996

[23] S. M.Gubanski and A. E.Vlastos, "Wettability of naturally aged silicone and EPDM composite insulators", IEEE Trans. on PD., Vol.5, No.3, pp.1527-1533, 1990

[24] E.A.Cherney and D.J.Stonkus, "Non-Ceramic Insulators for Contaminated Environments", IEEE Transactions on Power Apparatus and Systems, Vol.PAS-100, pp.131-142, 1981

[25] T. Sorqvist and Antonios E.Vlastos, "Outdoor polymeric insulators long-term exposed to HVDC", IEEE Trans. on PD, Vol.12, No.2, pp.1041-1047, 1997

[26] H. Deng, "Electrical performance of RTV silicone rubber coatings for H.V. outdoor insulators", Master thesis, University of Windsor, Ontario, Canada, 1995

[27] T. Tokoro and R. Hackam, "Recovery of hydrophobicity of ethylene propylene diene monomer aged by heat and saline water", Procedings of the 5th International Conference on Properties and Applications of Dielectric Materials, pp.82-85, 1997

[28] T. Tokoro and R. Hackam, "Effect of water salinity and temperature on the hydrophobicity of ethylene propylene diene monomer insulator", Conf. Record of CEIDP, pp.424-427, 1996

[29] D.K.Owens and R.C.Wendt, "Estimation of the surface free energy of polymers", J. Appl. Polym. Sci., Vol.13, pp.1741-1747, 1969

[30] J.Kinsweavwefwe, A.Schutz, H.C.Karner and R.v.d.Huir, "Service performance, material design and applications of composite insulators with silicone rubber housing", 1996 CIGRE, paper 33-303, 1996

[31] R. J. Good, "Contact angle, wetting, and adhesion: a critical review", in Contact angle, Wettability and Adhesion, pp.3-36, ed., K.L.Mittal

[32] L.H. Lee, "Roles of molecular interactions in adhesion, adsorption, contact angle, and wettability", in Contact angle, Wettability and Adhesion, pp.49-57, ed., K.L.Mittal, 1993

[33] L.Szepesy, C.Sc. "Gas chromatography", editor E.D.Morgan, M.A.D.Phil., and F.R.I.C, pp.1-7,1963

[34] H. S.Kroman and S. R.Bender, editor, "Theory and application of gas chromatography in industry and medicine", pp.58-60,1968

[35] H. A. Scymanski, "Lectures on gas chromatography", Plenum press, pp.19-31, 1963

[36] R.J.Abraham and P.Loftus, "Proton and carbon-13 NMR spectroscopy", pp.2-19, 1978

[37] I. NODA, "Contact angle studies of surface-hydrophilic elastomer films", in"Contact angle, wettability and adhesion", Ed. K.L.Mittal, pp691, 1993

[38] E. D.Becker, "High resolution NMR theory and chemical applications", pp.2-6, 1980

[39] P.G.Harris and A.D.Trigg, "Surface analysis techniques and their application to materials and device characterization", pp.88-95, 1987

[40] P.R.Thornton, "Scanning electron microscopy" in "application to materials and device science", Published by Chapman and Hall Ltd, pp.6-12, 1968

[41] J. I. Goldstein, "Scanning electron microscopy and X-ray microanalysis", pp.2-24, Plenum press

[42] A.E.Vlastos and S.M. Gubanski, "Surface structural changes of naturally aged silicone and EPDM composite insulators", IEEE Trans. on PD., Vol.6, No.2, pp.888-900, 1991

[43] R.S. Gorur, E.A.Cherney, R.Hackam and T.orbeck, "The electrical performance of polymeric materials under accelerated aging in a fog chamber", IEEE Trans. on PD., Vol.3, pp.1157-1164, 1988

[44] H. Deng, R.Hackam and E.A.Cherney, "Influence of thickness, substrate type, amount of silicone fluid and solvent type on the electrical performance of RTV silicone rubber coatings", IEEE Trans. on PD., Vol.11, No.1, pp.431-443, 1996

[45] H.Deng, R.Hackam and E.A.Cherney, "Role of the size of particles of alumina trihydrate filler in the life of RTV silicone rubber coating", IEEE Trans. on PD., Vol.10, pp.1012-1024, 1995

[46] S.K.Kim and R.Hackam, "Formation of silicone fluid at the surface of RTV silicone rubber coating due heat", IEEE Conference on CEIDP, Proc. pp.605-611, 1993

[47] D.K. Thomas, "Network scission processes in peroxide cured methylvinyl silicone rubber", Polymer, Vol.7, pp.99-105, 1966

[48] H.Deng, R.Hackam and E.A.Cherney, "Effects of applied heat on LMW silicone fluid in RTV silicone rubber coatings used in outdoor HV insulation", Conference on CEIDP, Proc. 95CH 35842, pp.459-46, 1995

[49] H. Deng and R.Hackam, "Electrical performance of RTV silicone rubber coating of different thickness on porcelain", IEEE Trans. on PD., Vol.8,1997

[50] H. Deng, R.Hackam and E.A.Cherney, "Role of the size of particles of alumina trihydrate filler on the life of RTV silicone rubber coating", IEEE Trans. on PD., Vol.10, pp.1012-1024, 1995

[51] R.S.Gorur, E.A.Cherney and R.Hackam, "Performance of polymeric insulating materials in salt-fog", IEEE Trans. on PD., Vol.PWRD-2, pp.486-492, 1987

[52] R.S.Gorur, J.Chang and O.G.Amburgey, "Surface hydrophobicity of polymeric materic materials used for outdoor insulation", IEEE Trans. on PD., Vol. 5, No.4, pp.1923-1933, 1990

[53] S.H.Kim, E.A.Cherney and R. Hackam, "Effects of filler level in RTV silicone rubber coatings used in HV insulators", IEEE Trans. on EI, Vol.27, No.6, 1065-1072, 1992

[54] S.H.Kim, E.A.Cherney and R. Hackam, "Suppression mechanism of leakage current on RTV coating porcelain and silicone rubber insulators", IEEE Trans. on PD., Vol.6, pp.1549-1556, 1991

[55] S.H.Kim, E.A.Cherney and R.Hackam, "The loss and recovery of hydrophobicity of RTV silicone rubber insulator coatings", IEEE Trans. on PD., Vol.5, pp.1491-1500, 1990

[56] S.M.Gubanski and A.E.Vlastos, "Wettability of natural aged silicone and EPDM composite insulators", IEEE Trans. PD., Vol.5, pp.1527-1535, 1990

[57] B.F.Hampton, "Flashover Mechanism of Polluted Insulation", Proc. IEE, Vol.111, pp.985-990, 1964

[58] N.K.Adam, "Principles of water-repellency", in "Waterproofing and water-repellency", Ed. By J.L.Moilliet, pp.1-147, Elsevier Publishing Comp., 1963

[59] M.Leclerc, Bouchard, Y.Gervais and D.Mukhedkar, "Wetting processes on a contaminated insulator surface", IEEE Trans. on P.A.S., Vol.101, pp.1005-1011, 1982

[60] R.S.Gorur, E.A.Cherney and R.Hackam, "Performance of polymeric insulating materials in salt-fog", IEEE Trans. on PD., Vol.PWRD-2, pp.486-492, 1987

[61] M.J.Owen, T.M.Gentle, T.Orbeck, and D.E. Williams, "Dynamic wettability of hydrophobic polymers", pp.101-110, in "Polymer surface dynamics", Ed. By J.D.Andrade, 1988

[62] R.J. Good, "A theory of hysteresis", J.Am.Chem. Soc. Vol.74, pp.5041-5045, 1953

[63] R.J. Good, L.A.Girifalco and G.Kraus, "A theory for the estimation of surface and interfacial energies", J.Phys.Chem. Vol.61, pp.1418-1422, 1958

[64] Wu, S. "Polymer interface and adhesion", Marcel Dekker, Inc., pp.98-104, 169-181, 1982

[65] W.Duncan-Hewitt and R.Nisman, "Investigation of the surface free energy of pharmaceutical materials from contact angle, sedimentation, and adhesion measurements", in Contact angle, Wettability and Adhesion, pp.791-810, ed., K.L.Mittal

PUBLICATIONS IN SUPPORT OF THIS THESIS

Refereed International Conferences:

1. Liwen Cao and Reuben Hackam "Low molecular weight fluid in EPDM" Conference on Electrical Insulation and Dielectric Phenomena, IEEE Proceeding, Vol. II, pp.423-426,1997

2. Liwen Cao and Reuben Hackam "Effects of heating on the presence of fluid in EPDM" 1998 International Symposium on Electrical Insulation (ISEI), IEEE Conference Proceeding Vol. II, pp.360-364,1998

3. Liwen Cao and Reuben Hackam "Diffusion of low molecular weight fluid in EPDM" IEEE Conference on Electrical Insulation and Dielectric Phenomena, Atlanta, U.S.A October 25-28, 1998

National Conferences: (Abstract only)

1. Liwen Cao and Reuben Hackam "Hydrophobic fluids in EPDM" CAGE CLUB, Canadian High Voltage Engineering Conference, Toronto, Ontario, 1997

2. Liwen Cao and Reuben Hackam, "Effects of heating on the hydrophobicity of EPDM", CAGE CLUB, Canadian High Voltage Engineering Conference, London, Ontario, 1998

VITA AUCTORIS

Liwen Cao was born in 1974 in Hebei Province, China. She received her B.Sc from University of Nanchang in Electrical Engineering Department in 1996, China. Currently she is a candidate for the degree of M.A.Sc., Electrical Engineering, University of Windsor, Windsor, Canada.